VOLUME 35, NUMBER 4, AUGUST 2012

HADRONIC JOURNAL

HADRONIC JOURNAL Volume 35, Number 4, August 2012

Founded in 1978 by Prof. R. M. Santilli at Harvard University. Some of the past Editors include Professors S. L. Adler, A. 0. Barut, L. C. Biedenharn, N. N. Bogoliubov, M. Froissart, J.Lohmus, S. Okubo, Nobel Laureate Ilya Prigogine, M. L. Tomber, J. P.Vigier, J. Wess, Nobel Laureate Chen Ning Yang.

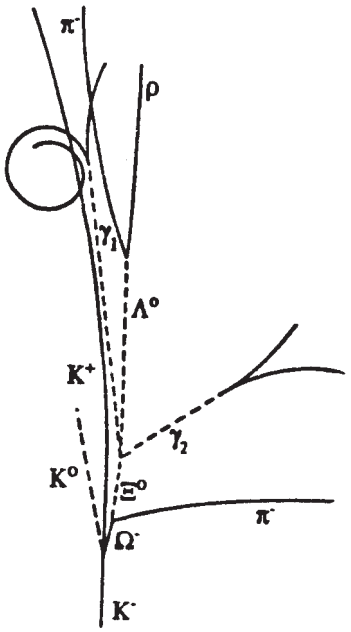

EDITORIAL BOARD
A.O.Animalu
D. P. Bhattacharyya
G.-C. Cavalleri
V. De Sabbata
T. L. Gill
L. P. Horwitz
H. Hurst
S. L. Kalla
S. I. Kruglov
S. S. Moskaliuk
M. Nishioka
R. F. O'Connell
Z. Oziewicz
E. Recami
M. Saleem
D. V. Shirkov
S. Silvestrov
D.S. Sourlas
H. M. Srivastava
A. I. Studenikin
R.I. Tsonchev
QI-Ren Zhang
C.A.Wolf
YI-Zhong Zhuo

FOUNDER:
RUGGERO M. SANTILLI

EDITOR IN CHIEF
CHRISTIAN CORDA

HADRONIC PRESS, INC.

HADRONIC JOURNAL

VOLUME 35, NUMBER 4, AUGUST 2012

THE RADIUS OF THE PROTON IN THE SELF-CONSISTENT MODEL, 349
Sergey G. Fedosin
Perm, Perm Region, Russia
Sviazeva Str. 22-79

GENERAL RELATIVITY AND OPERA EXPERIMENT, 365
Christian Corda
Institute for Theoretical Physics and
Advanced Mathematics
Einstein-Galilei, Via Santa Gonda 14
59100 Prato, Italy

RESPONSE TO CROTHERS' CATASTROPHE, 373
Jason J. Sharples
Applied and Industrial Mathematics Research Group
School of Physical, Environmental and Mathematical Sciences
University of South Wales, Canberra, 2600 Australia

SOLAR REDSHIFT CALCULATIONS BY THE RAYLEIGH SCATTERING MECHANISM, 379
Ivan Gandzha
Department of Theoretical Physics
Institute of Physics, National Academy of Sciences of Ukraine
03028 Kyiv, Prospect Nauky 46, Ukraine

COMMENTS ON I. GANDZHA'S PAPER: "SOLAR REDSHIFT CALCULATIONS BY THE RALEIGH SCATTERING MECHANISM", 389
Richard Cox
International Committee on Scientific
Ethics and Accountability

WHY BARYONS ARE YANG-MILLS MAGNETIC MONOPOLES, 399
Jay R. Yablon
Schenectady, New York 12309

THE RADIUS OF THE PROTON IN THE SELF-CONSISTENT MODEL

Sergey G. Fedosin
Perm, Perm Region, Russia
Sviazeva Str. 22-79
intelli@list.ru

Received August 20, 2012

Abstract

Based on the notion of strong gravitation, acting at the level of elementary particles, and on the equality of the magnetic moment of the proton and the limiting magnetic moment of the rotating non-uniformly charged ball, the radius of the proton is found, which conforms to the experimental data. At the same time the dependence is derived of distribution of the mass and charge density inside the proton. The ratio of the density in the center of the proton to the average density is found, which equals 1.57.

Keywords: *strong gravitation; de Broglie waves; magnetic moment; proton radius.*

Copyright © 2012 by Hadronic Press, Inc., Palm Harbor, FL 34682–1577, USA

1 Introduction

Since the discovery of the proton in 1917 the question arose how to determine the radius of this elementary particle. There are many theoretical models to estimate the radius of the proton. Most of these models is associated with the concept of the electromagnetic form factors as the amendment by which the scattering amplitude of particles by proton is different from the scattering amplitude by a point particle. The calculation of the form factors is complex and requires taking into account many factors, including the radial density distribution of charge and magnetic moment, the dynamics of quarks, partons and virtual particles. There may be a variety of approaches – scattering theory, chiral perturbation theory, lattice QCD, etc., description of which can be found in [1], [2]. Form factors are determined from scattering experiments, depend on the energy of the interacting particles, and allow us to find the root mean square of the charge distribution and magnetic moment as a measure of particle's size. Information on the radius of the proton can be extracted from the analysis of the Lamb shift in hydrogen and in a coupled system of a proton and a negative muon [3].

2 Other estimates of proton radius

Consider some simple methods for determining the radius of the proton. One of them is based on the fact that in the particles, when they are excited, standing electromagnetic waves emerge. The maximum energy of these standing waves does not exceed the rest energy in order to avoid the decay of particles. From this it can be derived that the de Broglie waves are electromagnetic oscillations, detectable in the laboratory frame in the interaction of moving particles. To describe these oscillations it is necessary to apply the Lorentz transformations to the standing waves inside the particles and to find their form in the laboratory reference frame [4], [5].

In the simplest case the spherical standing waves are modeled by two waves, one of which runs from the center to the surface of the particle and the other at the same time is moving backwards. We can assume that in the direction of a specified axis, for example OX, there are two counter-propagating waves of the following form:

$$U_1 = U_0 \sin(\omega' t' - K' x' + \varphi_1), \qquad U_2 = U_0 \sin(\omega' t' + K' x' + \varphi_2),$$

$$U = U_1 + U_2 = 2U_0 \cos\left(K'x' - \frac{\varphi_1 - \varphi_2}{2} \right) \sin\left(\omega' t' + \frac{\varphi_1 + \varphi_2}{2} \right), \qquad (1)$$

here φ_1, φ_2 are the initial phases of the oscillations with $t' = x' = 0$, U_0 is the amplitude of the periodic function, ω' and K' denote the angular frequency and wave number and the primes over the variables mean that they are considered in the rest frame of the particle.

As U any periodic function can be used, which satisfies the wave equation. For example, it can be the strength or the field potential of the wave. The phases of the waves in (1) must be shifted to π for emerging of the standing wave. If $\varphi_1 = \pi$, $\varphi_2 = 0$, then in the center of the particle with $x' = 0$ there will be always a node as the absence of visible oscillations, and (1) becomes as follows:

$$U = 2U_0 \sin(K'x') \cos(\omega' t'). \qquad (2)$$

As a result of oscillations (2) velocities of charges of the particle substance and the field potentials can periodically change inside the particle. This leads inevitably to periodic oscillations of the field potentials also outside the particle in the surrounding space.

Now we shall assume that the particle moves together with its standing wave along the axis OX in the laboratory reference frame at the velocity u. How are the field oscillations modified inside and outside the particle with respect to its movement? We should express in (2) the primed coordinates and the time inside the moving particle through the coordinates and the time in the laboratory reference frame using the Lorentz transformations (c refers to the speed of light):

$$t' = \frac{t - ux/c^2}{\sqrt{1 - u^2/c^2}}, \qquad x' = \frac{x - ut}{\sqrt{1 - u^2/c^2}}, \qquad y' = y, \qquad z' = z,$$

$$U = 2U_0 \sin\left(\frac{K'(x-ut)}{\sqrt{1-u^2/c^2}}\right)\cos\left(\frac{\omega'(t-ux/c^2)}{\sqrt{1-u^2/c^2}}\right). \qquad (3)$$

From (3) we see that as a result of displacement of the standing wave with the particle for the external motionless observer in the laboratory frame the wavelength and the frequency will change. More precisely, on the observed wave additional antinodes appear, with a wavelength between them, differing from the wavelength $\lambda' = \frac{2\pi}{K'}$ in the reference frame of the particle. We shall stop the wave (3) for a moment with $t = 0$ and shall find the wavelengths as the spatial separation between the points of the wave in the same phase. When $x = 0$ the sine in (3) will be zero, while when $x = \lambda_1$ the phase of the sine will change from 0 to 2π. Hence we obtain:

$$\sin\left(\frac{K'\lambda_1}{\sqrt{1-u^2/c^2}}\right) = \sin(2\pi), \qquad \lambda_1 = \frac{2\pi\sqrt{1-u^2/c^2}}{K'} = \lambda'\sqrt{1-u^2/c^2}. \qquad (4)$$

Similarly for the wavelength of the cosine in (3) we find:

$$\cos\left(-\frac{\omega' u\lambda_2/c^2}{\sqrt{1-u^2/c^2}}\right) = \cos(-2\pi), \qquad \lambda_2 = \frac{2\pi c^2\sqrt{1-u^2/c^2}}{\omega' u}. \qquad (5)$$

We shall now estimate the temporal separation between the points of the wave in one phase with $x = 0$, considering this separation as the corresponding period of the wave:

$$\sin\left(-\frac{K'uT_1}{\sqrt{1-u^2/c^2}}\right) = \sin(-2\pi), \qquad T_1 = \frac{2\pi\sqrt{1-u^2/c^2}}{K'u}. \qquad (6)$$

$$\cos\left(\frac{\omega' T_2}{\sqrt{1-u^2/c^2}}\right)=\cos(2\pi), \qquad T_2 = T'\sqrt{1-u^2/c^2}\,. \tag{7}$$

From (4) – (7) we obtain the following expressions for the velocities:

$$\frac{\lambda_1}{T_1}=u\,, \qquad \frac{\lambda_2}{T_2}=\frac{c^2}{u}=v_b\,. \tag{8}$$

As we see from (8) the oscillations of the wave (3) associated with the cosine, are propagating at the phase velocity of de Broglie v_b. Besides, the oscillations of the wave (3) associated with sine, move in space at the same velocity u as the particle itself. The wavelength λ_2 in (5) can be transformed so as to bring it to the standard form for the de Broglie wavelength. We shall associate the angular frequency of the oscillations inside the particle, similarly to the electromagnetic wave, with the energy of oscillations: $W' = \hbar\omega'$, where $\hbar = \frac{h}{2\pi}$ is Dirac constant, h is Planck constant. This gives the following:

$$\lambda_2 = \frac{hc^2\sqrt{1-u^2/c^2}}{W'u}\,. \tag{9}$$

Similarly from (4) we have:

$$\lambda_1 = \frac{hc\sqrt{1-u^2/c^2}}{W'}\,. \tag{10}$$

In the limiting case when the oscillation energy is compared with the rest energy of the particle, $W' = mc^2 = \hbar\omega'$, from (9) it follows:

$$\lambda_{2f} = \frac{h\sqrt{1-u^2/c^2}}{mu} = \frac{h}{\wp}, \tag{11}$$

where m is the mass of particle, $\wp$ is relativistic momentum of the particle.

The formula (11) defines de Broglie wavelength with the help of particle momentum. We shall note that de Broglie wrote (11) on condition that the energy of the particle $W = \frac{mc^2}{\sqrt{1-u^2/c^2}}$ is equal to the energy of the wave accompanying the particle. According to the obtained expression (9), the wavelength λ_2 must be present in the particle also at low excitation energy W'. In this case as the excitation energy decreases, the wavelength should increase.

As a rule in the experiments only $\lambda_b = \lambda_{2f} = \frac{h}{\wp}$ is found from (11), and not the wavelength λ_2 from (9). This can occur because among the number of interacting particles at the same time there are particles with different excitation energies W' and different λ_2, so that the wave phenomena are blurred. The same is true for the waves with wavelength λ_1 in (10). Only for the most actively interacting particles, the excitation energies W' of which are close to the rest energy of the particles, the limiting value of the wavelength is reached equal to the de Broglie wavelength. Thus this wavelength is revealed in the experiment. When $W' = mc^2 = \hbar\omega'$ we can also predict for the particles the wave phenomena with the critical wavelength $\lambda_{1f} = \frac{h\sqrt{1-u^2/c^2}}{mc}$. In particular, $\lambda_c = \frac{h}{mc}$ is the Compton wavelength, discovered in the Compton effect. According to our point of view, emerging of de Broglie wave should be treated as a purely relativistic effect, which arises as a consequence of the Lorentz transformation of the standing wave, moving with the particle.

As a result, we have to assume that the wave-particle duality is realized in full only in those particular particles, the excitation energies of which reach their rest energies. In this case the difference of particles and field quanta, if they are treated from the point of view of their wave properties, becomes

minimal. At low excitation energies the particles can not emit their energy greatly, and the amplitudes of the oscillations of the field potentials near the particles are small. Then the particles would interact with each other not in the wave way, but rather in the usual way, and the wave phenomena become invisible.

If we assume that the length of the standing wave is equal to $\lambda' = 2R$, where R is the radius of the proton, then from the equality of the wave energy and the rest energy of the proton we obtain:

$$\nu' = \frac{c}{\lambda'} = \frac{c}{2R}, \qquad M_p c^2 = h\nu' = \frac{hc}{2R}, \qquad R = \frac{h}{2M_p c} = 6.6 \cdot 10^{-16} \text{ m},$$

here ν' is the oscillation frequency, M_p is the mass of the proton.

Another way to estimate the radius of the proton assumes that the difference between the rest energy of the neutron and the proton is due to the electrical energy of the proton charge. In this case, it should be:

$$(M_n - M_p)c^2 = \frac{ke^2}{4\pi\varepsilon_0 R}, \tag{12}$$

where M_n is the mass of the neutron, e is the elementary charge, ε_0 is the vacuum permittivity.

In (12) for the case of the uniform distribution of the charge in the volume of the proton $k = 0.6$, as a result the estimation of the proton radius gives the value of $R = 6.68 \cdot 10^{-16}$ m.

In [6] and [7], the radius of the proton was found from the condition that the limiting angular momentum of the strong gravitation field inside the proton is equal in magnitude to the spin of the proton. This leads to the following formula:

$$R = \frac{5\Gamma M_p}{21c^2} = 6.7 \cdot 10^{-16} \text{ m}. \tag{13}$$

In (13) the strong gravitational constant Γ is used. According to [4], this constant is determined from the equation of electric force and the force from the strong gravitation field, acting in the hydrogen atom on the electron with the mass M_e, which is located in the ground state on the Bohr radius R_B:

$$\frac{e^2}{4\pi\varepsilon_0 R_B^2} = \frac{\Gamma M_p M_e}{R_B^2}, \qquad \Gamma = \frac{e^2}{4\pi\varepsilon_0 M_p M_e} = 1.514 \cdot 10^{29}\ \mathrm{m^3 \cdot kg^{-1} \cdot s^{-2}}, \qquad (14)$$

In addition to the attractive forces from gravitation and the charges of the nucleus and the electron, in the hydrogen atom the electron substance in the form of the rotating disc is influenced by the repulsive forces acting away from the nucleus. One of these forces is the electric force of repulsion of the charged substance of the electron cloud from itself. In the rotating non-inertial reference frame in which an arbitrary part of the electron substance is at rest, there is also the force of inertia in the form of the centrifugal force, which depends on the velocity of rotation of this substance around the nucleus. In the first approximation, these forces are equal in magnitude, which leads to (14).

We shall remind that the idea of strong gravitation was introduced into science in the works of Abdus Salam and his colleagues [8], [9] as the alternative explanation of the strong interaction of the particles. Assuming that hadrons can be represented as Kerr-Newman black holes, they estimated the strong gravitational constant as $6.7 \cdot 10^{27}\ \mathrm{m^3 \cdot kg^{-1} \cdot s^{-2}}$.

With the help of the strong gravitation constant (14) we can express the fine structure constant:

$$\alpha = \frac{\Gamma M_p M_e}{\hbar c} = \frac{1}{137.035999}.$$

Another estimate of the radius of the proton follows from the equality of the rest energy and the absolute value of the total energy, which, taking into account the virial theorem, is approximately equal to the half of the absolute value of the strong gravitation energy associated with the proton [4]:

$$M_p c^2 = \frac{k\Gamma M_p^2}{2R}. \qquad (15)$$

If we take $k = 0.6$ for the case of the uniform mass distribution, then from (15) it follows that $R = 8.4 \cdot 10^{-16}$ m.

All of the above estimates are based on the classical approach to the proton as to the material object of small size in the form of the ball with the radius R. It is assumed that the strong gravitation acts at the level of elementary particles in the same way as ordinary gravitation at the level of planets and stars.

In the Standard model of elementary particles and in quantum chromodynamics it is assumed that the nucleons and other hadrons consist of quarks, and baryons have three quarks, while mesons have two quarks. Instead of the strong gravitation, the action of gluon fields is assumed to hold the quarks in hadrons. Quarks are considered to be charged elementary particles, therefore as the radius of the proton the charge and magnetic root mean square radii are considered. These radii are determined by the electric and magnetic interactions of the proton and can differ from each other.

The estimate of the proton charge radius can be made with the help of the experiments on the scattering of charged particles on the proton target [10]. In such experiments the total cross sections of interaction of the particles σ are found. For the case of the protons scattering on nucleons with energies more than 10 GeV we can assume that $\sigma = \pi R^2$, and $\sigma = 3.8 \cdot 10^{-30}$ m^2. Hence we obtain $R = 7.8 \cdot 10^{-16}$ m.

3 The self-consistent model

Our aim will be to find a more exact value of the radius of the proton by using classical methods. In the calculations we shall use only the tabular data on the mass, charge and magnetic moment of the proton. The proton will be considered from the standpoint of the theory of infinite nesting of matter [11], in which the analogue of the proton at the level of stars is a magnetar or a charged neutron star with a very large magnetic and gravitational field. Similarly to the magnetar, the substance of the proton must be magnetized and held by a strong gravitation field.

To take into account the non-uniformity of the substance density inside the proton we shall use the simple formula in which the substance density changes linearly increasing to the center:

$$\rho = \rho_c (1 - Ar), \tag{16}$$

where ρ_c is the central density, r is the current radius, $0 < A < \frac{1}{R}$ is the coefficient which should be determined.

Formula (16) should be considered as a first approximation to the actual distribution of the density of matter inside the proton. Approximate linear dependence of the density of matter in neutron stars has been shown in [12], and we assume that this is also true for the proton as an analogue of the neutron stars.

To estimate the values A and the radius R we shall consider the integral for the proton mass in the spherical coordinates:

$$M_p = \int \rho_c (1 - Ar) r^2 dr \sin\theta \, d\theta \, d\varphi = \frac{4\pi R^3 \rho_c}{3}\left(1 - \frac{3AR}{4}\right). \tag{17}$$

For accurate calculation of state of neutron stars, and thus protons as their analogues we should consider the curvature of spacetime in a strong gravitational field, as well as the contribution of the energy of the gravitational field to the total mass-energy. We shall assume that in (16), in dependency of matter density on the radius all relativistic effects are taken into account, and the mass of the proton (17) is the gravitational mass from the point of view of a distant observer.

In (17) there are three unknown quantities, to obtain which two more equations are required. We shall assume the virial theorem to be valid and equate the rest energy of the proton to the half of the absolute value of the energy of the static field of strong gravitation:

$$M_p c^2 = -\frac{1}{2}\int_0^\infty \varepsilon \, dV = \frac{1}{16\pi\Gamma}\int_0^\infty G^2 dV, \tag{18}$$

where $\varepsilon = -\dfrac{G^2}{8\pi\Gamma}$ is the energy density of the strong gravitation field according to [4], G is the gravitational acceleration or strength of gravitational field.

In (18), the integration of the energy density of the field should be done both inside and outside of the proton. The value G inside the proton can be conveniently found by integrating the equation for the strong gravitation field $\nabla \cdot \boldsymbol{G} = -4\pi\Gamma\rho$, which is part of the equations of the Lorentz-invariant theory of gravitation [13]. After integrating over the spherical volume with the radius $r \le R$, and then using the Gauss theorem, that is making transition to integrating over the area of the indicated sphere inside this proton, in view of (17) we obtain:

$$\int \nabla \cdot \boldsymbol{G}_i \, dV = \oint \boldsymbol{G}_i \cdot \boldsymbol{n} \, dS = 4\pi r^2 G_i = -\int 4\pi\Gamma\rho \, dV ,$$

$$\boldsymbol{G}_i = -\frac{4\pi\Gamma\rho_c \boldsymbol{r}}{3}\left(1 - \frac{3Ar}{4}\right). \tag{19}$$

Outside the proton the gravitational acceleration is equal to:

$$\boldsymbol{G}_o = -\frac{\Gamma M_p \boldsymbol{r}}{r^3}. \tag{20}$$

Substituting (19) and (20) in (18), we obtain the relation:

$$M_p c^2 = 4\pi^2 \Gamma \rho_c^2 R^5 \left(\frac{1}{45} - \frac{AR}{36} + \frac{A^2 R^2}{112}\right) + \frac{\Gamma M_p^2}{4R}. \tag{21}$$

In (21) we can eliminate the value ρ_c using (17), which give the dependence of A on R in the form of the quadratic equation:

$$A^2R^2\left(\frac{\Gamma M_p}{14}-\frac{Rc^2}{4}\right)+AR\left(-\frac{7\Gamma M_p}{36}+\frac{2Rc^2}{3}\right)+\frac{2\Gamma M_p}{15}-\frac{4Rc^2}{9}=0.$$

The analysis of this equation shows that it has the following solution:

$$AR=\frac{\frac{7\Gamma M_p}{36}-\frac{2Rc^2}{3}+\sqrt{\frac{\Gamma M_p Rc^2}{945}-\frac{13\Gamma^2 M_p^2}{45360}}}{\frac{\Gamma M_p}{7}-\frac{Rc^2}{2}}, \qquad (22)$$

on condition that when $0.3<\frac{Rc^2}{\Gamma M_p}<\frac{13}{35}\approx 0.371$, then accordingly $0<AR<1$.

We shall now turn to the magnetic moment of the proton. As in [4], we assume that the magnetic moment of the proton is equal to the magnetic moment, which is formed due to the maximum rapid rotation of the charged substance of the proton. In spherical coordinates, the magnetic moment can be approximately calculated as the sum of the elementary magnetic moments of the separate rings with their radius $r\sin\theta$, which have the magnetic moment due to the current di flowing in them from the rotation of the charge:

$$\begin{aligned} P_m &= \int dP_m = \int \pi r^2 \sin^2\theta\, di = \int \pi r^2 \sin^2\theta \frac{dq}{dt} = \\ &= \int \pi r^2 \sin^2\theta\, \rho_{qc}(1-Ar) r^2 dr \sin\theta\, d\theta \frac{d\varphi}{dt} = \frac{4\pi R^5 \omega_L \rho_{qc}}{15}\left(1-\frac{5AR}{6}\right). \end{aligned} \qquad (23)$$

The angular velocity $\omega_L=\frac{d\varphi}{dt}$ of the maximum rotation of the proton can be found from the condition of limiting rotation, with the equality of the centripetal force and the gravitation force at the equator: $\frac{\Gamma M_p}{R^2}=\omega_L^2 R$. Further

we believe that for the charge density and the substance density the equation $\frac{\rho_{qc}}{\rho_c} = \frac{e}{M_p}$ holds, and we use (17). This gives the following:

$$P_m = \frac{4e\sqrt{\Gamma M_p R}\,(6-5AR)}{30(4-3AR)}. \qquad (24)$$

4 Conclusions

The relation (24) together with (22) allow us to find the radius of the proton $R = 8.73 \cdot 10^{-16}$ m, as well as the value $A = \frac{0.48}{R}$. From (17) we obtain then the central substance density $\rho_c = 9.4 \cdot 10^{17}$ kg/m^3, which exceeds the average density of the proton 1.57 times. The maximum angular velocity of rotation of the proton in view of (23) is equal to $\omega_L = 6.17 \cdot 10^{23}$ rad/s. At the same time, if the spin of the proton in the approximation of the uniform density of substance would be equal to the standard value for the spin of the fermion $L = 0.4 M_p R^2 \omega = \frac{\hbar}{2}$, then the angular velocity of rotation $\omega = 1.03 \cdot 10^{23}$ rad/s would correspond to this spin.

For comparison with the experimental data we shall point to the results of calculations of electron scattering from [14], where the charge radius $R_E = 8.7 \cdot 10^{-16}$ m is obtained taking into account only the scattering on protons, $R_E = 8.71 \cdot 10^{-16}$ m – taking into account the data on the pion scattering, and $R_E = 8.8 \cdot 10^{-16}$ m – taking into account the data on the neutron scattering. In [3] the charge radius $R_E = 8.4184 \cdot 10^{-16}$ m was found in the study of the coupled system of the proton and the negative muon. The study of the scattering cross section of polarized photons by protons [15] gives the charge radius $R_E = 8.75 \cdot 10^{-16}$ m and the magnetic radius $R_M = 8.67 \cdot 10^{-16}$ m. The charge radius $R_E = 8.77 \cdot 10^{-16}$ m and the magnetic radius $R_M = 7.77 \cdot 10^{-16}$ m of the proton are listed on the site of *Particle data group* [16]. In the database CODATA [17] the proton charge radius is equal to $R_E = 8.775 \cdot 10^{-16}$ m.

The value $R = 8.73 \cdot 10^{-16}$ m obtained in the framework of the self-consistent model is close to the experimental values of the radius of the proton, which confirms the possibility of applying the idea of strong gravitation to describe the strong interaction of elementary particles.

References

[1] C. F. Perdrisat, V. Punjabi and M. Vanderhaeghen, Nucleon Electromagnetic Form Factors. Prog. Part. Nucl. Phys. **59** (2) (2007), 694–764.

[2] J. Arrington, C. D. Roberts and J. M. Zanotti, Nucleon electromagnetic form factors. Journal of Physics G **34** (7) (2007), S23.

[3] Randolf Pohl at al, The size of the proton. Nature, **466** (2010), 213–216.

[4] S.G. Fedosin, *Fizika i filosofiia podobiia: ot preonov do metagalaktik*, Style-MG, Perm (1999).

[5] S.G. Fedosin, *Fizicheskie teorii i beskonechnaia vlozhennost' materii*, Perm (2009).

[6] S.G. Fedosin, *Sovremennye problemy fiziki: v poiskakh novykh printsipov*, Editorial URSS, Moskva (2002).

[7] S.G. Fedosin and A.S. Kim, The Moment of Momentum and the Proton Radius. Russian Physics Journal, **45** (2002), 534–538.

[8] A. Salam and C. Sivaram, Strong Gravity Approach to QCD and Confinement. Mod. Phys. Lett. **A8** (4) (1993), 321–326.

[9] C. Sivaram and K.P. Sinha, Strong gravity, black holes, and hadrons. Physical Review D, **16** (6) (1977), 1975–1978.

[10] В.С. Барашенков, *Сечения взаимодействия элементарных частиц*, Наука, Москва (1966).

[11] Infinite Hierarchical Nesting of Matter – en.wikiversity.org.

[12] Riccardo Belvedere, Daniela Pugliese, Jorge A. Rueda, Remo Ruffini, She-Sheng Xue, Neutron star equilibrium configurations within a fully relativistic theory with strong, weak, electromagnetic, and gravitational interactions. Nuclear Physics A, **883** (2012), 1–24.

[13] S.G. Fedosin, Electromagnetic and Gravitational Pictures of the World. Apeiron, **14** (4) (2007), 385–413.

[14] Richard J. Hill and Gil Paz, Model independent extraction of the proton charge radius from electron scattering. Physical Review D, **82** (11) (2010), 113005.

[15] X. Zhan et al, High Precision Measurement of the Proton Elastic Form Factor Ratio $\mu_p G_E / G_M$ at low Q^2. Phys. Lett. **B705** (2011), 59–64.

[16] J. Beringer et al, (Particle Data Group), Review of Particle Physics. Phys. Rev. **D86**, 010001 (2012).

[17] P.J. Mohr, B.N. Taylor and D.B. Newell (2011), The 2010 CODATA Recommended Values of the Fundamental Physical Constants. National Institute of Standards and Technology, Gaithersburg, MD 20899.

HADRONIC JOURNAL 35, 365-371 (2012)

GENERAL RELATIVITY AND OPERA EXPERIMENT

Christian Corda
Institute for Theoretical Physics and
Advanced Mathematics
Einstein-Galilei, Via Santa Gonda 14,
59100 Prato, Italy
cordac.galilei@gmail.com

Received November 8, 2012

Abstract

In his paper "A very simple solution to the OPERA neutrino velocity problem" the author J. Manuel Garcia-Islas claims to have very easily solved and explained within the general theory of relativity that OPERA's neutrinos are not traveling faster than the speed of light and the early time arrival is due to the presence of the Earth's gravitational field. In this letter we easily show that the argument by Garcia-Islas does not work.

Although it looks that data suggesting that neutrinos can travel faster than light probably resulted from a faulty connection in a GPS timing system, it is important to clarify that, in any case, the general relativistic effect discussed by Garcia-Islas cannot explain the original OPERA's data.

PACS numbers: 04.20.-q, 14.60.Lm.

The OPERA collaboration claimed that "the measurement indicates an early arrival time of CNGS muon neutrinos with respect to the one computed assuming the speed of light in vacuum" [1]. Such a claim generated an interesting debate within the Scientific Community. Various authors try

Copyright © 2012 by Hadronic Press, Inc., Palm Harbor, FL 34682–1577, USA

to justify or invalidate the results of OPERA by using theoretical analyses, other authors discuss potential errors in OPERA's experimental methodology, especially concerning the clocks' synchronization, see for example refs. [2, 3, 4, 5, 6, 7]. Now, it looks that data suggesting that neutrinos can travel faster than light probably resulted from a faulty connection in a GPS timing system [13].

In [8] the author claims to have very easily solved and explained within the general theory of relativity that OPERA's neutrinos are not traveling faster than the speed of light and the early time arrival is due to the presence of the Earth's gravitational field. In this letter we easily show that the argument in [8] does not work. In fact, although the original OPERA's data could be wrong, see for example [13], it is important to clarify that, in any case, the general relativistic effect discussed in [8] cannot explain such original OPERA's data.

In [8] the problem is simplified by assuming that on Earth a massive particle is traveling at velocity v in a circular orbit (or just in an arc $\triangle\varphi$) at a fixed radial distance $r = R$. Then, the proper time of travel measured by an observer which is fixed at the same radial distance is calculated [8]. The analysis is performed by using the well known Schwarzschild solution to Einstein's field equation [8]. A first comment is needed. Actually, general relativistic effects, i.e. the presence of the gravitational field, are taken into due account in the process of clocks' synchronization when the GPS receivers are used [9]. This is exactly the case of the OPERA experiment, which worked with two identical systems installed at CERN and LNGS and composed of a GPS receiver for time-transfer applications Septentrio PolaRx2e operating in "common-view" mode and a Cs atomic clock Symmetricom Cs4000 [1]. More, synchronization of GPS does not work in Schwarzschild coordinates. Indeed, it works in the Universal Coordinated Time as maintained by the U.S. Naval Observatory on the rotating geoid, but with synchronization established in an underlying, locally inertial, reference frame [9]. In such a reference frame, by setting $G = c = 1$ with the sign conventions for the line element $(-,+,+,+)$, an approximate solution of Einstein's field equations in isotropic coordinates is used [9]

$$ds^2 = -\left(1 + 2(V - \Phi_0)\right) dt^2 + (1 - 2V)\left(dr^2 + r^2(\sin^2\theta d\varphi^2 + d\theta^2)\right) \qquad (1)$$

where

$$V = -\frac{M}{r}\left[1 - J_2\left(\frac{a_1}{r}\right)^2 P_2 \cos\theta\right], \tag{2}$$

$$\Phi_0 = -\left(\frac{M}{a_1} + \frac{MJ_2}{2a_1} + \frac{1}{2}\omega^2 a_1^2\right). \tag{3}$$

M is the Earth's mass, J_2 is Earth's quadrupole moment coefficient, a_1 is Earth's equatorial radius and ω the Earth's angular velocity.

In any case, we start by showing that the conclusions in [8] are not correct in the framework of the Schwarzschild solution. Then, we will discuss the coordinates (1) too.

Let us review the analysis in [8].

The Schwarzschild line element reads [8, 10] (but see [11] for clarifying historical notes to this notion)

$$ds^2 = -(1 - \frac{2M}{r})dt^2 + \frac{dr^2}{1 - \frac{2M}{r}} + r^2(\sin^2\theta d\varphi^2 + d\theta^2), \tag{4}$$

being M the Earth's mass.

Hence, the world line for a massive particle which travels in a circular orbit $r = R$ at a velocity v in the space-time of eq. (4) is [8]

$$x^\mu(\tau) = \left(\gamma\tau,\ R,\ \frac{\pi}{2},\ \frac{\gamma v\tau}{R}\right), \tag{5}$$

where

$$\gamma = \frac{1}{\sqrt{1 - v^2 - \frac{2M}{R}}} \tag{6}$$

is the general "gamma factor" in presence of a gravitational field and τ is the proper time for the world line (5). The gamma factor (6) is obtained by imposing the 4-velocity to be orthogonal for the world line [8, 10]

$$g_{\mu\nu}\frac{dx^\mu}{d\tau}\frac{dx^\nu}{d\tau} = -1. \tag{7}$$

Eq. (5) gives [8]

$$\frac{d\varphi}{d\tau} = \frac{\gamma v}{R}. \tag{8}$$

An observer which uses Schwarzschild coordinates measures [8]

$$\frac{d\varphi}{dt} = \frac{d\varphi}{d\tau}\frac{d\tau}{dt} = \frac{v}{R}. \tag{9}$$

On the other hand, a stationary observer fixed at the radial distance R measures a proper time related to the Schwarzschild time coordinate by [8, 12]

$$dt' = \sqrt{1 - \frac{2M}{R}}dt. \tag{10}$$

Such a stationary observer also sees a displacement along a circular arc [8]

$$dl = Rd\varphi. \tag{11}$$

Then, one can compute the velocity of the particle in orbital motion as measured by the stationary observer at R like [8]

$$\frac{dl}{dt'} = \frac{R}{\sqrt{1 - \frac{2M}{R}}}\frac{d\varphi}{dt} = \frac{v}{\sqrt{1 - \frac{2M}{R}}}. \tag{12}$$

By integrating this expression one gets the time measured by the stationary observer at R for the particle to travel an arc displacement $\triangle l$ on Earth [8]

$$\triangle t' = \frac{\triangle l}{v}\sqrt{1 - \frac{2M}{R}}. \tag{13}$$

The neutrinos' trajectory can be approximately thought as a circular arc $\triangle l$, which as a numerical value is 731 kilometers [8]. The author of [8] claims that eq. (13) gives the correct answer of the measured time by a stationary observer when these particles travel an angle distance $\triangle l$ because the time given by formula (13) is shorter than the time $\frac{\triangle l}{v}$ the particles will take if they were traveling in flat space-time. Even if the above analysis is correct we easily show that the final conclusion is not correct. In fact, the value of $\frac{2M}{R}$ is of order $6.9 * 10^{-10}$ [4] which gives a correction on $\frac{\triangle l}{v}$ of order $3.4 * 10^{-10}$. The effect originally measured by the OPERA Collaboration was of order 10^{-5} [1]. Therefore the gravitational effect is five orders of magnitude less than the one originally measured by OPERA.

Now, let us make the computation by using the approximate solution (1). Again, we simplify the problem by assuming a circular orbit, i.e. $r = R$,

$\theta = \frac{\pi}{2}$. If one sets such values in the coordinates (1) the particle travels at the equator, i.e. $R = a_1$ [9]. The world line for a massive particle which travels in a circular orbit $r = R$ at a velocity v' in the spacetime of eq. (1) is

$$x^{\mu}(\tau) = \left(\gamma'\tau,\ R,\ \frac{\pi}{2},\ \frac{\gamma' v'\tau}{R}\right), \tag{14}$$

where the condition (7) now sets the general gamma factor γ' as

$$\gamma' = \frac{1}{\sqrt{1 + \frac{MJ_2}{R} + \omega^2 R^2 - \frac{v'^2}{R^2}\left(1 + \frac{2M}{R}\right)}}. \tag{15}$$

Eq. (14) gives

$$\frac{d\varphi}{d\tau} = \frac{\gamma' v'}{R}. \tag{16}$$

An observer which uses the coordinates (1) measures

$$\frac{d\varphi}{dt} = \frac{d\varphi}{d\tau}\frac{d\tau}{dt} = \frac{v'}{R}. \tag{17}$$

Now, a stationary observer fixed at the radial distance R measures a proper time related to the time coordinate by [8, 12]

$$dt' = \sqrt{1 + \frac{MJ_2}{R} + \omega^2 R^2}\, dt. \tag{18}$$

Such a stationary observer also sees a displacement along a circular arc

$$dl = \sqrt{1 + \frac{2M}{R}}\, R d\varphi. \tag{19}$$

Hence, we can compute the velocity of the particle in orbital motion as measured by the stationary observer at R like

$$\frac{dl}{dt'} = \frac{\sqrt{1 + \frac{2M}{R}}\, R}{\sqrt{1 + \frac{MJ_2}{R} + \omega^2 R^2}}\frac{d\varphi}{dt} = \frac{\sqrt{1 + \frac{2M}{R}}\, v'}{\sqrt{1 + \frac{MJ_2}{R} + \omega^2 R^2}}. \tag{20}$$

By integrating this expression one gets the time measured by the stationary observer at R for the particle to travel an arc displacement $\triangle l$ on Earth in the coordinates (1)

$$\triangle t' = \frac{\triangle l}{v'} \frac{\sqrt{1 + \frac{MJ_2}{R} + \omega^2 R^2}}{\sqrt{1 + \frac{2M}{R}}}. \tag{21}$$

$\frac{MJ_2}{R}$ is order 10^{-13} while $\omega^2 R^2$ is order 10^{-12} [9]. These values, together with the value of $\frac{2M}{R}$, give a correction on $\triangle l$ again of order 10^{-10} which cannot explain the original OPERA's results as the effect originally measured by the OPERA Collaboration was of order 10^{-5} [1].

In summary, in this letter we have shown that the claims of the author of [8] to have very easily solved and explained within the general theory of relativity that OPERA's neutrinos are not traveling faster than the speed of light and the early time arrival is due to the presence of the Earth's gravitational field are not correct. In fact, the presence of the gravitational field generates a variation of the proper time of order 10^{-10} in both of the Schwarzschild solution of Einstein's field equations and the approximate solution of Einstein's field equations where GPS receivers are usually synchronized, while the effect originally measured by the OPERA Collaboration is of order 10^{-5} [1]. Thus, although it looks that data suggesting that neutrinos can travel faster than light probably resulted from a faulty connection in a GPS timing system [13], it is important to clarify that, in any case, the general relativistic effect discussed by Garcia-Islas in [8], cannot explain the original OPERA's data [1].

Acknowledgements The R. M. Santilli Foundation has to be thanked for partially supporting this letter (Research Grant Number RMS-TH-5735A2310). It is a pleasure to thank Ruggero M. Santilli, Erasmo Recami, Ammar Sakaji, Ignazio Licata, Herman Mosquera Cuesta, Gaetano Lambiase and Lawrence Crowell for various interesting comments and discussions on the issue of the neutrino faster than the speed of light.

References

[1] The OPERA Collaboration, arXiv:1109.4897.

[2] G. Amelino-Camelia et al., arXiv:1109.5172.

[3] J. P. Mbelek, arXiv:1110.4095.

[4] O. Besida, arXiv:1110.2909.

[5] C.R. Contaldi, arXiV:1109.6160.

[6] J. W. Moffat, arXiv:1110.1330.

[7] A. G. Cohen and S. L. Glashow, arXiv:1109.6562.

[8] J. Manuel Garcia-Islas, arXiv:1110.5866.

[9] N. Ashby, Liv. Rev. Rel. 2003, 1.

[10] C. W. Misner , K. S. Thorne, J. A. Wheeler, *"Gravitation"*, Feeman and Company (1973).

[11] C. Corda, Electr. J. Theor. Phys. 8, 25, 65-82 (2011).

[12] L. Landau and E. Lifsits, *Classical Theory of Fields* (3rd ed.), London: Pergamon (1971).

[13] E. Cartlidge, Science 335 (6072): 1027 (2012).

RESPONSE TO CROTHERS' CATASTROPHE

Jason J. Sharples
Applied and Industrial Mathematics Research Group
School of Physical, Environmental and Mathematical Sciences
University of New South Wales
Canberra, 2600 Australia

Received November 8, 2012

Abstract

In this article I respond to Stephen J. Crothers' paper "The black hole catastrophe: a short reply to J.J. Sharples" (*Hadronic Journal*, 34, 2011), which is a reply to my original rebuttal to Crothers' relativistic claims. This paper again highlights some of Crothers' misunderstandings and mathematical errors.

Keywords: Schwarzschild solution; coordinate transformation.
PACS: 02.40.-k; 04.20.Cv; 04.20.Jb; 04.20.Dw

Copyright © 2012 by Hadronic Press, Inc., Palm Harbor, FL 34682–1577, USA

1 Introduction

The Schwarzschild solution to the Einstein field equations is an important and much celebrated result in the general theory of relativity. Historically, it was obtained as the first analytical solution of the field equations. Specifically, Schwarzschild determined a spherically symmetric solution to the field equations arising from a point mass. Interestingly, the form of the solution delivered by Schwarzschild was the subject of much subsequent inquiry, and continues to be the source of some debate (for example, see [1]). Stephen J. Crothers has been one of the most ardent participants in this debate since circa 2005, and has written a number of articles concerning the interpretation of the Schwarzwschild solution.

Unfortunately, however, Mr Crothers' papers contain a number of elementary mathematical and conceptual errors. After becoming aware that Mr Crothers' works were being discussed on a number of internet fora, and were being cited as theoretical evidence for the non-existence of black holes, I published a paper [2] in the journal *Progress in Physics*, rebutting Mr Crothers' relativistic claims. In reply, Mr Crothers published a lengthy article [3] – the present paper is my response to Mr Crothers' article.

I aim to keep my response very short – far shorter than Mr Crothers' short[1] reply. In fact, in my opinion, the only response that is really required on my behalf is to simply note that Mr Crothers does not understand the concept of a coordinate function in differential geometry. This much is clear from his writings, and many mathematically qualified scientists (myself included) have tried to convince him of this point to no avail. To illustrate this point it is most convenient to actually reply to another paper of Mr Crothers', namely [4]. In fact, I already alluded to the problems with [4] in the Postscript of [2] – further details will now be provided.

2 Crothers' 'counter-examples' to the Kruskal-Szekeres extension

Mr Crothers [4] considers the following pair of line-elements[2]

$$ds^2 = \left(1-\frac{2m}{2m-r}\right)dt^2 - \left(1-\frac{2m}{2m-r}\right)^{-1} dr^2 - (r-2m)^2\, d\Omega^2, \quad (1)$$

$$ds^2 = \left(1-\frac{2m}{4m-r}\right)dt^2 - \left(1-\frac{2m}{4m-r}\right)^{-1} dr^2 - (r-4m)^2\, d\Omega^2. \quad (2)$$

[1] Curiously, Mr Crothers' "short" reply was far longer than my original rebuttal...

[2] Note that for brevity I will use $d\Omega^2$ as a shorthand for the spherical line-element $d\theta^2 + \sin^2\theta\, d\varphi^2$ throughout the paper.

In defining these line-elements he remarks that they satisfy all the requirements of a static, spherically symmetric solution to the vacuum field equations, and so are just as good as the Schwarzschild metric. This remark is perfectly correct, but due to his lack of understanding of coordinate functions Mr Crothers fails to realise that the line-elements (1) and (2) correspond identically to restrictions of the Schwarzschild metric,

$$ds^2 = \left(1 - \frac{2m}{r}\right) dt^2 - \left(1 - \frac{2m}{r}\right)^{-1} dr^2 - r^2\, d\Omega^2. \tag{3}$$

Mr Crothers [4] calculates that the line-element (1) has a coordinate singularity at $r = 0$ and a point singularity at $r = 2m$. Similarly for the line-element (2), a coordinate singularity is found at $r = 2m$ and a point singularity is found at $r = 4m$. In light of these calculations he concludes that the analytical considerations employed by the "astrophysical scientists" in asserting the existence of a black hole, are invalid.

I will treat both of the cases (1) and (2) simultaneously by considering the following line-element:

$$ds^2 = \left(1 - \frac{2m}{M_0 - r}\right) dt^2 - \left(1 - \frac{2m}{M_0 - r}\right)^{-1} dr^2 - (r - M_0)^2\, d\Omega^2, \tag{4}$$

where M_0 is an arbitrary positive constant. Note that setting $M_0 = 2m$ and $M_0 = 4m$ recovers the line-elements (1) and (2), respectively. Let us also assume, as Mr Crothers does, that the coordinate r in (4) varies over the set $[0, \infty)$.

As noted in [2], or indeed in any textbook that deals with differential geometry, changing coordinates does not alter the metric represented by the line-element, though it will generally alter the appearance of the line-element. Some differences may also arise due to the inability of the new coordinates to cover the same regions covered by the old coordinates, but again these differences do not alter the underlying metric. On regions of the spacetime covered by both coordinate systems, the respective line-elements must represent the same metric.

Thus introducing the change of coordinates

$$\rho = M_0 - r, \tag{5}$$

the line-element (4) can be written in terms of the coordinate ρ as

$$ds^2 = \left(1 - \frac{2m}{\rho}\right) dt^2 - \left(1 - \frac{2m}{\rho}\right)^{-1} d\rho^2 - \rho^2\, d\Omega^2, \tag{6}$$

which is just the standard expression for the Schwarzschild line-element.

It is important to note that since $0 \leq r < \infty$, it follows that $-\infty < \rho \leq M_0$. However, to avoid degeneracy of the metric we require that $\rho \geq 0$. Thus $0 \leq \rho \leq M_0$ and so the line-element (6) is seen to represent a subset of the Schwarzschild spacetime. In particular, it represents the subset whose spatial section is foliated by 2-spheres of area less than $4\pi M_0^2$.

Equation (4) is simply the standard Schwarzschild line-element written in terms of an "inverted" radial coordinate. For example when $M_0 = 2m$, the inversion of the radial coordinate defined by $\rho = 2m - r$, takes the point singularity at $\rho = 0$ to a point singularity at $r = 2m$. Similarly, the coordinate singularity at $\rho = 2m$ is transformed to a coordinate singularity at $r = 0$. If $a \leq 2m$ then the subsets of Schwarzschild spacetime defined by $r = a$ and $\rho = 2m - a$ are one and the same. Similarly setting $M_0 = 4m$ it is no surprise that the point singularity is at $r = 4m$ ($\rho = 0$) and the coordinate singularity is at $r = 2m$ ($\rho = 2m$).

3 Some of Crothers' other mistakes

The above discussion highlights Mr Crothers' misunderstanding of coordinate functions in differential geometry. To further illustrate Mr Crother's shortcomings, we now address a few more telling examples of mistakes from his reply [3] (or indeed in any of his papers):

- In [3], Mr Crothers continually emphasizes his point that "a geometry is completely determined by the *form* of its line-element". This is false and betrays his poor understanding of global differential geometry. A line-element is a *coordinate-dependent* representation of a metric and as such is entirely irrelevant to the global structure of a manifold. Indeed, paraphrasing Weyl, the introduction of a coordinate system to geometry is an act of violence! The *form* of a line-element representing a geometry is really only restricted by the creativity of the cartographer.

- On page 210 of [3], Mr Crothers provides a baffling "proof" of the inextendibility of Euclidean 3-space. The "proof" starts out following Szekeres [5] by asking the reader to consider the line-element for Euclidean 3-space expressed in the standard spherical coordinates:

$$ds^2 = dr^2 + r^2 d\Omega^2, \quad r \in [0, \infty). \tag{7}$$

Again following [5], Mr Crothers then makes the substitution $r = \bar{r} - 2m$, where m is a positive constant, so that the line-element is written as

$$ds^2 = d\bar{r}^2 + (\bar{r} - 2m)^2 d\Omega^2, \tag{8}$$

and where, owing to the definition of $\bar{r}$, we must now have $\bar{r} \in [2m, \infty)$.

Mr Crothers then quotes Szekeres' point about the formation of an apparent singularity on the sphere $\bar{r} = 2m$ before showing that the "*claim is easily proven false*" by performing an essentially redundant calculation. The calculation amounts to rewriting the line-element back in the original radial coordinate r. For some reason Mr Crothers insists on writing r as $\rho = |\bar{r} - 2m|$; but since $\bar{r} \geq 2m$, by definition, we must have $|\bar{r} - 2m| = \bar{r} - 2m = r$. Mr Crothers then claims that this calculation shows that the metric is inextendable. But of course no calculation was necessary to show this! The line-element (7) was inextendible from the outset since it covered all of Euclidean 3-space – at no point did Szekeres, or indeed anyone else, claim that Euclidean 3-space had a "*hole in its centre*"...!?!?

- In the 'Epilogue' of [3], Mr Crothers states that his arguments, which purport to show that a black hole cannot form in Schwarzschild space, have been reaffirmed by D. Rabounski [6]. However, Rabounski states repeatedly throughout his short paper that Mr Crothers' solution doesn't eliminate the classical "black hole solution". Thus it would seem that Mr Crothers has been a bit overzealous in his reading of [6].

4 Final remarks

The claim that Schwarzschild's original solution of the field equations prohibits the existence of black holes is patently false. The belief that it does prohibit the existence of black holes stems from a lack of understanding of coordinate functions in differential geometry. The original Schwarzschild solution is completely equivalent to a subset (the exterior) of the standard 'Schwarzschild solution' as espoused by Hilbert and others.

Of course we note that just because the notion of a black hole, as embodied in the Schwarzschild solution, is mathematically consistent, it does not provide direct confirmation that black holes exist as a physical entity

– though modern observational astronomy does tend to support the physical reality of black holes, at galactic centres for example [7], though some debate is still underway on this issue ([8],[9],[10]).

Acknowledgement

I am grateful to the *Hadronic Journal* Editor in Chief, Dr. Christian Corda, for the invitation to formally respond to Mr Crothers' reply.

References

[1] C. Corda, A clarification on the debate on "the original Schwarzschild solution". Electronic Journal of Theoretical Physics, 8 (2011), 65-82.
[2] J.J. Sharples, Coordinate transformations and metric extension: a rebuttal to the relativistic claims of Stephen J. Crothers. Progress in Physics, 1 (2010), L1-L6.
[3] S.J. Crothers, The black hole catastrophe: a short reply to J.J. Sharples. Hadronic Journal, 34 (2011), 197-224.
[4] S.J. Crothers, The Kruskal-Szekeres "extension": Counter-examples. Progress in Physics, 1 (2010), 3-7.
[5] G. Szekeres, On the singularities of a Riemannian manifold. General Relativity and Gravitation, 34 (2002), 2001-2016.
[6] D. Rabounski, On the current situation concerning the black hole problem. Progress in Physics, 1 (2008), 101-103.
[7] S. Gillessen, F. Eisenhauer, S. Trippe, T. Alexander, R. Genzel, F. Martins and T. Ott, Monitoring stellar orbits around the massive black hole in the galactic center.The Astrophysical Journal, 692 (2009), 1075-1109.
[8] S. Robertson and D. Leiter, On intrinsic magnetic moments in black hole candidates. The Astrophysical Journal, 596 (2003), L203.
[9] C. Barceló, S. Liberati, S. Sonego and M. Visser, Fate of gravitational collapse in semiclassical gravity. Physical Review D, 77 (2008), 044032.
[10] A. Mitra, Comments on "The Euclidean gravitational action as black hole entropy, singularities, and space-time voids" [J. Math. Phys. 49, 042501 (2008)]. Journal of Mathematical Physics, 50 (2009), 042502.

HADRONIC JOURNAL 35, 379-389 (2012)

SOLAR REDSHIFT CALCULATION BY THE RAYLEIGH SCATTERING MECHANISM

Ivan Gandzha
Department of Theoretical Physics
Institute of Physics, National Academy
of Sciences of Ukraine
03028 Kyiv, Prospect Nauky 46, Ukraine
gandzha@iop.kiev.ua

Received November 5, 2012

Abstract

This note gives a descriptive validation to a classical model where the redness of the Sun at sunset is attributed to the Rayleigh scattering mechanism ($\sim \lambda^{-4}$, λ being the wavelength). The motivation for this study has no intention in dismissal of other existing approaches to the problem, such as the recent isoredshift explanation by Santilli et al. [1].

Keywords: Solar redshift; Rayleigh scattering; Solar radiation intensity; Isoredshift.

Copyright © 2012 by Hadronic Press, Inc., Palm Harbor, FL 34682–1577, USA

1 Introduction

The colors of the Sun and the sky have been a fascinating subject for numerous physical studies. The blue color of the sky is generally attributed to the scattering of blue rays in the atmosphere with the domination of the yellow and red color in the spectrum of the Sun when recorded on the Earth's surface. The scattering mechanism was first addressed by Lord Rayleigh in 1871 [2], who considered the elastic scattering of light by particles much smaller than the wavelength of light. Later, in 1908, Gustav Mie formulated a more general approach based on the scattering of electromagnetic radiation by spherical particles of various sizes [3].

The solar radiation has a wide continuous spectrum reproduced in Fig. 1. The energy generated in the core of the Sun propagates to the outer solar layers and exhibits a sequence of absorption-reemission processes. The radiation in the visible optical range is mainly generated in the outer layer of the Sun, which is called photosphere. In the upper photosphere and lower chromosphere, radiation is partially absorbed by the atoms located therein, and this leads to the formation of peculiar absorption lines in the spectrum, each line corresponding to a specific atom (H, He, Ca, Mg, Fe, etc.) and wavelength. These lines are called the Fraunhofer lines, their list can be found elsewhere. The corresponding spectrum of the Sun is represented by curve 2 in Fig. 1. The color of the Sun as seen from the space outside the Earth's atmosphere is white because of the superposition of various wavelengths with different colors.

After entering the Earth's atmosphere, the solar spectrum attains a distorted pattern due to molecular absorption and scattering on aerosols, water molecules, CO_2, and ozone. The corresponding spectrum at the Earth's surface is represented by curve 3 in Fig. 1. This spectrum is given for the Sun located at the zenith, when the solar zenith angle Z is equal to zero, which corresponds to the unit air mass. The color of the Sun at the zenith appears yellow because of the partial scattering of the blue light in the atmosphere (see Section 2).

When the Sun passes from the zenith to the horizon, the solar radiation spectrum shifts to the red side, as confirmed by many independent measurements, see, e.g. papers [5, 6]. As a result, the Sun attains the orange and red color. Recently Santilli et al. [1] made very meticulous records of

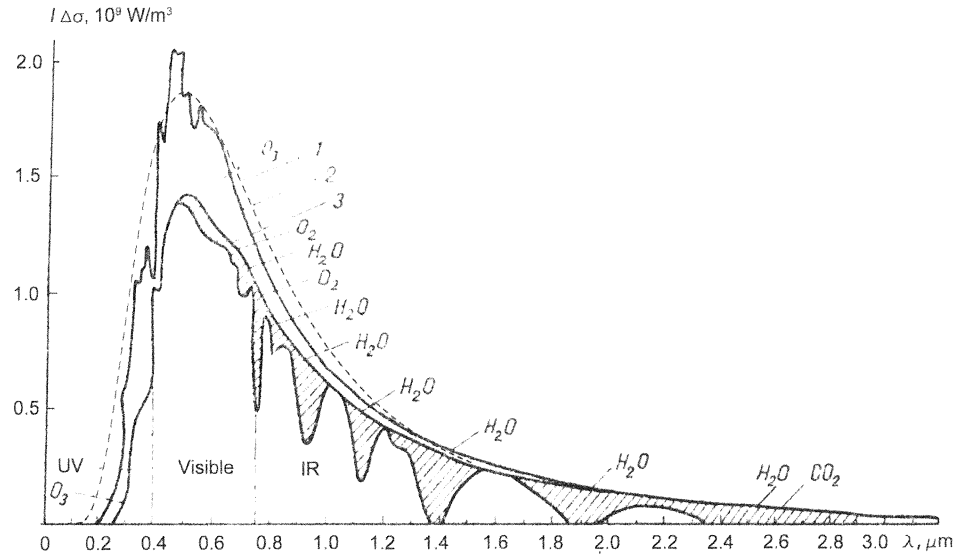

Figure 1: Energy distribution in the solar spectrum and absorbing components of the Earth's atmosphere (adapted from Fig. 1.3 of monograph [4] and normalized to the source solid angle $\Delta\sigma = 6.8 \times 10^{-5}$ srad): (1) blackbody spectrum at 5777 K, (2) the Sun at the boundary of the Earth's atmosphere, (3) the Sun at sea level at unit mass ($Z = 0$) of the pure atmosphere at average humidity.

the spectrum of the Sun in direct light by proceeding from small zenith angles, when the Sun is at the zenith, to the maximum possible zenith angles (close to 90°), when the Sun is at the horizon. They recorded a substantial redshift of the solar spectrum (measured up to 200 nm), which manifests itself in the reddening of the Sun at sunset.

Santilli et al. [1] used their experimental data as the experimental validation of the isorelativity theory introduced earlier by Prof. Santilli (see a detailed review in [7]). In particular, the redshift of the solar spectrum was attributed to the isoredshift effect (IRS), which occurs without any necessary relative motion between the source, the medium and the observer,

according to the general isolaw

$$\lambda_{IRS} = \frac{\lambda_0}{1 - \frac{v}{c}\frac{n_4}{n_s}},$$

where λ_0 is the non-shifted wavelength, v is the tangential speed of the observer due to the rotation of the Earth, c is the speed of light in vacuum, n_4 is the local index of refraction of light in air, and n_s is the space characteristic quantity of the atmosphere in the selected direction s, which was estimated by the fit to the experimental data for $\Delta\lambda = \lambda_{IRS} - \lambda_0 = 200$ nm [1]. The IRS origin of the redness of the Sun at sunset is based upon the preposition about the loss of energy by light to a cold medium.

By giving all the credit to the measurements done by Prof. Santilli and his associates as well as to Santilli's isorelativity theory, we would like to briefly outline an alternative (classical) explanation to the origin of the redness of the Sun at sunset based on the Rayleigh scattering mechanism. This explanation should by no means be regarded as the dismissal of Prof. Santilli's paper [1]. On the contrary, it can serve as a supplement to that paper because the IRS mechanism does not describe the intensity drop of the redshifted solar light.

2 Solar radiation intensity and Rayleigh scattering

The solar radiation profile can be roughly approximated by the black-body radiation spectrum described by the celebrated Planck law (originally proposed in 1900)

$$I_0(\lambda) = \frac{2\,h\,c^2}{\lambda^5}\frac{1}{\exp\left(hc/\lambda kT\right) - 1} \quad [\mathrm{W/(m^3\,srad)}]. \tag{1}$$

Here $I_0(\lambda)\mathrm{d}\lambda$ is the radiation power per unit area per unit solid angle in the wavelength range from λ to $\lambda + \mathrm{d}\lambda$, h is the Planck constant, c is the speed of light, k is the Boltzmann Constant, T is the absolute temperature of the black body. The temperature of the solar photosphere is estimated at $T = 5777$ K [8]. The solar radiation power coming to the Earth is usually normalized to the solid angle of the solar disk, $\Delta\sigma = 6.8 \times 10^{-5}$ srad [9].

The integral intensity of the solar radiation at the boundary of the Earth's atmosphere is estimated as

$$I_\sigma = \Delta\sigma \int_0^\infty I_0(\lambda)\mathrm{d}\lambda = 1637 \text{ W/m}^2.$$

While passing through the atmosphere, the solar light is partially scattered by the molecules that constitute the atmosphere and bigger particles (aerosols, etc.). Among different scattering mechanisms, the Rayleigh molecular scattering has the largest effect on the solar light traveling through the atmosphere. More specific effects are attributed to the Mie scattering on larger particles and molecular absorption. Here we restrict our consideration to the Rayleigh scattering only. Other scatterings are well described in [10].

The intensity of light traveled through the atmosphere is described by the Beer-Lambert-Bouguer law

$$I(\lambda) = I_0(\lambda)\exp\big(-\tau(\lambda)\, m(Z)\big), \tag{2}$$

where the quantity $\tau(\lambda)$ is called the characteristic optical depth of the atmosphere, $m(Z)$ is the optical path in air measured in relative air masses and proportional to the path traveled by light in the atmosphere, and Z is the solar zenith angle (0 when the Sun is at the zenith and 90° when the Sun is at the horizon). In the first approximation the optical path is calculated as

$$m(Z) = \frac{1}{\cos Z}.$$

At high Z a more accurate expression should be used, which still assumes the spherical form of the Earth but gives a reasonable approximation to the optical path:

$$m(Z) = \sqrt{(r\cos Z)^2 + 2r + 1} - r\cos Z, \quad r = \frac{R_{\text{Earth}}}{h_{\text{atmosphere}}} \approx 708, \tag{3}$$

R_{Earth} being the Earth's radius, $h_{\text{atmosphere}}$ being the atmosphere height [11]. At the horizon $m(Z = 90°) = 37.6$, i.e. the optical path of the light coming

from the Sun at the horizon is 37.6 times longer than the optical path of the light coming from the Sun at the zenith.

The Rayleigh optical depth is defined as

$$\tau(\lambda) = \frac{8\pi^3 (n^2-1)^2 N_c}{3\lambda^4 N_s^2} \left(\frac{6+3\gamma}{6-7\gamma}\right) \frac{p}{p_0} \frac{T_0}{T},$$

where n is the refractive index of air, γ is the depolarization factor, N_c is the columnar number density ($= 2.154 \times 10^{29}$ m^{-2} for standard conditions), N_s is the molecular number density ($= 2.547 \times 10^{25}$ m^{-3} for standard conditions), p is pressure (equal to atmospheric pressure p_0 for standard conditions), T is temperature ($= T_0 = 288.15$ K for standard conditions). For standard conditions this law is well approximated by the numerical fit [12]

$$\tau(\lambda) = \frac{0.008569}{\lambda^4}, \tag{4}$$

where λ is expressed in μm. This λ^{-4} law means that shorter waves are more readily scattered than longer waves, i.e. blue light is scattered more than red light. This fact explains the blue color of the sky and red color of the Sun at sunset. Indeed, the direct light coming from the Sun at sunset lacks the wavelengths corresponding to the blue color (their intensity becomes very small) with the red light prevailing.

Figure 2 presents results of calculation of the solar spectrum by formulas (1)–(4). The black curve is the solar radiation curve outside the atmosphere, the dark-yellow curve is the solar radiation curve at the Earth's surface on the equator when the Sun is at zenith ($Z = 0$), orange curve is the solar radiation curve when the Sun is approaching the horizon ($Z = 87°$). The red curve is the solar radiation curve at sunset ($Z = 89°$).

The maximum position on the dark-yellow curve is

$$\lambda = 546 \text{ nm}, \quad I\Delta\sigma = 1.6 \times 10^9 \text{ W/m}^3.$$

The maximum position on the red curve is

$$\lambda = 840 \text{ nm}, \quad I\Delta\sigma = 6.6 \times 10^8 \text{ W/m}^3.$$

Thus, the Rayleigh scattering mechanism well predicts a solar radiation redshift of about 300 nm and an intensity drop at maximum of about 2.5

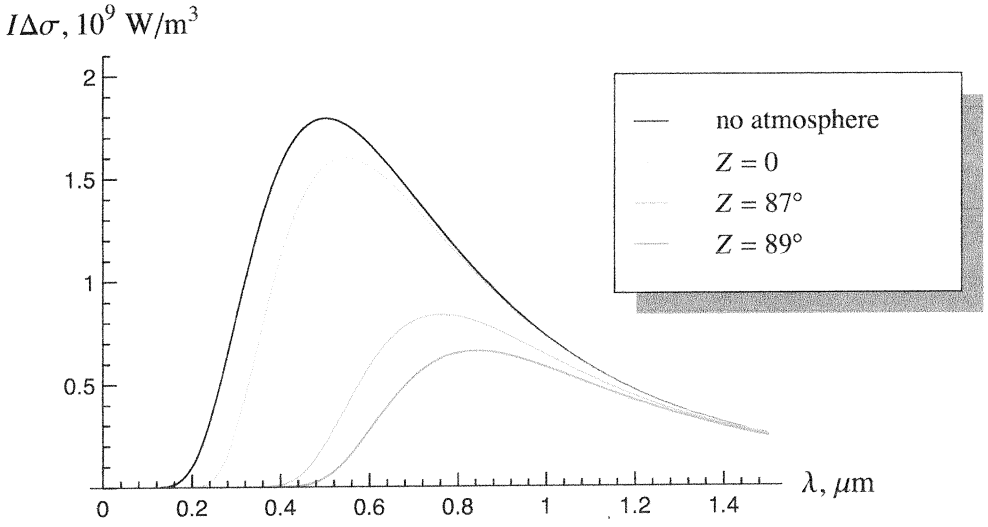

Figure 2: Solar radiation intensity (black-body approximation) at various zenith angles calculated by the Rayleigh scattering mechanism: $Z = 0$ (zenith), $Z = 87°$ (approaching the horizon), and $Z = 89°$ (near horizon).

times between the Sun's positions at the zenith and sunset. These data are in good agreement with the recent measurements performed by Santilli et al. [1], see Fig. 7 thereon.

Note that this note gives only illustrative calculations of the solar radiation spectra and Rayleigh scattering. More accurate models and corrections for various atmospheric effects are described elsewhere, e.g. refer to monograph [10].

3 Conclusion

In this note we proved that the Rayleigh scattering mechanism provides an unambiguous phenomenological explanation to the redshift nature of the solar light while the Sun passes from the zenith to horizon. The scattering mechanism

1) Does give the correct wavelength redshift value, which is in full agreement with the experiment,

2) Does give the correct radiation intensity drop, which is in full agreement with the experiment,

3) Does not require introduction of any fitting parameters.

Acknowledgement

The author would like to thank Prof. Ruggero Maria Santilli for his motivation in writing this note and to Dr. René Verreault for his constructive comments.

References

[1] R.M. Santilli, G. West and G. Amato, Experimental confirmation of the IsoRedShift at sunset and sunrise, with consequential absence of the universe expansion and related conjectures. Journal of Computational Methods in Sciences and Engineering, 12 (2012), 141–168.

[2] John Strutt (Lord Rayleigh), On the light from the sky, its polarization and colour. Philosophical Magazine, Series 4, 41 (1871), 107–120, 274–279; John Strutt, On the scattering of light by small particles. Philosophical Magazine, Series 4, 41 (1871), 447–454.

[3] M.I. Mishchenko and L.D. Travis, Gustav Mie and the evolving discipline of electromagnetic scattering by particles. Bulletin American Meteorological Society, Dec. 2008, 1853–1861.

[4] *Variations in Global Characteristics of the Sun* [in Russian], Ed. E.A. Gurtovenko, Naukova Dumka, Kiev, 1992.

[5] D.L. King, J.A. Kratochvil and W.E. Boyson, Measuring solar spectral and angle-of-incidence effects on photovoltaic modules and solar irradiance sensors. Sandia National Laboratories Report, September 1997.

[6] C. Cornado and A. Andreotti, Solar spectral irradiance measurements relevant to photovoltaic applications. Proceedings of the Third International Conference on Applied Energy, Perugia, Italy, 16–18 May 2011.

[7] I. Gandzha and J. Kadeisvili, *New Sciences for a New Era: Mathematical, Physical and Chemical Discoveries of Ruggero Maria Santilli.*

Sankata Printing Press, Nepal, 2011,
http://www.santilli-foundation.org/docs/RMS.pdf.

[8] See webpage http://solarsystem.nasa.gov/planets/profile.cfm?Display =Facts&Object=Sun.

[9] M.M. Franco, S.D. Slobin and C.T. Stelzried, 20.7 and 31.4-GHz solar disk temperature measurements. TDA Progress Report, 42–64 (1981), 140–159.

[10] C. Gueymard and H. Kambezidis, *Solar Spectral Radiation*: Chapter 5 in *Solar Radiation and Daylight Models*, Ed. T. Muneer, Elsevier, 2004.

[11] E. Schoenberg, *Theoretische Photometrie*, g) Über die Extinktion des Lichtes in der Erdatmosphäre: In *Handbuch der Astrophysik*. Band II, erste Hälfte, Springer, Berlin, 1929.

[12] P.M. Teillet, Rayleigh optical depth comparisons from various sources. Applied Optics, 29 (1990), 1897–1900.

COMMENTS ON I. GANDZHA'S PAPER: "SOLAR REDSHIFT CALCULATION BY THE RAYLEIGH SCATTERING MECHANISM"

Richard Cox
International Committee on Scientific Ethics and Accountability
cox6797@gmail.com

Received December 5, 2012

Abstract

In the recent paper [14], the Ukrainian physicist I. Gandzha has expressed the view that the Rayleigh scattering model on light *intensity* provides the basic representation of Santilli's IsoRedShift origin of the redshift of*frequencies* of direct Sun at Sunset [7-12]. In this paper we point out that such a view is unsubstantiated on various counts, such as: scattering cannot occur for light propagating along a straight line, thus preventing the use of any scattering model on the behavior of frequencies of direct Sunlight; the data on Santilli's IsoRedShift cannot be used to fit Rayleigh scattering since their accuracy is for frequencies, rather than on intensity; Santilli's IsoRedShift is centered in the physical origin of the redness of the Sun at Sunset as being due to loss of energy by light to air, while Rayleigh scattering provides no interpretation of said redness; and other reasons. However, it is pointed out that, following a due reformulation, Rayleigh scattering [15] should be applicable to the part of direct Sunlight lost to scattering, since that is the origin of the colors of our atmosphere. Thereafter, following experimental confirmations on intensities independently from Santilli's measurements of frequency shifts, Rayleigh or other scattering models on intensities are expected to be complementary to Santilli's IsoRedShift in the frequencies in the same way as Doppler's frequency shift and intensity (luminosity) models of far away galaxies are complementary to each other without conflict.

Key words: solar redness, Rayleigh scattering, Santilli IsoRedShift

PACS 42.68.-w, 98.62.Py, 96.10.+i,

Copyright © 2012 by Hadronic Press, Inc., Palm Harbor, FL 34682–1577, USA

The Italian-American physicist R. M. Santilli has dedicated decades of mathematical, theoretical and experimental studies on the origin of the redness of Sunlight at the horizon by:

1) Identifying the appropriate mathematics for the correct geometric representation of the inhomogeneity and anisotropy of our atmosphere [1-3];

2) Showing that said correct geometric representation predicts Sunlight to lose energy to our atmosphere without any relative motion between the sun and the observer, an effect today called *Santilli IsoRedShift* (IRS) [3-6]; and

3) Conducting systematic experimental confirmations, firstly, on monochromatic laser light propagating within a pipe at pressure, and then via direct measurements of the frequency of Sunlight in the transition from the Zenith to the horizon [7-10].

The result of this research is that , *in the transition from the Zenith to the horizon (both for Sunset and Sunrise), the entire spectrum of Sunlight experiences an IRS of about* 100 nm. In particular, blue light completely disappears at the horizon and it is shifted to the red by about 100 nm, while red light is shifted also of about 100 nm toward the infrared according to lines that did not exist for the Sun at the Zenith.

The above result have received independent confirmations in Ref./ [11] for the IRS of monochromatic laser light, and in Ref. [12] for the IRS of the entire spectrum of sunlight (see also Ref. [13]). In particular, the numerical value of the frequency shift for monochromatic laser light in the pipe, when prorated to the trajectory of Sunlight in Earth's atmosphere, yields precisely about 100 nm as needed for Sunset and Sunrise . Consequently, Santilli's measurements of IRS for ,monochromatic laser light constitute, *per se,* an independent confirmation of the IRS of all frequencies of Sunlight at the horizon.

Subsequent to the appearance of this rather vast research, the Ukrainian physicist I. Gandzha released paper [14] according to which the redness of the Sun at Sunset is due to the Rayleigh scattering mechanism [15] essentially expressible via the following classical phenomenological approximation

$$I\,(\lambda) = I_0(\lambda)\exp(-\tau(\lambda)\,m(Z)) \;\approx N\frac{1}{\lambda^4}, \qquad (1)$$

where: the quantity $\tau(\lambda)$ is called the characteristic optical depth of the

atmosphere; $m(Z)$ is the optical path in air measured in relative air masses and proportional to the path traveled by light in the atmosphere; Z is the solar zenith angle (0 when the Sun is at the zenith and 90° when the Sun is at the horizon)' and N is approximately a constant.

While confirming the historical and physical value of Rayleigh scattering, this paper is intended to express the following comments on Gandzha's [14] interpretation of Santilli's IRS [1-12]:

A. On historical ground, Rayleigh [15] conceived and developed his scattering model for the colors of the *atmosphere* and *not* for the color of direct Sunlight, because he knew that the colors of our atmosphere are indeed due to scattering of light (in the absence of scattering, our sky would be black day and night), and that scattering cannot occur along a straight line by its very conception and technical realization. It should be noted in this respect the intense redness of the atmosphere at Sunset that fully confirms its scattering origin in support of Rayleigh and other models. Moreover, the redness of the atmosphere at Sunset is bigger than the redness of direct Sunlight also at Sunset, g thus being evidence of the occurrence in our atmosphere of inelastic scattering causing indeed a redshift, but again, solely for the "scattering" of light defined according to the Webster Dictionary as the disorderly dispersal of light in all directions and positively not for Sunlight propagating along a straight line.

B. In the propagation of Sunlight in our atmosphere, part of Sunlight is indeed lost due to scattering, but the remaining part does reach us. Since the main mechanist of Eq. (1) is scattering, when dealing with direct Sunlight, Rayleigh model should be applied to the intensity of Sunlight lost to scattering and cannot be consistently applied to the remaining part of direct Sunlight reaching us, again, because of the absence of scattering in the latter case.

C. According to its original conception [15], Rayleigh scattering is solely a *phenomenological* description of the intensity of light with no hint whatsoever for the physical origin of its variation depending on the position of the Sun, while Santilli's IRS is primarily intended to provide the physical origin of the redness of the Sun at Sunset, namely, the loss of energy by all frequencies of light to air.

D. Rayleigh scattering provides a phenomenological representation of the *intensity* of light, while Santilli's IRS deals with *frequencies* as clearly illus-

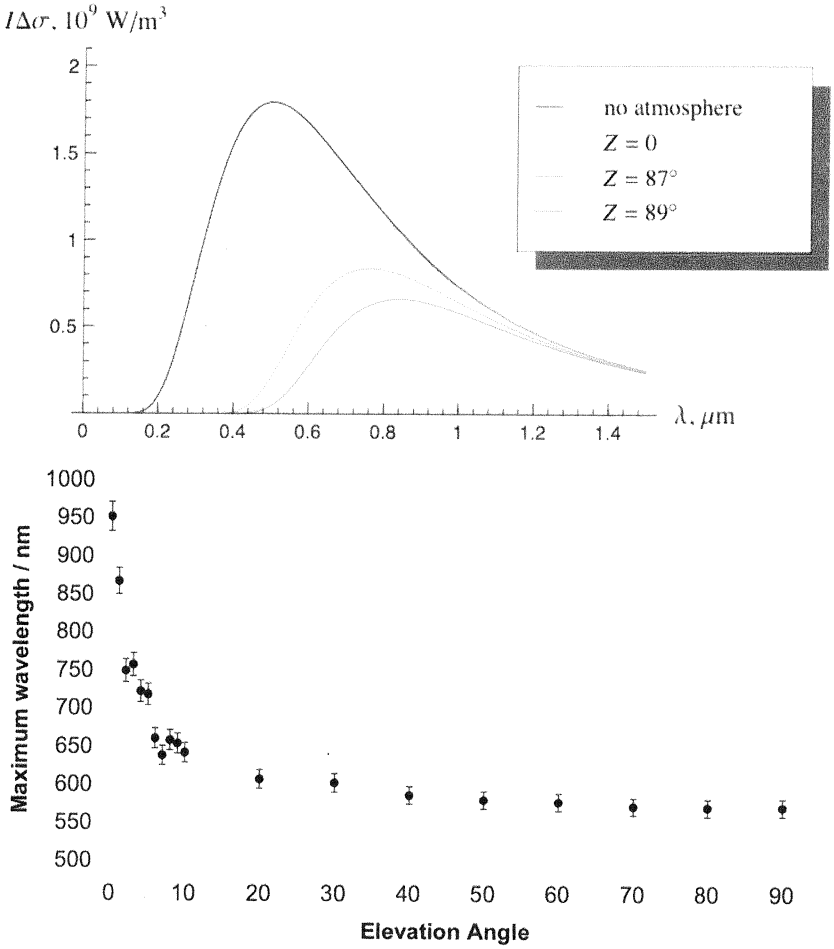

Figure 1: Copy of the main figure of Ref. [14] in the top, clearly illustrating its referral to *intensities*, and a representative figure of Ref. [12] at the bottom, clearly illustrating its referral to *frequencies* (or wavelengths).

trated by the differences of the two diagrams of Fig. 1. Consequently, under proper reformulation, the formulation of Rayleigh scattering presented in Ref. [14] is expected to be a rather natural complement of Santilli's IRS with no identifiable conflict. This is established by the fact that the Minkowski-Santilli IsoGeometry 4] recovers uniquely and identically the Minkowskian geometry when light propagates in vacuum, thus recovering the complementarity of the Doppler's law and the intensity (luminosity) established in astrophysics following about one century of measurements. Accepting this duality in astrophysics, but denying it for our atmosphere, would be non-scientific because it would imply a double standard for physical laws that are known to be universal.

E. Contrary to Gandzha view [14], Santilli's measurements of IRS *cannot* be consistently applied to the Rayleigh scattering because, as clearly stated in Refs. [7-12], the telescope used in all measurements of Sunlight from the Zenith to the horizon was manually adjusted toward the Sun, thus leading to evident variations of the intensity depending on the orientation of the telescope. However, it is equally stress that all analyzers were set for accurate detections of *wavelengths (frequencies)* under an intensity sufficient to have accurate wavelengths detections (see the confirmation in scan analyses of Ref. [13]).

Therefore, according to a consensus by colleagues in the field contacted b y the author, Gandzha [14] view in assuming Rayleigh scattering as the physical origin of the redness of the Sun at Sunset is conceptually, theoretically and experimentally unsubstantiated because:

1) Rayleigh "scattering" was conceived and developed for the colors of our *atmosphere,* where scattering is indeed dominant, and definitely not for visible direct Sunlight;

2) No scattering can be consistently introduced in the propagation of Sunlight along of light along a straight line, no quantitative treatment of this central assumption of Ref. [14] is on record at this time to our knowledge and, in the event it exists, it can be dismissed on numerous grounds [12];

3) Assuming that scattering might somehow be admitted for direct Sunlight following structural modifications of Rayleigh original conception, by remembering that blue and red are shifted for about 100 nm at the horizon, scattering cannot possibly cause a redshift of blue light into redlight of of the order of 100 nm as needed to represent the redness at Sunset;

4) Rayleigh scattering is a purely phenomenological model and, therefore, provides no clue whatsoever on the physical origin of said redness, thus preventing any consistent use as the dominant even t for the redness of the Sun at Sunset while, by comparison, said physical origin is indeed the main aim of Santilli IRS for which reason it can be assumed as fundamental; and

5) Rayleigh scattering has no experimental verification at this writing since no experimental verification is on record to our knowledge for the colors of or atmosphere, and the wavelength analyzers used by Santilli for the IRS scans are accurate for the measurement of frequencies under varying intensities, e.g., irrespective of whether from a spec of Sunlight or from highly intense Sunlight at the Zenith, thus preventing Santilli's IRS measurements from being consistently used for intensity based models (see as done by Gandzha for the plot in the top of Figure 1 also Section 9 of Ref. [12]).

Additionally, we have to recall the corresponding situation in astrophysics where there is a complementary between the Doppler frequency shift law and the intensity (luminosity) description of light from fart away galaxies. It is evident that the same complementary is expected for the behavior of Sunlight in our atmosphere in order to avoid double standards, thus mandating the use of Santilli's IRS as the fundamental physical description, and the use of intensity models as a complement.

In any case, Santilli's IRS recovers identically Doppler';s law in vacuum for the cosmological redshift and related intensity (luminosity) data. Therefore, solely accepting Rayleigh scattering for Sunlight in pour atmosphere would be in contradiction with about one century of astrophysical knowledge.

In summary, also according to a consensus among the colleagues consulted by the author, Gandzha presentation of Rayleigh or other forms of scattering [14] should be reformulated for sound physical conditions (e.g., for the loss of intensity of Sunlight due to scattering, rather than for the intensity of direct Sunlight where no scattering can coninsistently be admitted) and, additionally, should be experimentally verified via tests independent from those on frequencies and via the use of detectors measuring the *intensity of light from our atmosphere,* ratehr than the *wavelength of direct Sunlight.* Following such a reformulation and experimental verification, Rayleigh or other scattering models can indeed be complementary to

Santilli's IRS without any conflict.

Acknowledgments.

The author would like to thank I. Gandzha for critical comments on this note as well as for the publication of paper [14] because it has permitted important scientific clarifications in a new and rather complex field. Also, the author would like to express its appreciation to R. M. Santilli for invaluable assistance without which this paper would not have seen the light of the day. Additional thanks are due to two referees for penetrating comments and suggestions. Thanks are additionally due to various colleagues who participated to the *2012 Seminar Course on Hadronic Mathematics, mechanics and Chemistry* for in depth comments and suggestions. Thanks are finally due to Josh Manuel for the editorial control of the paper.

References

[1] R. M. Santilli. *Foundation of Theoretical Mechanics,* Volume I (1978) [2a], and Volume II (1982) [2b], Springer-Verlag, Heidelberg, Germany, http://www.santilli-foundation.org/docs/Santilli-209.pdf
http://www.santilli-foundation.org/docs/santilli-69.pdf

[2] R. M. Santilli, "Nonlocal-Integral Isotopies of Differential Calculus, Mechanics and Geometries," in Isotopies of Contemporary Mathematical Structures, P. Vetro Editor, Rendiconti Circolo Matematico Palermo, Suppl. Vol. 42, 7-82 (1996),
http://www.santilli-foundation.org/docs/Santilli-37.pdf

[3] D. S. Sourlas and Gr. T. Tsagas, *Mathematical Foundation of the Lie-Santilli Theory,* Ukraine Academy of Sciences (1993),
http://www.santilli-foundation.org/docs/santilli-70.pdf

[4] R. M. Santilli, "Isominkowskian Geometry for the Gravitational Treatment of Matter and its Isodual for Antimatter," Intern. J. Modern Phys. D **7**, 351 (1998),
http://www.santilli-foundation.org/docs/Santilli-35.pdf

[5] R. M. Santilli, "Lie-isotopic Lifting of Special Relativity for Extended Deformable Particles," Lettere Nuovo Cimento **37**, 545 (1983), http://www.santilli-foundation.org/docs/Santilli-50.pdf

[6] R. M. Santilli, *Isotopic Generalizations of Galilei and Einstein Relativities,* Vols. I [7a] and II [7b] (1991), International Academic Press http://www.santilli-foundation.org/docs/Santilli-01.pdf http://www.santilli-foundation.org/docs/Santilli-61.pdf

[7] R. M. Santilli, "Experimental Verifications of IsoRedShift with Possible Absence of Universe Expansion, Big Bang, Dark Matter, and Dark Energy," The Open Astronomy Journal **3**, 124 (2010), http://www.santilli-foundation.org/docs/Santilli-isoredshift.pdf

[8] R. M. Santilli, "Experimental Verification of IsoRedShift and its Cosmological Implications," American Institute of Physics Conference Proceedings Vol. 1281, pp. 882-885 (2010) http://www.santilli-foundation.org/docs/Isoredshift-Letter.pdf

[9] R. M. Santilli, "Iso-Minkowskian Geometry for Interior Dynamical Problems," Contributed paper to *Cosmology, Quantum Vacuum, and Zeta Functions,* Diego Sez-Gmez Sergei Odintsov Sebasti Xamb Editors, Springer, 2011 http://www.santilli-foundation.org/docs/Isominkowskian-Geom.pdf].

[10] R. M. Santilli, G. Amato and G. West, "Experimental Confirmation of the IsoRedShift at Sun at Sunset and Sunrise with Consequential Absence of Universe Expansion and Related Conjectures," Journal of Computational Methods in Sciences and Engineering, Vol. 12, pages 165-188 (2012). http://www.santilli-foundation.org/docs/Confirmation-sun-IRS.pdf

[11] G. West and G. Amato, "Experimental Confirmation of Santilli's IsoRedShift and IsoBlueShift," contributed paper to the *Proceedings of the San Marino Workshop on Astrophysics and Cosmology for Matter and Antimatter,* Republic of San Marino, September 5 to 9, 2011, in press (2012).

[12] H. Ahmar, G. Amato, J. V. Kadeisvili, J. Manuel, G. West, and O. Zogorodnia, "Additional experimental confirmations of Santilli's IsoRedShift and the consequential expected absence of universe expansion," in press.
http://www.santilli-foundation.org/docs/IRS-confirmations-212.pdf

[13] R. Verreault, "Experimental confirmation of Santilli's prediction of the anisotropy of Earth's gravitational field via the spherical pendulum," Journal of Computational Methods in Sciences and Engineering, in press (2012)

[14] I. Gandzha, "Solar Redshift Calculation by the Rayleigh Scattering Mechanism, in press at" Hadronic Journal **35**, issue no., 4 (2012).
http://www.scientificethics.org/Gandzha-2012.pdf

[15] (Lord Rayleigh, "On the light from the sky, its polarization and colour." Philosophical Magazine, Series 4, 41 (1871), 107–120, 274–279; John Strutt, On the scattering of light by small particles. Philosophical Magazine, Series 4, 41 (1871), 447–454.

HADRONIC JOURNAL 35, 399-467 (2012)

WHY BARYONS ARE YANG-MILLS MAGNETIC MONOPOLES

Jay R. Yablon
Schenectady, New York 12309

Received December 10, 2012

Abstract

We demonstrate that Yang-Mills Magnetic Monopoles naturally confine their gauge fields, naturally contain three colored fermions in a color singlet, and that mesons also in color singlets are the only particles they are allowed to emit or absorb. $SU(3)_C$ QCD as it has been extensively studied and confirmed is understood in broader context, with no contradiction, to be a consequence of baryons being Yang-Mills magnetic monopoles. Protons and neutrons are naturally represented in the fundamental representation of this group. We use the t'Hooft monopole Lagrangian with a Gaussian ansatz for fermion wavefunctions to demonstrate that these monopoles can be made to interact only at very short range as is required for nuclear interactions, and we establish topological stability following symmetry breaking from an SU(4) group using the B-L (baryon minus lepton number) generator. Finally, the mass of the electron is accurately predicted based on the masses of the up and down quarks to about 3% from the experimental mean for the quark masses, and confinement of quarks occurs energetically via fantastically strong negative binding energies that accord very well with experimental nuclear data. All of this makes Yang-Mills magnetic monopoles worthy of serious consideration and further development as baryons.

Copyright © 2012 by Hadronic Press, Inc., Palm Harbor, FL 34682–1577, USA

Contents

Introduction and Summary .....

1. Yang-Mills Magnetic Monopoles Naturally Confine their Gauge Fields through Spacetime Geometry .....

2. Yang-Mills Magnetic Monopoles Contain Fermion Wavefunctions .....

3. Yang-Mills Magnetic Monopoles Contain Three Fermions and Fermion Propagators .....

4. Yang-Mills Magnetic Monopoles Contain Spin 0, 1 and 2 Terms in "Vector (V)" and "Axial (A)" Variants, Consistent with Nuclear Phenomenology .....

5. Fermi-Dirac Exclusion Requires Using $SU(3)_C$ Quantum Chromodynamics for Yang-Mills Magnetic Monopoles, Yielding the Correct Baryon and Meson Color Wavefunctions .....

6. Yang-Mills Magnetic Monopoles Require the Topologically-Stable Gauge Group $SU(3)_C \times U(1)$ .....

7. Protons and Neutrons Naturally Fit Fundamental $SU(3)_{C'} \times U(1)_{B-L}$ Representations of Yang-Mills Magnetic Monopoles .....

8. Protons and Neutrons and Electrons and Neutrinos Emerge from Spontaneous Symmetry Breaking of a Simple $SU(4)_{B-L}$ Group Down to $SU(3)_{C'} \times U(1)_{B-L}$ .....

9. Using a Gaussian *Ansatz* for Fermion Wavefunctions, the t'Hooft Monopole Model Fully Specifies the Dynamical Properties of Yang-Mills Magnetic Monopole Baryons .....

10. Yang-Mills Magnetic Monopoles with a Gaussian *Ansatz* Interact only at Very Short Range as is Required for Nuclear Interactions .....

11. The Electron Mass is Predicted from Up and Down Quark Masses to about 3% from the Experimental Mean .....

12. Quark Confinement Results from Predicted Binding Energies which Coincide Extremely Closely with Nuclear Binding Energies .....

Conclusion .....

References .....

Introduction and Summary

The thesis of this paper is simple: magnetic monopole densities which come into existence in a non-Abelian Yang-Mills gauge theory of non-commuting fields are synonymous with baryon densities. Baryons, including the protons and neutrons which form the vast preponderance of matter in the universe, are Yang-Mills magnetic monopoles! Conversely, magnetic monopoles, long pursued since the time of Maxwell, have always been hiding in plain sight as baryons.

We first show how Yang-Mills magnetic monopoles naturally confine their gauge fields for the same formal reasons that there are no magnetic monopoles in Abelian gauge theories (section 1). When we replace the gauge fields of a Yang-Mills magnetic monopole with associated currents via an inverse relation $G_\nu \equiv I_{\sigma\nu} J^\sigma$ based on Maxwell's classical chromoelectric charge equation $J^\nu = \partial_\mu F^{\mu\nu}$ and then introduce fermion fields via currents $J_i^\mu = \overline{\psi} T_i \gamma^\mu \psi$, we find that these magnetic monopoles naturally contain three fermions and associated propagators (sections 2 and 3). After showing some ways in which these propagators may be mathematically expanded (section 4), we employ Fermi-Dirac statistics to require that each of the three fermions contained in this magnetic monopole system must possess unique quantum numbers, and this *compels* the introduction of $SU(3)_C$ QCD. We thus uncover a natural system containing three colored quarks which has the precise antisymmetric color wavefunction $R[G,B]+G[B,R]+B[R,G]$ expected of a baryon, and which passes through its closed surfaces objects with the symmetric wavefunction configuration $\overline{R}R+\overline{G}G+\overline{B}B$ expected of a meson. Thus, we naturally arrive at all the required features of QCD including three valence quarks and gluons and quark-anti-quark pairs (mesons). $SU(3)_C$ QCD as it has been extensively studied and confirmed is thereby understood in broader context, *with no contradiction*, to be a *natural consequence* of baryons being Yang-Mills magnetic monopoles (section 5).

These magnetic monopoles, however, cannot be made stable with the gauge group SU(3) alone, and will vanish unless one employs a product group SU(3)xU(1) with a U(1) generator for which the trace in non-vanishing. This leads us to obtain the required SU(3)xU(1) from a larger group SU(4) via spontaneous symmetry breaking, to both ensure renormalizability and provide topological stability (section 6). Close consideration of this SU(4) group reveals that its λ^{15} generator can naturally represent the difference between

baryon number and lepton number, $B-L$, and that the SU(3) subgroup provides a natural fundamental representation for protons and for neutrons (section 7) which emerge as distinct entities following spontaneous symmetry breaking (section 8).

The t'Hooft [1] and Polyakov [2] model may be used without alteration to specify the dynamics of this magnetic monopole system which includes protons and neutrons. However, rather than apply an *ansatz* $G^a_\mu = \varepsilon_{\mu ab} x_b G(r)$ to the *spin 1 gauge fields* to determine radial behaviors, we apply a *Gaussian ansatz* $\psi(r) = u(p)(\pi\lambda^2)^{-3/4} e^{-(1/2)(r-r_0)^2/\lambda^2}$ as in [3] to the *spin ½ fermion fields*. Because Gaussians are well-behaved and easily integrable, the monopoles vanish at the boundaries, have finite, calculable energies, and are indeed stable (section 9). Moreover, unlike the known monopoles which all exhibit inverse square-law field strengths, monopoles based on the Gaussian *ansatz* from [3] interact *only at extremely short range*, which is precisely what is to be expected and is experimentally observed for baryons such as protons and neutrons (section 10).

Finally, integrating the energy tensor of these magnetic monopoles over an entire spatial volume d^3x with all gauge field interactions and vacuum effects turned off (zero perturbation) allows us to obtain expressions for the "uncovered" proton and neutron mass as a function of the up and down "current quark" masses. For experimental validation we show how the observed electron mass m_e=0.510998928 MeV may be predicted from the 2012 PDG values of the up and down quark masses m_u, m_d, not only within experimental errors, *but with only a 3% difference from the mean experimental data* which itself has a spread about the mean of about 20% for the down mass and 50% for the up mass. Specifically, it is predicted that $m_e = 3(m_d - m_u)/(2\pi)^{\frac{3}{2}}$, with the $(2\pi)^{\frac{3}{2}}$ divisor directly emergent from three-dimensional Gaussian integration (section 11). The "uncovered" masses of the proton and neutron turn out to be more than 80% smaller than the total mass of the three quarks that they contain. This is understood as being due to a fantastically strong binding energy which confines the quarks. Moreover, latent (available) binding energies B for the proton and neutron are predicted to be $B_P = 7.640679\,MeV$ and $B_N = 9.812358\,MeV$, which accords well with empirical per-nucleon binding data for many nuclei and provides a basis to better understand nuclear bonding and fusion. Finally, it is shown how nuclear binding is intimately related to quark confinement, with extremely tight empirical data concurrence (section 12).

1. Yang-Mills Magnetic Monopoles Naturally Confine their Gauge Fields through Spacetime Geometry

First, we demonstrate how Yang-Mills magnetic monopoles naturally confine their gauge fields. We use the language of differential forms, and assume the reader has sufficient familiarity with this so no tutorial explanations are required.

In an Abelian (commuting field) gauge theory such as QED, the field strength tensor F is specified in relation to the vector potential gauge field (e.g., photon) A according to $F=dA$. The magnetic monopole source density P is then specified classically (for high-action $S(\varphi)=\int d^4x\mathcal{L}(\varphi)>>\hbar$ where the Euler Lagrange equation may be applied) by the classical field equation $P=dF=ddA=0$. This makes use of the geometric law that the exterior derivative of an exterior derivative is zero, $dd=0$. In integral form, this becomes $\iiint P=\iiint dF=\iiint ddG=\oiint F=\oiint dA=0$. All of the foregoing "zeros" are what tell us that there are no magnetic monopoles in an Abelian gauge theory such as QED. This absence of magnetic monopole charges at all attainable experimental energies is well borne out in the 140 years since James Clerk Maxwell published his 1873 *A Treatise on Electricity and Magnetism*.

In a non-Abelian (non-commuting field) Yang-Mills gauge theory such as QCD, the fundamental difference is that the field strength tensor F is now specified in relation to the vector gauge field potential G (e.g., gluon in QCD) according to $F=dG-iG^2$. For SU(N), both F and G are NxN matrices. In this relationship, $G^2=[G^\mu,G^\nu]dx_\mu dx_\nu$ expresses the non-commuting nature of the gauge fields and the non-linearity of Yang-Mills gauge theory. Therefore, although $ddG=0$ as always because of the exterior geometry, the classical (high-action) magnetic monopole density becomes the non-zero $P=dF=d\left(dG-iG^2\right)=-idG^2$. For SU(N), P is also an NxN matrix. In integral form, using Gauss'/ Stokes' law, this becomes:

$$\iiint P=\iiint dF=\iiint d\left(dG-iG^2\right)=-i\iiint dG^2=\oiint F=\oiint dG-i\oiint G^2=-i\oiint G^2 \quad (1.1)$$

and from the last two terms above, we also derive the companion equation:

$$\oiint dG=0. \quad (1.2)$$

Of course, (1.2), albeit with the different field name, is just the relationship $\oiint dA=0$ which tells us that there are no magnetic monopoles in Abelian gauge theory. But in light of (1.1), which provides us with a non-zero

magnetic monopole $\iiint P = -i\oiint G^2 \neq 0$, what can we learn from (1.2), which is the Yang-Mills analogue to the Abelian "no magnetic monopole" relationship $\oiint dA = 0$?

If we perform a local transformation $F \rightarrow F' = F - dG$ on the field strength F, which in expanded form is written as $F^{\mu\nu} \rightarrow F^{\mu\nu\prime} = F^{\mu\nu} - \partial^{[\nu}G^{\mu]}$, then we find from (1.1) as a direct and immediate result of the Abelian "no magnetic monopole" relationship $\oiint dG = 0$ in (1.2), that:

$$\iiint P = \oiint F \rightarrow \oiint F' = \oiint (F - dG) = \oiint F \,. \tag{1.3}$$

This means that the flow of the field strength $\oiint F = -i\oiint G^2$ across a two dimensional surface is invariant under the local gauge-like transformation $F^{\mu\nu} \rightarrow F^{\mu\nu\prime} = F^{\mu\nu} - \partial^{[\nu}G^{\mu]}$. We know in QED that invariance under the similar transformation $A^{\mu} \rightarrow A^{\mu\prime} = A^{\mu} + \partial^{\mu}\Lambda$ means the gauge parameter Λ is not a physical observable. We know in gravitational theory that invariance under $g^{\mu\nu} \rightarrow g^{\mu\nu\prime} = g^{\mu\nu} + \partial^{\{\mu}\Lambda^{\nu\}}$ likewise means the gauge vector Λ^{ν} is not a physical observable. In this case, the invariance of $\oiint F$ under the transformation $F^{\mu\nu} \rightarrow F^{\mu\nu\prime} = F^{\mu\nu} - \partial^{[\nu}G^{\mu]}$ tells us the gauge field G^{μ} is not an observable over the surface through which the field $\oiint F = -i\oiint G^2$ is flowing. But G^{μ} are simply the gauge fields, which in QCD, are the gluon fields. So, simply put: <u>the Yang-Mills gauge fields G^{μ}, including gluons in $SU(3)_C$, are not observables across any closed surface surrounding a magnetic monopole density P</u>. No matter what may transpire inside the volume represented by $\iiint P$, the gauge fields remain confined.

Taking this a step further, we see that the origins of this gauge field confinement rest in the 140-year old mystery as to why there are no magnetic monopoles in Abelian gauge theory. In differential forms, the statement of this is $ddG = 0$. In integral form, this becomes $\oiint dG = 0$, equation (1.2). Yet it is precisely this same "zero" which renders $\oiint F \rightarrow \oiint F' = \oiint F$ invariant under $F^{\mu\nu} \rightarrow F^{\mu\nu\prime} = F^{\mu\nu} - \partial^{[\nu}G^{\mu]}$ in (1.3). So the physical observation that there are no magnetic monopoles in Abelian gauge theory translates into a symmetry condition in non-Abelian gauge theory that gauge boson flow is not an observable over the surface of a magnetic charge. Again: In Abelian gauge theory there are no magnetic monopoles. In non-Abelian theory, this absence of Abelian magnetic monopoles translates into there being no flow of gauge

bosons (e.g., gluons) across any closed surface surrounding a Yang-Mills magnetic monopole. Consequently, *the absence of gluon flux, hence color, across surfaces surrounding non-Abelian chromo-magnetic monopoles is fundamentally equivalent to the absence of magnetic monopoles in Abelian gauge theory.* And, because this is turn originates in $dd=0$, we see that *this confinement is mandated by the differential forms geometry, imposed by spacetime itself.* The very same "zero" which in Abelian gauge theory says that there are no magnetic monopoles, in non-Abelian gauge theory says that there is no observable flux of Yang-Mills gauge fields across a closed surface surrounding a Yang-Mills magnetic monopole. We do not find a net flow of gluons across a closed monopole surface in Yang-Mills gauge theory any more than we find Abelian magnetic monopoles in electrodynamics, for identical geometric reasons.

2. Yang-Mills Magnetic Monopoles Contain Fermion Wavefunctions

While gauge field confinement is a necessary prerequisite for Yang-Mills magnetic monopoles to be considered baryon "candidates," it is by no means sufficient. At minimum, we must also show that these monopoles are capable of naturally containing three fermions in suitable color eigenstates, because we know that baryons contain three colored quarks. So, we now show how the hypothesis that Yang-Mills magnetic monopoles are baryons is fully consistent with $SU(3)_C$ QCD as it has been extensively studied and confirmed, replete with three valence quarks and gluons and quark-anti-quark pairs (mesons), and that QCD can in fact be viewed as the very *consequence* of this thesis. This will be the central focus of sections 2 through 5.

For this purpose, we start with the classical "chromoelectric" and "chromomagnetic" Maxwell field equations, using $D^\mu \equiv \partial^\mu - iG^\mu$:

$$J^\nu = \partial_\mu F^{\mu\nu} = \partial_\mu D^{[\mu} G^{\nu]} = \partial_\mu D^\mu G^\nu - \partial_\mu D^\nu G^\mu = \left(g^{\mu\nu}\partial_\sigma D^\sigma - \partial^\mu D^\nu\right) G_\mu \qquad (2.1)$$

$$P^{\sigma\mu\nu} = \partial^\sigma F^{\mu\nu} + \partial^\mu F^{\nu\sigma} + \partial^\nu F^{\sigma\mu}, \qquad (2.2)$$

together with the Yang-Mills field strength tensor:

$$F^{\mu\nu} = \partial^\mu G^\nu - \partial^\nu G^\mu - i\left[G^\mu, G^\nu\right] = D^\mu G^\nu - D^\nu G^\mu = D^{[\mu} G^{\nu]}. \qquad (2.3)$$

Above, group generators T^i are related by the group structure relation $f^{ijk}T_i = -i\left[T^j, T^k\right]$, and $F^{\mu\nu} \equiv T^i F_i^{\mu\nu}$ and $G^\mu \equiv T^i G_i^{\ \mu}$ are *N*x*N* matrices for any given SU(N) (same for J^ν and $P^{\sigma\mu\nu}$). (2.2) and (2.3) respectively are just expanded restatements of the classical field relationships $P=dF$ and

$F = dG - iG^2$ which we used in (1.1). We do not in general show the interaction charge strength g, but scale this into the gauge bosons $gG^\mu \to G^\mu$.

As soon as one substitutes the non-Abelian (2.3) into Maxwell's equation (2.2), while the terms based on $\partial^\mu G^\nu - \partial^\nu G^\mu$ continue to zero out by identity in the usual way (via $dd = 0$ which as shown in section 1 confines the gauge fields), one nonetheless arrives at a residual non-zero magnetic charge:

$$\begin{aligned} P^{\sigma\mu\nu} &= -i\left(\partial^\sigma\left[G^\mu, G^\nu\right] + \partial^\mu\left[G^\nu, G^\sigma\right] + \partial^\nu\left[G^\sigma, G^\mu\right]\right) \\ &= -i\left(\left[\partial^\sigma G^\mu, G^\nu\right] + \left[G^\mu, \partial^\sigma G^\nu\right] + \left[\partial^\mu G^\nu, G^\sigma\right] + \left[G^\nu, \partial^\mu G^\sigma\right] + \left[\partial^\nu G^\sigma, G^\mu\right] + \left[G^\sigma, \partial^\nu G^\mu\right]\right) \end{aligned} \quad . (2.4)$$

This is a longhand version of $P = -idG^2 = -2idG$ used in (1.1). The balance of this paper will largely be devoted to studying this $P^{\sigma\mu\nu}$ monopole closely. In sections 2 through 5 we will essentially study its symmetry properties and show how these coincide with those of QCD. In section 6 through 9 we shall study the circumstances under which it is topologically stable. In sections 10 through 12 we shall study a Gaussian *ansatz* for fermion wavefunctions which gives this monopole a short interaction range and yields calculable mass and binding energy predictions according with experimental observations.

To begin, we make use of the commutator relationship $\partial^\sigma G^\mu = i\left[k^\sigma, G^\mu\right]$ to replace the various $\partial^\sigma G^\mu$ in (2.4). Expanding, $G^\mu k^\sigma G^\nu - G^\mu k^\sigma G^\nu$ appears throughout, so these terms drop out. Re-consolidating yields:

$$P^{\sigma\mu\nu} = -\left(\left[\left[G^\mu, G^\nu\right], k^\sigma\right] + \left[\left[G^\nu, G^\sigma\right], k^\mu\right] + \left[\left[G^\sigma, G^\mu\right], k^\nu\right]\right). \quad (2.5)$$

Now, by way of brief preview, in the t'Hooft model [1] which we shall review in detail in section 9, the *spin 1 gauge fields* are specified as a function of radial distance r using the *ansatz* $G_{a\mu} = \varepsilon_{\mu ab} x_b G(r)$. Solutions of Lagrangian (9.2) infra are then used to find $G(r)$ and lead to the t'Hooft monopole solutions. Here, we will instead seek an inverse relation $G_\nu \equiv I_{\sigma\nu} J^\sigma$ for Maxwell's (2.1) to replace each G^μ above with a J^μ which can then be used to introduce fermion field wavefunctions ψ via $J^\mu = \overline{\psi}\gamma^\mu\psi$. The *ansatz* we employ will then be based on the radial behavior of these *spin ½ fermion fields*. *Using spin ½ fermion fields rather than spin 1 gauge fields to introduce an ansatz about the radial behavior of the G^μ, is the primary difference between the monopoles to be developed here, and the t'Hooft monopoles.*

Proceeding using $\partial^\sigma G^\mu = i\left[k^\sigma, G^\mu\right]$, inverse $I_{\sigma\nu}$ is specified in terms of a $\mu \leftrightarrow \sigma$ symmetrized configuration space operator based on the $g^{\mu\sigma}\partial_\alpha D^\alpha - \partial^\mu D^\sigma$ contained (2.1), with a hand-added Proca mass, by:

$$I_{\sigma\nu}\left(-g^{\mu\sigma}\left(k^{\alpha}k_{\alpha}+i\left[k^{\alpha},G_{\alpha}\right]-m^{2}\right)+k^{\mu}k^{\sigma}+\tfrac{1}{2}i\left[k^{\{\mu},G^{\sigma\}}\right]\right)=\delta^{\mu}{}_{\nu}\,. \tag{2.6}$$

We also use a $\sigma\leftrightarrow\nu$ symmetrized $I_{\sigma\nu}\equiv Ag_{\sigma\nu}+Bk_{\sigma}k_{\nu}+\tfrac{1}{2}Ci\left[k_{\{\sigma},G_{\nu\}}\right]$ to calculate $I_{\sigma\nu}$. In doing so, we keep in mind that the G^{σ} is an NxN matrix for the Yang-Mills gauge group SU(N), so any time G^{σ} appears in a denominator we must actually form a *Yang-Mills matrix inverse*. So that expressions we develop have a similar "look" to familiar expressions from QED, we use a "quoted denominator" notation $1/"M"\equiv M^{-1}$ to designate a Yang-Mills matrix inverse. Thus, $G^{\sigma^{-1}}=1/"G^{\sigma}"$, etc. This inverse from (2.6) is calculated to be:

$$I_{\sigma\nu}=\frac{-g_{\sigma\nu}+\dfrac{k_{\sigma}k_{\nu}+\tfrac{1}{2}i\left[k_{\{\sigma},G_{\nu\}}\right]}{"m^{2}-k^{\alpha}k_{\alpha}-i\left[k^{\alpha},G_{\alpha}\right]"}}{"k^{\alpha}k_{\alpha}-m^{2}+i\left[k^{\alpha},G_{\alpha}\right]"}\,, \tag{2.7}$$

and can only be formed if we simultaneously impose the covariant gauge condition, in configuration space:

$$\left(\partial_{\sigma}\partial_{\nu}-\tfrac{1}{2}\partial_{\{\sigma}G_{\nu\}}\right)\left(\partial^{\mu}\partial^{\sigma}-\tfrac{1}{2}\partial^{\{\mu}G^{\sigma\}}\right)=0\,. \tag{2.8}$$

Note that the often-employed $i\left[k^{\sigma},G_{\sigma}\right]=\partial^{\sigma}G_{\sigma}=0$ is *not* a gauge condition here; this is replaced by (2.8).

Now, inverse (2.7) has many interesting properties which we shall not take the time to explore here which would require an entire separate paper to do them justice. Special cases of interest include $i\left[k_{\nu},G_{\sigma}\right]=\partial_{\nu}G_{\sigma}\to 0$; $m=0$; both $\partial_{\nu}G_{\sigma}\to 0$ and $m=0$; and on shell $k^{\alpha}k_{\alpha}-m^{2}=0$ for $m\neq 0$, or $k^{\alpha}k_{\alpha}=0$ for $m=0$. We will also note that when working towards a quantum path integral formulation, $i\left[k^{\sigma},G_{\sigma}\right]=\partial^{\sigma}G_{\sigma}$ in (2.7) is replaced by a gauge-invariant perturbation $-V=\left(\partial^{\sigma}G_{\sigma}+G_{\sigma}\partial^{\sigma}\right)+G^{\sigma}G_{\sigma}$, contracted from a perturbation tensor $-V^{\mu\nu}=\left(\partial^{\mu}G^{\nu}+G^{\nu}\partial^{\mu}\right)+G^{\mu}G^{\nu}$. But our interest at the moment is in the low-perturbation limit, which is specified by $i\left[k_{\nu},G_{\sigma}\right]=\partial_{\nu}G_{\sigma}\to 0$. Thus, using (2.7) in the inverse relation $G_{\nu}=I_{\sigma\nu}J^{\sigma}$, we "turn off" all the perturbations by setting $i\left[k_{\nu},G_{\sigma}\right]=\partial_{\nu}G_{\sigma}=0$. When we do so, all the inverses (quoted denominators) in (2.7) become ordinary denominators. We then reduce using the fact that in momentum space, current conservation $\partial_{\mu}J^{\mu}(x)=0$ becomes $k_{\mu}J^{\mu}(k)=0$ (see [4] after I.5(4)). We thus obtain:

$$G_{\nu}=-\frac{g_{\sigma\nu}}{k^{\alpha}k_{\alpha}-m^{2}}J^{\sigma}\,. \tag{2.9}$$

The above is just like the expressions we encounter for inverses with a Proca mass in QED. It says, not unexpectedly, that in the low-perturbation limit, when we set $\partial_\nu G_\sigma \to 0$ (and in a deeper analysis, $-V^{\mu\nu} = \left(\partial^\mu G^\nu + G^\nu \partial^\mu\right) + G^\mu G^\nu \to 0$) QCD looks like QED.

The point of developing this inverse, is to be able to use (2.9) in (2.5) and then deploy fermion wavefunctions via $J^\mu = \bar{\psi}\gamma^\mu\psi$. Because (2.5) contains six different appearances of G_ν, there are six independent substitutions of (2.9) into (2.5), and what we must presume to be six independent Proca masses m. To track this, we will use the first six letters of the Greek alphabet $\alpha,\beta,\gamma,\delta,\varepsilon,\zeta$ to carry out the internal index summations and to label each of these six Proca masses. This substitution yields:

$$\begin{aligned} P^{\sigma\mu\nu} = &-\left[\left[\frac{g^{\alpha\mu}J_\alpha}{k^\alpha k_\alpha - m_{(\alpha)}{}^2}, \frac{g^{\nu\beta}J_\beta}{k^\beta k_\beta - m_{(\beta)}{}^2}\right], k^\sigma\right] \\ &-\left[\left[\frac{g^{\gamma\nu}J_\gamma}{k^\gamma k_\gamma - m_{(\gamma)}{}^2}, \frac{g^{\sigma\delta}J_\delta}{k^\delta k_\delta - m_{(\delta)}{}^2}\right], k^\mu\right] \\ &-\left[\left[\frac{g^{\varepsilon\sigma}J_\varepsilon}{k^\varepsilon k_\varepsilon - m_{(\varepsilon)}{}^2}, \frac{g^{\mu\zeta}J_\zeta}{k^\zeta k_\zeta - m_{(\zeta)}{}^2}\right], k^\nu\right] \end{aligned} \tag{2.10}$$

Here, we see *six massive vector boson propagators* each coupled with a current vector J_α. We raise the indexes on all the currents and absorb the $g^{\alpha\mu}$. We use $J^\mu = T^i J_i{}^\mu$, $i = 1,2,3...N^2-1$ to explicitly introduce the SU(N) generators. We factor out the resulting commutators $\left[T^i, T^j\right]$. And finally, we employ $J_i^\mu = \bar{\psi}T_i\gamma^\mu\psi$ and the like to introduce fermion wavefunctions. With this, and moving all currents into the same numerator, (2.10) becomes:

$$\begin{aligned} P^{\sigma\mu\nu} = -\left[T^i, T^j\right] \Bigg(&\left[\left[\left(\frac{1}{k^\alpha k_\alpha - m_{(\alpha)}{}^2}\frac{\bar{\psi}T_i\gamma^\mu\psi\bar{\psi}T_j\gamma^\nu\psi}{k^\beta k_\beta - m_{(\beta)}{}^2}\right), k^\sigma\right]\right] \\ &+\left[\left[\left(\frac{1}{k^\gamma k_\gamma - m_{(\gamma)}{}^2}\frac{\bar{\psi}T_i\gamma^\nu\psi\bar{\psi}T_j\gamma^\sigma\psi}{k^\delta k_\delta - m_{(\delta)}{}^2}\right), k^\mu\right]\right] \\ &+\left[\left[\left(\frac{1}{k^\varepsilon k_\varepsilon - m_{(\varepsilon)}{}^2}\frac{\bar{\psi}T_i\gamma^\sigma\psi\bar{\psi}T_j\gamma^\mu\psi}{k^\zeta k_\zeta - m_{(\zeta)}{}^2}\right), k^\nu\right]\right] \Bigg) \end{aligned} \tag{2.11}$$

The above monopole now contains fermion wavefunctions in three additive terms. In the next three sections, we shall show how these are the wavefunctions of the three colored quarks of QCD.

3. Yang-Mills Magnetic Monopoles Contain Three Fermions and Fermion Propagators

Let us first take a close look at the fermion term $\overline{\psi}T_i\gamma^\mu\psi\overline{\psi}T_j\gamma^\nu\psi/\left(k^\beta k_\beta - m_{(\beta)}{}^2\right)$ and the other two like-terms in (2.11). First, we focus on $\overline{\psi}T_i\gamma^\mu\psi\overline{\psi}T_j\gamma^\nu\psi$, and refer to sections 6.2 and 6.14 of [5]. If these two spacetime indexes μ, ν, had been summed with one another in the form of $\overline{\psi}T_i\gamma^\mu\psi\overline{\psi}T_j\gamma_\mu\psi$, then this would represent Moeller scattering. But because these are *free* spacetime indexes, the Feynman diagram associated with this term will be that for Compton scattering. The two lowest-order diagrams for this, as will be developed in the discussion to follow, are shown in Figure 1 below. Specifically, the left vertex contains the factor $T_j\gamma^\nu$ and the right vertex contains $T_i\gamma^\mu$, with the free indexes μ, ν shown at the end of the respective boson lines. For the four-momentum of the wavefunctions, we designate p^σ to represent the initial incoming momentum of the rightmost ψ, and p'^σ to represent the final, outgoing momentum of the leftmost $\overline{\psi}$. Thus, we rewrite this term as $\overline{\psi}(p')T_i\gamma^\mu\psi\overline{\psi}T_j\gamma^\nu\psi(p)$.

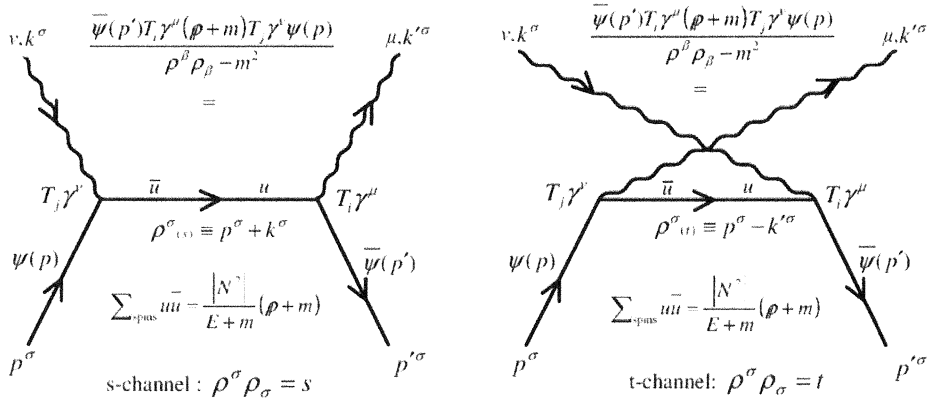

Figure 1

Appearing in the center of the numerator is $\psi\overline{\psi}$. For Compton scattering, these two wavefunctions have no intervening vertex and so are

represented by a single fermion line in the middle of the diagram. The four-momentum is either $\rho^{\sigma}{}_{(s)} \equiv p^{\sigma} + k^{\sigma}$ for the left diagram of Figure 1, or $\rho^{\sigma}{}_{(t)} \equiv p^{\sigma} - k'^{\sigma}$ for the right diagram, with k^{σ} and k'^{σ} respectively representing the four-momentum added to or subtracted from the fermion wavefunctions at the $T_j \gamma^{\nu}$ vertex. In terms of the Mandelstam variables, $\rho^{\sigma}{}_{(s)} \rho_{\sigma(s)} = s$, while $\rho^{\sigma}{}_{(t)} \rho_{\sigma(t)} = t$, which explains the choice of s, t labels. For notational compactness, we shall often make use of ρ^{σ} while keeping in mind that this may represent either of $\rho^{\sigma}{}_{(s)}$ or $\rho^{\sigma}{}_{(t)}$ as defined above. Because these wavefunctions are directly back to back in the form of $\psi\bar{\psi}$ with no intervening vertex γ^{μ}, the momenta of the two wavefunctions in $\psi\bar{\psi}$ are equal $p^{\sigma}(\psi) = p^{\sigma}(\bar{\psi}) = \rho^{\sigma}$, so we may set $\psi\bar{\psi} = u\bar{u}$, where u and $\bar{u}$ are a Dirac spinor and its adjoint. For U(1), $\psi\bar{\psi} = u\bar{u}$ is a 4x4 Dirac matrix because each spinor has four components. But for SU(N), it is important to keep in mind that $\psi\bar{\psi} = u\bar{u}$ is a $(4\times N)\times(4\times N)$ matrix.

Next, we sum $u\bar{u}$ over all spins states, $\Sigma_{\text{spins}} u\bar{u}$. Often, this spin sum is written as $\Sigma_{\text{spins}} u\bar{u} = \not{p} + m$ (see e.g., [5], section 5.5). But there is an implied covariant (real) normalization $N^2 = E + m$ in this expression. So to be fully explicit, this should really be written (see [5], problem solution 5.9):

$$\sum_{\text{spins}} u\bar{u} = \frac{N^2}{\mathrm{E} + m}(\not{p} + m), \tag{3.1}$$

where $\not{p} + m$ is also a $(4\times N)\times(4\times N)$ matrix for SU(N), and where we have made use of $\not{p} = \gamma^{\alpha} \rho_{\alpha}$ using the s and t-channel ρ^{σ} as defined above, with $\rho^{0} \equiv \mathrm{E}$. So we use the foregoing including (3.1) in (2.11) to obtain

$$\frac{\bar{\psi} T_i \gamma^{\mu} \psi \bar{\psi} T_j \gamma^{\nu} \psi}{k^{\beta} k_{\beta} - m_{(\beta)}{}^2} = \frac{\bar{\psi} T_i \gamma^{\mu} u \bar{u} T_j \gamma^{\nu} \psi}{k^{\beta} k_{\beta} - m_{(\beta)}{}^2} \rightarrow \frac{\bar{\psi} T_i \gamma^{\mu} \Sigma_{\text{spins}} u \bar{u} T_j \gamma^{\nu} \psi}{k^{\beta} k_{\beta} - m_{(\beta)}{}^2} = \frac{N^2}{\mathrm{E} + m} \frac{\bar{\psi} T_i \gamma^{\mu} (\not{p} + m) T_j \gamma^{\nu} \psi}{k^{\beta} k_{\beta} - m_{(\beta)}{}^2} \tag{3.2}$$

for top line term in (2.11), and similarly for the other two like-terms.

Now, let us take a moment to discuss propagators. In general, a propagator (times -i) is specified by $\Sigma_{\text{spins}} / (p^{\sigma} p_{\sigma} - m^2)$, where p^{σ} and m are the four-momentum and rest mass of the propagating particle. For fermions, we specifically employ (3.1) including ρ^{σ} as defined above, so that:

$$\frac{\Sigma_{\text{spins}}}{\rho^{\sigma}\rho_{\sigma}-m^2}=\frac{N^2}{\mathrm{E}+m}\frac{\not p+m}{\rho^{\sigma}\rho_{\sigma}-m^2}=\frac{N^2}{\mathrm{E}+m}\frac{\not p+m}{(\not p+m)(\not p-m)}=\frac{N^2}{\mathrm{E}+m}\frac{1}{\not p-m}=\frac{N^2}{\mathrm{E}+m}(\not p-m)^{-1}\,.(3.3)$$

For $N^2=\mathrm{E}+m$, the propagator becomes the familiar $(\not p-m)^{-1}=1/(\not p-m)$. Of course, having a $(4\times N)\times(4\times N)$ (or even a 4x4) matrix such as $\not p-m$ in a denominator is really not a proper mathematical expression, but merely a convenient shorthand to designate a *matrix inverse*. Thus, as we have done previously in section 2, we will use a quoted denominator $1/"\not p-m"$ to gently remind us of this. With the earlier definitions of ρ^{σ}, (3.3) has two alternative formulations corresponding to s and t channel diagrams in Figure 1:

$$\frac{\Sigma_{\text{spins}}}{s-m^2}=\frac{N^2}{\mathrm{E}+m}\frac{\not p+\not k+m}{(p+k)^{\sigma}(p+k)_{\sigma}-m^2}=\frac{N^2}{\mathrm{E}+m}\frac{1}{"\not p+\not k-m"}=\frac{N^2}{\mathrm{E}+m}(\not p+\not k-m)^{-1}\,.(3.4)$$

$$\frac{\Sigma_{\text{spins}}}{t-m^2}=\frac{N^2}{\mathrm{E}+m}\frac{\not p-\not k'+m}{(p-k')^{\sigma}(p-k')_{\sigma}-m^2}=\frac{N^2}{\mathrm{E}+m}\frac{1}{"\not p-\not k'-m"}=\frac{N^2}{\mathrm{E}+m}(\not p-\not k'-m)^{-1}\,.(3.5)$$

Now, let us closely contrast (3.2) with (3.4) and (3.5). The final term in (3.2) contains at its center, the expression $(\not p+m)/\left(k^{\beta}k_{\beta}-m_{(\beta)}{}^2\right)$. This looks intriguingly like the fermion propagator in the second terms of (3.4) and (3.5). However, $m_{(\beta)}$ in (3.2) started out in (2.10) as a *gauge boson* mass in the denominator of a gauge boson propagator $g^{\nu\beta}/\left(k^{\beta}k_{\beta}-m_{(\beta)}{}^2\right)$, with k^{β} being the associated four-momentum. By contrast, the numerator of (3.2), with either $\not p_{(s)}+m=\not p+\not k+m$ or $\not p_{(t)}+m=\not p-\not k'+m$ contains a *fermion* mass m and associated Dirac-daggered four-momentum $\not p$. That is, (3.2) looks to have "apples" (bosons) in the denominator and "oranges" (fermions) in the numerator. So the question arises: is there some way to mix "apples" and "oranges" and actually treat (3.2) – and therefore the terms in (2.11) – as a fermion propagator? And if so, what is required for us to be able to do so?

First, the generalized expression (3.3) does not discriminate fermions from bosons. If the Σ_{spins} in the left term of (3.3) operates on $u\bar{u}$, then $\rho^{\sigma}\rho_{\sigma}-m^2$ in the denominator produces a fermion propagator. If the Σ_{spins} operates on an expression $\varepsilon_{\mu}{}^{*}\varepsilon_{\nu}$ with boson polarization vectors, $\rho^{\sigma}\rho_{\sigma}-m^2$ produces a boson propagator. That is, it is the Σ_{spins} in the numerator of a propagator such as (3.3) which sets the tone for whether the propagator is that of a fermion or a boson. This suggests, because $\not p+m$ is in the numerator of

(3.2), and of (2.11) via $\psi\bar{\psi} = u\bar{u}$, that the denominators $k^{\beta}k_{\beta} - m_{(\beta)}{}^{2}$ in (2.11) and (3.2) should be associated with fermions, not bosons.

Second, more fundamentally, it is instructive to consider spontaneous symmetry breaking, because that entails a similar mixing of apples and oranges. In weak $SU(2)_W$, for example, we start with three massless gauge bosons $W^{1\mu}, W^{2\mu}, W^{2\mu}$ each with two degrees of freedom for a subtotal of six, and a complex scalar doublet ϕ which contains four scalar degrees of freedom, for a total of ten degrees of freedom. After spontaneous symmetry breaking, three of the scalar degrees of freedom are "swallowed" by the three gauge bosons via the Goldstone mechanism. The gauge bosons become massive, each with three degrees of freedom for a total of nine, and the remaining scalar degree of freedom goes to the Higgs field. We still end up with ten degrees of freedom, but they are redistributed from the scalars ("apples") to the gauge bosons ("oranges"). In SU(2)W×U(1)Y electroweak theory, we start with four massless gauge bosons rather than three, but the photon remains massless. So twelve degrees of freedom before symmetry breaking (eight from the four massless gauge bosons and four from the complex scalar doublet) remain twelve degrees of freedom afterwards (three massive vector bosons, one massless photon, and one Higgs field).

Equation (2.11), which is what we are working with at the moment, started in (2.10) with a total of six Proca (presumed massive) *boson propagators*, thus totaling 18 degrees of freedom. So if we want to mix apples and oranges in (3.2) using a Goldstone-like mechanism that shifts degrees of freedom from one particle type to another, we must be sure to end up with eighteen degrees of freedom in total once we are all done.

Consequently, let us now introduce the hypothesis that each of $k^{\beta}k_{\beta} - m_{(\beta)}{}^{2}$, $k^{\delta}k_{\delta} - m_{(\delta)}{}^{2}$ and $k^{\zeta}k_{\zeta} - m_{(\zeta)}{}^{2}$ in the (2.11) denominators are to be associated with the *fermion* masses and momenta in the $\Sigma_{\text{spins}} u\bar{u} \propto \not{p} + m$ of their respective numerators in (3.2). We shall validate this "propagator hypothesis" by showing that it leads to QCD. This means that (2.11) will now contain three massive fermion propagators, and therefore three fermions, which is highly desirable if we are attempting to demonstrate that the Yang-Mills magnetic monopole is a baryon. And since a massive fermion contains four degrees of freedom, (2.11) will now contain a total of twelve degrees of freedom for the fermions. This leaves six of the 18 degrees of freedom for the three remaining vector bosons propagators, and so means that these bosons must drop down to <u>two</u> degrees of freedom apiece and thus become massless,

i.e., that we must now set their Proca masses to zero, $m_{(\alpha)},m_{(\gamma)},m_{(\varepsilon)}=0$. Now, the 18 degrees of freedom that initially belonged three apiece to six massive vector bosons have been redistributed: 12 of these now belong to the 3 fermions, and only 6 belong to the 3 remaining bosons. That this hypothesis leads to the requirement that the gauge bosons remain massless, is one of several results we shall soon derive that are fully consistent with QCD and indeed are required by QCD.

To implement this, using (3.2) in (2.11) and the s and t channel diagrams in Figure 1, we promote $k^\beta \rightarrow \rho^\beta{}_{(s)} = p^\beta + k^\beta$ and $k^\beta \rightarrow \rho^\beta{}_{(t)} = p^\beta - k'^\beta$ to the momentum of the associated fermion lines in the middle of both of Figures 1, and similarly for the other terms in (2.11). Thus, at the $T_j\gamma^\nu$ vertex of the s-channel Figure 1, we are taking the original incoming gauge boson momentum k^β and adding it to the incoming fermion momentum p^β to arrive at $p^\beta + k^\beta$. And, at the $T_j\gamma^\nu$ vertex of the t-channel Figure 1, we are taking the original incoming gauge boson momentum k^β, associating it with the outgoing momentum by setting $k^\beta \rightarrow -k'^\beta$, and then adding this to the incoming fermion momentum p^β to obtain $p^\beta - k'^\beta$. The final fermion momentum, in either diagram, is then $p'^\beta = p^\beta + k^\beta - k'^\beta \equiv p^\beta + q^\beta$. We then generally label all objects associated with these three fermions with either β, δ or ζ, while setting $m_{(\alpha)},m_{(\gamma)},m_{(\varepsilon)}=0$ to balance the degrees of freedom, and we show the initial and final fermion momenta. With all of this, (2.11) now becomes:

$$P^{\sigma\mu\nu} = -\left[T^i,T^j\right]\left(\begin{array}{l}\left[\left(\frac{1}{k^\alpha k_\alpha}\frac{{N_{(\beta)}}^2}{\mathrm{E}_{(\beta)}+m_{(\beta)}}\frac{\overline{\psi}_{(\beta)}(p'_\beta)T_i\gamma^\mu\left(\rho_{(\beta)}+m_{(\beta)}\right)T_j\gamma^\nu\psi_{(\beta)}(p_\beta)}{\rho^\beta\rho_\beta-{m_{(\beta)}}^2}\right),k^\sigma\right] \\ +\left[\left(\frac{1}{k^\gamma k_\gamma}\frac{{N_{(\delta)}}^2}{\mathrm{E}_{(\delta)}+m_{(\delta)}}\frac{\overline{\psi}_{(\delta)}(p'_\delta)T_i\gamma^\mu\left(\rho_{(\delta)}+m_{(\delta)}\right)T_j\gamma^\nu\psi_{(\delta)}(p_\delta)}{\rho^\delta\rho_\delta-{m_{(\delta)}}^2}\right),k^\mu\right] \\ +\left[\left(\frac{1}{k^\varepsilon k_\varepsilon}\frac{{N_{(\zeta)}}^2}{\mathrm{E}_{(\zeta)}+m_{(\zeta)}}\frac{\overline{\psi}_{(\zeta)}(p'_\zeta)T_i\gamma^\mu\left(\rho_{(\zeta)}+m_{(\zeta)}\right)T_j\gamma^\nu\psi_{(\zeta)}(p_\zeta)}{\rho^\zeta\rho_\zeta-{m_{(\zeta)}}^2}\right),k^\nu\right]\end{array}\right) \quad (3.6)$$

The Higgs / Goldstone mechanism has long been known to enable massless gauge bosons to become massive by swallowing degrees of freedom from scalars. Here, fermions become massive by swallowing degrees of freedom from massive bosons, which then revert to massless bosons. This turns out to

be perfect for QCD, which is known to require massless gluons and which is expected to have massive quarks.

Looking closely at (3.6), we now also see a path to choosing normalizations N which simultaneously: 1) are covariant; 2) retain the original mass dimensionality of +3 for $\overline{uu}$; and 3) greatly simplify (3.6). Specifically, we now *choose* the covariant, mass dimension-preserving normalizations:

$$N_{(\beta)}{}^2 = \left(\mathrm{E}_{(\beta)} + m_{(\beta)}\right)k^\alpha k_\alpha; \quad N_{(\delta)}{}^2 = \left(\mathrm{E}_{(\delta)} + m_{(\delta)}\right)k^\gamma k_\gamma; \quad N_{(\zeta)}{}^2 = \left(\mathrm{E}_{(\zeta)} + m_{(\zeta)}\right)k^\varepsilon k_\varepsilon . \quad (3.7)$$

Using these in (3.6), and re-labeling $\beta \to 1; \delta \to 2; \zeta \to 3$, yields the further simplified expression:

$$P^{\sigma\mu\nu} = -\left[T^i, T^j\right]\left(\begin{array}{l} \left[\left(\dfrac{\overline{\psi}_{(1)}T_i\gamma^\mu\left(\not{p}_{(1)} + m_{(1)}\right)T_j\gamma^\nu\psi_{(1)}}{\rho^\beta\rho_\beta - m_{(1)}{}^2}\right), k^\sigma\right] \\ + \left[\left(\dfrac{\overline{\psi}_{(2)}T_i\gamma^\mu\left(\not{p}_{(2)} + m_{(2)}\right)T_j\gamma^\nu\psi_{(2)}}{\rho^\delta\rho_\delta - m_{(2)}{}^2}\right), k^\mu\right] \\ + \left[\left(\dfrac{\overline{\psi}_{(3)}T_i\gamma^\mu\left(\not{p}_{(3)} + m_{(3)}\right)T_j\gamma^\nu\psi_{(3)}}{\rho^\zeta\rho_\zeta - m_{(3)}{}^2}\right), k^\nu\right] \end{array}\right). \quad (3.8)$$

By virtue of (3.7) explicitly preserving the mass dimensionality, (3.8) retains a mass dimension +3 which one expects for a source current density $P^{\sigma\mu\nu}$ corresponding with the second spacetime derivatives of a gauge potential G^μ with mass dimension +1. We also removed the initial and final p and p' which appeared in (3.6), which are now regarded to be implicit in (3.8). The above should be contrasted with [6.103] and [6.104] in [5].

Now we return to the commutator $\left[T^i, T^j\right]$. This operates to antisymmetrically commute the vertices $\left(T_i\gamma^\mu\right)\left(T_j\gamma^\nu\right)$, and so visibly restores the antisymmetric character of the spacetime indexes, thus:

$$\left[T^i, T^j\right]\frac{\overline{\psi}T_i\gamma^\mu\left(\not{p} + m\right)T_j\gamma^\nu\psi}{\rho^\beta\rho_\beta - m^2} = \frac{\overline{\psi}\gamma^{[\mu}\left(\not{p} + m\right)\gamma^{\nu]}\psi}{\rho^\beta\rho_\beta - m^2} \equiv \frac{\overline{\psi}\left[\gamma^\mu{}_\vee\,\gamma^\nu\right]\psi}{\text{"}\not{p} - m\text{"}} . \quad (3.9)$$

where in the final term, we have *defined* the shorthand operator

$$\vee \equiv \frac{\not{p} + m}{\not{p} + m} = 1 . \quad (3.10)$$

This operator allows us to write consolidated expressions with "$\not{p} - m$" fermion propagator denominators and clearly display the spacetime symmetries, while at the same time providing a placeholder to restore the full

propagator. The "quasi-commutator" $[\gamma^\mu \vee \gamma^\nu]$ says that one inserts (3.10) into the final term of (3.9) at the location designated by $\vee$, and then commutes γ^μ and γ^ν with one another in antisymmetric combination about the $\not{p}+m$ in the numerator to arrive at the next to last term in (3.9).

Using the compact notation of (3.9) (which we shall momentarily re-expand), we now write (3.8) as:

$$P^{\sigma\mu\nu} = -\left(\left[\left(\frac{\overline{\psi}_{(1)} [\gamma^\mu \vee \gamma^\nu] \psi_{(1)}}{"\not{p}_{(1)} - m_{(1)}"} \right), k^\sigma \right] + \left[\left(\frac{\overline{\psi}_{(2)} [\gamma^\mu \vee \gamma^\nu] \psi_{(2)}}{"\not{p}_{(2)} - m_{(2)}"} \right), k^\mu \right] + \left[\left(\frac{\overline{\psi}_{(3)} [\gamma^\mu \vee \gamma^\nu] \psi_{(3)}}{"\not{p}_{(3)} - m_{(3)}"} \right), k^\nu \right] \right). \quad (3.11)$$

This explicitly highlights the antisymmetric commutation $[G^\mu, G^\nu]$ of free indexes μ, ν with which everything started back in (2.5), and even further back, in the underlying field density $F^{\mu\nu} = \partial^\mu G^\nu - \partial^\nu G^\mu - i[G^\mu, G^\nu]$ of (2.3) which is the heart of non-commuting Yang-Mills field theory. This also illustrates the "clean" compactness provided by quasi-commutator $[\gamma^\mu \vee \gamma^\nu]$.

All that now remains in (3.11) is the final commutator with momentum terms such as k^σ. Going back to the earlier-employed $\partial^\sigma G^\mu = i[k^\sigma, G^\mu]$ which tells us that commuting a spacetime field with k^σ is just a clever way to take its derivatives, we can similarly write $i\partial^\sigma M^{\mu\nu} = [M^{\mu\nu}, k^\sigma]$ for a second rank tensor field $M^{\mu\nu}(x^\sigma)$. So, if we also use (3.11) to *define* a second rank Dirac "quasi-covariant" $-2i\sigma^{\mu \vee \nu} \equiv [\gamma^\mu \vee \gamma^\nu]$, we may finally consolidate (3.11) to:

$$P^{\sigma\mu\nu} = -2\left(\partial^\sigma \frac{\overline{\psi}_{(1)} \sigma^{\mu \vee \nu} \psi_{(1)}}{"\not{p}_{(1)} - m_{(1)}"} + \partial^\mu \frac{\overline{\psi}_{(2)} \sigma^{\nu \vee \sigma} \psi_{(2)}}{"\not{p}_{(2)} - m_{(2)}"} + \partial^\nu \frac{\overline{\psi}_{(3)} \sigma^{\sigma \vee \mu} \psi_{(3)}}{"\not{p}_{(3)} - m_{(3)}"} \right). \quad (3.12)$$

This is our final expression for a Yang-Mills magnetic monopole $P^{\sigma\mu\nu}$. We shall now explore its symmetries and other properties in a variety of ways.

4. Yang-Mills Magnetic Monopoles Contain Spin 0, 1 and 2 Terms in "Vector (V)" and "Axial (A)" Variants, Consistent with Nuclear Phenomenology

Before proceeding further with development, we pause in this section to first evaluate the compact expression in (3.9) explicitly, so we can see what is contained in each of the terms in the monopole (3.12). Separating the terms with $\not{p} = \rho_\alpha \gamma^\alpha$ and m yields:

$$\frac{\bar{\psi}\left[\gamma^{\mu}{}_{\vee}\,\gamma^{\nu}\right]\psi}{"\not{p}-m"}=\frac{\bar{\psi}\gamma^{[\mu}(\not{p}+m)\gamma^{\nu]}\psi}{\rho^{\beta}\rho_{\beta}-m^{2}}=\frac{\rho_{\alpha}\bar{\psi}\gamma^{[\mu}\gamma^{\alpha}\,\gamma^{\nu]}\psi}{\rho^{\beta}\rho_{\beta}-m^{2}}+\frac{m\bar{\psi}\left[\gamma^{\mu},\gamma^{\nu}\right]\psi}{\rho^{\beta}\rho_{\beta}-m^{2}}. \qquad (4.1)$$

The second separated term contains the ordinary second rank Dirac covariants $-2i\sigma^{\mu\nu}=\left[\gamma^{\mu},\gamma^{\nu}\right]$. But the former term contains a third rank formation of Dirac matrices $\gamma^{[\mu}\gamma^{\alpha}\,\gamma^{\nu]}$, summed over the α index with ρ_{α}. So, we expand the numerator in this term to write:

$$\rho_{\alpha}\bar{\psi}\gamma^{[\mu}\gamma^{\alpha}\,\gamma^{\nu]}\psi=\rho_{0}\bar{\psi}\gamma^{[\mu}\gamma^{0}\,\gamma^{\nu]}\psi+\rho_{1}\bar{\psi}\gamma^{[\mu}\gamma^{1}\,\gamma^{\nu]}\psi+\rho_{2}\bar{\psi}\gamma^{[\mu}\gamma^{2}\,\gamma^{\nu]}\psi+\rho_{3}\bar{\psi}\gamma^{[\mu}\gamma^{3}\,\gamma^{\nu]}\psi \qquad (4.2)$$

Then, we evaluate each of the six independent components for $\mu\nu=01,02,03,12,23,31$. The terms where either the μ or ν index is equal to the middle α index drop out because of the μ,ν antisymmetry. Applying the Dirac relation $\gamma^{5}=i\gamma^{0}\gamma^{1}\gamma^{2}\gamma^{3}$ in various combinations to the remaining terms, then using $g_{\mu\nu}=\eta_{\mu\nu}$ in geodesic (flat spacetime tangential) coordinates to lower indexes, the result can be covariantly-summarized via the Levi-Civita tensor (in a basis where $\varepsilon_{0123}=\sqrt{-g}$) as:

$$\bar{\psi}\gamma^{[\mu}\not{p}\,\gamma^{\nu]}\psi=2i\varepsilon^{\mu\nu\alpha\beta}\rho_{[\alpha}\bar{\psi}\gamma_{\beta]}\gamma^{5}\psi\,. \qquad (4.3)$$

Therefore, the explicit evaluation of (4.1), using the earlier-defined second rank Dirac "quasi-covariant" $-2i\sigma^{\mu}{}_{\vee}{}^{\nu}=\left[\gamma^{\mu}{}_{\vee}\gamma^{\nu}\right]$ and (3.10) for ${}_{\vee}$, and also the ordinary covariant $-2i\sigma^{\mu\nu}=\left[\gamma^{\mu},\gamma^{\nu}\right]$, is:

$$\frac{\bar{\psi}\sigma^{\mu}{}_{\vee}{}^{\nu}\psi}{"\not{p}-m"}=\frac{i}{2}\frac{\bar{\psi}\left[\gamma^{\mu}{}_{\vee}\,\gamma^{\nu}\right]\psi}{"\not{p}-m"}=\frac{i}{2}\frac{\bar{\psi}\gamma^{[\mu}(\not{p}+m)\gamma^{\nu]}\psi}{\rho^{\beta}\rho_{\beta}-m^{2}}=\frac{m\bar{\psi}\sigma^{\mu\nu}\psi}{\rho^{\beta}\rho_{\beta}-m^{2}}-\frac{\varepsilon^{\mu\nu}{}_{\alpha\beta}\rho^{[\alpha}\bar{\psi}\gamma^{\beta]}\gamma^{5}\psi}{\rho^{\beta}\rho_{\beta}-m^{2}}. \qquad (4.4)$$

This expression contains both a second rank antisymmetric tensor $\bar{\psi}\sigma^{\mu\nu}\psi$, and a first rank *axial* vector $\bar{\psi}\gamma^{\beta]}\gamma^{5}\psi$. This is the first of many instances where we shall discover that Yang-Mill magnetic monopoles inherently contain certain chiral asymmetries that introduce axial objects which may account for the chiral asymmetries and the many axial objects observed in strong interaction hadron phenomenology. *This sort of non-chiral result will provide one very strong basis upon which to experimentally validate the thesis that baryons are Yang-Mills magnetic monopoles.*

Let us now go one step further, and use the Gordon decomposition (see, e.g., [6] at 343-345) :

$$\bar{\psi}\gamma^{\nu}\psi=\frac{1}{2m}\bar{\psi}\left[(p'+p)^{\nu}+\frac{g}{2}(p'-p)_{\alpha}i\sigma^{\nu\alpha}\right]\psi \qquad (4.5)$$

where g is the gyromagnetic g-factor, with an axial wavefunction $\psi \to \gamma^5\psi = \psi_A$, to further decompose (4.4) into:

$$\frac{\bar{\psi}\sigma^{\mu\nu}\psi}{\text{"}\not{p}-m\text{"}} = \frac{m}{\rho^\beta\rho_\beta - m^2}\bar{\psi}\sigma^{\mu\nu}\psi - \frac{1}{2m}\frac{\varepsilon^{\mu\nu}{}_{\alpha\beta}\rho^{[\alpha}(p'+p)^{\beta]}}{\rho^\beta\rho_\beta - m^2}\bar{\psi}\gamma^5\psi - \frac{1}{2m}\frac{g}{2}\frac{\varepsilon^{\mu\nu}{}_{\alpha\beta}(p'-p)_\delta\rho^{[\alpha}}{\rho^\beta\rho_\beta - m^2}\bar{\psi}i\sigma^{\beta]\delta}\gamma^5\psi \quad ,(4.6)$$

with $q = p' - p$ as previously defined. This illustrates a) why (3.10) is desirable for compactness and b) how when fully-expanded, this compact notation reveals not only the second rank (spin 2) antisymmetric tensor $\bar{\psi}\sigma^{\mu\nu}\psi$ and first rank (spin 1) axial vector $\bar{\psi}\gamma^\beta\gamma^5\psi$ of (4.4), but also a second rank (spin 2) axial tensor $\bar{\psi}i\sigma^{\beta\delta}\gamma^5\psi$ (in the form of an axial magnetic moment term summed with q_δ) and a zero-rank (spin 0) pseudoscalar $\bar{\psi}\gamma^5\psi$. Most importantly, the magnetic monopole of (3.12) is built out of the term expanded in (4.4) and (4.6), and so contains all of these spin 0, 1 and 2 "vector" and "axial" objects. This will be very important to understanding the phenomenology of the observed strong interaction mesons, and in the next section, we shall show how these terms are indicative of the types of "vector (V)" and "axial (A)" mesons which mediate nuclear interactions.

5. Fermi-Dirac Exclusion Requires Using SU(3)$_C$ Quantum Chromodynamics for Yang-Mills Magnetic Monopoles, Yielding the Correct Baryon and Meson Color Wavefunctions

Returning to the main development, the Yang-Mills magnetic monopole $P^{\sigma\mu\nu}$ (3.12), when contracted to the differential three-form used in section 1, namely $P = P^{\sigma\mu\nu}dx_\sigma dx_\mu dx_\nu$, is an NxN matrix for SU(N). We have not yet chosen a particular Yang-Mills gauge group to associate with (3.12), and in principle, are free to use $P^{\sigma\mu\nu} = T^i P_i^{\sigma\mu\nu}$ with $f^{ijk}T_i = -i[T^j, T^k]$ generators and structure constants for whatever gauge group we wish to explore. But, (3.12) does contain exactly three fermion wavefunctions $\psi_{(1)}$, $\psi_{(2)}$ and $\psi_{(3)}$ and their associated propagators, so one is certainly motivated to *consider* the Yang-Mills gauge group SU(3). But is there anything that might *require* us to apply SU(3) via purely deductive logic?

The answer is yes: The Fermi-Dirac Exclusion Principle (with which Pauli's name is also often associated) requires that no two fermions within a

given system may simultaneously occupy the same quantum state. So if we regard $P^{\sigma\mu\nu}$ in (3.12) as a "system" containing three fermion wavefunctions and associated propagators, then we *must* utilize a gauge group that enables each of these three fermions to be distinguishable from one another with unique quantum numbers, similarly to how every electron within a given atom must possess a unique set of quantum numbers n, l, m, s generally associated with energy, orbital angular momentum and spin. The natural gauge group to achieve this exclusion, of course, is SU(3) (or SU(3)xU(1) as we shall momentarily discuss).

In fact, this is where QCD usually starts: If we understand baryons as containing three fermions which are quarks, and we know that Fermi-Dirac exclusion mandates these three quarks not simultaneously occupy the same quantum state, then we must introduce SU(3) or a variant thereof to enforce exclusion. So we call the quarks Red, Green, Blue as a matter of convention, set up an SU(3) Dirac Lagrangian for these quarks, impose gauge symmetry, and arrive at $SU(3)_C$ QCD.

In the present development, we discover that Yang-Mills magnetic monopoles naturally contain three fermions, we similarly require exclusion and so introduce $SU(3)_C$, *and we thereby arrive at exactly the same $SU(3)_C$ QCD theory, with no contradiction, simply from a different starting point*.

Accordingly, we now take the formal step of imposing quantum exclusion upon the three fermions in (3.12) by introducing the gauge group $SU(3)_C$ with generators $T^i = \lambda^i; i = 1...8$ normalized to $tr(\lambda^i)^2 = \frac{1}{2}$, and assigning these three fermions to one of three exclusive color eigenstates R, G, B, with associated quantum eigenvalues, as follows:

$$\psi_{(1)} \equiv \left|\lambda^8 = \tfrac{1}{\sqrt{3}}; \lambda^3 = 0\right\rangle = \begin{pmatrix} \psi_R \\ 0 \\ 0 \end{pmatrix}; \psi_{(2)} \equiv \left|\lambda^8 = -\tfrac{1}{2\sqrt{3}}; \lambda^3 = \tfrac{1}{2}\right\rangle = \begin{pmatrix} 0 \\ \psi_G \\ 0 \end{pmatrix}; \psi_{(3)} \equiv \left|\lambda^8 = -\tfrac{1}{2\sqrt{3}}; \lambda^3 = -\tfrac{1}{2}\right\rangle = \begin{pmatrix} 0 \\ 0 \\ \psi_B \end{pmatrix}. \quad (5.1)$$

These fermions are now specified in precisely the same way as the three colored *quarks* of QCD with $SU(3)_C$. Similarly, referring back to sections 1 and 2, the eight associated gauge bosons now become $G^\mu \equiv \lambda^i G_i^{\ \mu}$. And because of (2.2), all of the non-linear gluon interactions of QCD will be present here too. Further, earlier, between (3.3) and (3.6), we determined these gauge bosons *must* be massless for the quarks to acquire their expected non-zero mass. So these G^μ now have all the required characteristics to be the eight bi-colored, massless *gluons* of QCD. *The thesis that baryons are Yang-Mills magnetic monopoles does not contradict QCD in any way! Moreover, when combined with the Exclusion Principle, this thesis actually mandates*

QCD! But as shown in section 1, there is a bonus in this approach to QCD: the confinement of gauge fields is built into the theory from the start, whereas in many instances it is imposed by separate, ad-hoc mechanisms, see for example, the MIT bag model in, e.g., [7] section 18. This emergence of QCD also validates the "propagator hypothesis" which earlier yielded (3.6) from (2.11). Now, let's use (5.1) in the $P^{\sigma\mu\nu}$ of (3.12).

In the section 3, the spin sum (3.1) played a central role. From (5.1), let us form the three spin sum operands:

$$\psi_{(1)}\bar{\psi}_{(1)} = \begin{pmatrix} \psi_R\bar{\psi}_R & 0 & 0 \\ 0 & 0 & 0 \\ 0 & 0 & 0 \end{pmatrix}; \quad \psi_{(2)}\bar{\psi}_{(2)} = \begin{pmatrix} 0 & 0 & 0 \\ 0 & \psi_G\bar{\psi}_G & 0 \\ 0 & 0 & 0 \end{pmatrix}; \quad \psi_{(3)}\bar{\psi}_{(3)} = \begin{pmatrix} 0 & 0 & 0 \\ 0 & 0 & 0 \\ 0 & 0 & \psi_B\bar{\psi}_B \end{pmatrix} \quad (5.2)$$

We see very explicitly that each of these is a 3x3 color matrix in which the non-zero elements are 4x4 Dirac matrices $\psi\bar{\psi}$ (and the zeros are all 4x4 zeros). If we then start with (3.12) and backtrack through section 3 by applying $\sigma^{\mu\vee\nu} = \frac{i}{2}\left[\gamma^{\mu}\vee\gamma^{\nu}\right]$; (3.9); (3.7); (3.1) and $\psi\bar{\psi} = u\bar{u}$, and if we then substitute (5.2) into the backtracked result, we may obtain (with $\Sigma_{\text{spins}} \rightarrow \Sigma$ for notational compactness):

$$P^{\sigma\mu\nu} = -i\begin{pmatrix} \frac{1}{k^{\alpha}k_{\alpha}}\partial^{\sigma}\frac{\bar{\psi}_R\gamma^{\lambda\mu}\Sigma\psi_R\bar{\psi}_R\gamma^{\nu\rceil}\psi_R}{\rho_R{}^{\beta}\rho_{R\beta} - m_R{}^2} & 0 & 0 \\ 0 & \frac{1}{k^{\gamma}k_{\gamma}}\partial^{\mu}\frac{\bar{\psi}_G\gamma^{\lambda\nu}\Sigma\psi_G\bar{\psi}_G\gamma^{\sigma\rceil}\psi_G}{\rho_G{}^{\delta}\rho_{G\delta} - m_G{}^2} & 0 \\ 0 & 0 & \frac{1}{k^{\varepsilon}k_{\varepsilon}}\partial^{\nu}\frac{\bar{\psi}_B\gamma^{\lambda\sigma}\Sigma\psi_B\bar{\psi}_B\gamma^{\mu\rceil}\psi_B}{\rho_B{}^{\zeta}\rho_{B\zeta} - m_B{}^2} \end{pmatrix} \quad (5.3)$$

Then, forward tracking again through section 3, we reapply spin sums and normalizations, and arrive back at:

$$P^{\sigma\mu\nu} = -2\begin{pmatrix} \partial^{\sigma}\frac{\bar{\psi}_R\sigma^{\mu\vee\nu}\psi_R}{"\not{p}_R - m_R"} & 0 & 0 \\ 0 & \partial^{\mu}\frac{\bar{\psi}_G\sigma^{\nu\vee\sigma}\psi_G}{"\not{p}_G - m_G"} & 0 \\ 0 & 0 & \partial^{\nu}\frac{\bar{\psi}_B\sigma^{\sigma\vee\mu}\psi_B}{"\not{p}_B - m_B"} \end{pmatrix}. \quad (5.4)$$

The difference between (5.4) and (3.12) is that when we explicitly use the colored wavefunctions ψ_R, ψ_G, ψ_B rather than $\psi_{(1)}$, $\psi_{(2)}$ and $\psi_{(3)}$, the character of $P^{\sigma\mu\nu}$ as a 3x3 color matrix is made explicit. And, in a step that will have great topological significance, extracting the trace, we write:

$$\mathrm{Tr}P^{\sigma\mu\nu} = -2\left(\partial^{\sigma} \frac{\overline{\psi}_R \sigma^{\mu\wedge\nu} \psi_R}{"\not{p}_R - m_R"} + \partial^{\mu} \frac{\overline{\psi}_G \sigma^{\nu\wedge\sigma} \psi_G}{"\not{p}_G - m_G"} + \partial^{\nu} \frac{\overline{\psi}_B \sigma^{\sigma\wedge\mu} \psi_B}{"\not{p}_B - m_B"} \right). \tag{5.5}$$

The above is identical to (3.12), but for the fact that when we wish for the colored wavefunctions to appear explicitly in lieu of $\psi_{(1)}$, $\psi_{(2)}$ and $\psi_{(3)}$ in an analogous form, *we are required to employ the trace equation.*

Now, we have pointed out at the start of this section that developing Yang-Mills magnetic monopoles and then applying exclusion yields the basic required elements of QCD such as three colors of quark and eight bi-colored massless gluons, plus the added bonus of a gauge field confinement naturally built in from the start. But there is more: First, let us associate each color wavefunction with the spacetime index in the related ∂^{σ} operator in (5.5), i.e., $\sigma \sim R$, $\mu \sim G$ and $\nu \sim B$. Keeping in mind that $\mathrm{Tr}P^{\sigma\mu\nu}$ is antisymmetric in all spacetime indexes, we express this antisymmetry with wedge products as $\sigma \wedge \mu \wedge \nu \sim R \wedge G \wedge B$. So the natural antisymmetry of the magnetic monopole $P^{\sigma\mu\nu}$ leads straight to the required antisymmetric color singlet wavefunction $R[G,B]+G[B,R]+B[R,G]$ for a baryon (see [5] equation [2.70], and compare the top line term $\partial^{\sigma}[G^{\mu},G^{\nu}]+\partial^{\mu}[G^{\nu},G^{\sigma}]+\partial^{\nu}[G^{\sigma},G^{\mu}]$ of (2.4)). *That is, (5.5) has what is known to be the required antisymmetric color wavefunction for a baryon!* Indeed, one can argue that the antisymmetric indexes in $P^{\sigma\mu\nu}$ should have been a tip-off that magnetic monopoles would make good baryons.

Next, we showed in (1.3) that the invariance of $\oiint F$ under a gauge-like transformation $F^{\mu\nu} \rightarrow F^{\mu\nu\prime} = F^{\mu\nu} - \partial^{[\nu}G^{\mu]}$ means that no gauge bosons G^{μ} (now gluons $G^{\mu} \equiv \lambda^{i} G_{i}^{\ \mu}$) are allowed to flow across a closed surface surrounding a Yang-Mills magnetic monopole. So for $SU(3)_C$, the gluons are confined. So far, so good. But that only tells us what cannot flow. To find out what <u>*can*</u> flow, we return to $\iiint P = \oiint F = -i \oiint G^2$ from (1.1). Because $P = P^{\sigma\mu\nu} dx_{\sigma} dx_{\mu} dx_{\nu}$, let us multiply both sides of (5.5) by the anticommuting volume element $dx_{\sigma} dx_{\mu} dx_{\nu}$, form matching trace equations, take the triple integral, then apply Gauss' / Stokes' law to the right hand side and rename spacetime indexes. What we get is:

$$\iiint \mathrm{Tr}P = \oiint \mathrm{Tr}F = -i \oiint \mathrm{Tr}G^2 = -2 \iint \left(\frac{\overline{\psi}_R \sigma^{\mu\wedge\nu} \psi_R}{"\not{p}_R - m_R"} + \frac{\overline{\psi}_G \sigma^{\mu\wedge\nu} \psi_G}{"\not{p}_G - m_G"} + \frac{\overline{\psi}_B \sigma^{\mu\wedge\nu} \psi_B}{"\not{p}_B - m_B"} \right) dx_{\mu} dx_{\nu} . \tag{5.6}$$

The Gaussian integration has removed the ∂^σ operators from (5.5), and what remains by inspection in (5.6) is the symmetric color singlet wavefunction $\overline{R}R+\overline{G}G+\overline{B}B$. *This is precisely the symmetric color combination required for a meson!* But look at the context in which this meson wavefunction is revealed: if the integrand in (5.6) is in fact representative of mesons, then (5.6) taken together with section 1 makes a very clear statement: Mesons, not gluons, are what net flow across any closed surface surrounding a Yang-Mills magnetic monopole. *But one can say the exact same thing about what flows in and out of baryons!* And, the observed phenomenology of strong interactions makes very clear that baryons in fact emit and absorb mesons, and not individual quarks or gluons (see [8] especially 14.2 and [9] for a full exposition of experimentally-observed mesons and their spin classifications as scalars, vectors, tensors, etc. and axial variants). So this revelation of meson flow across the surface of a Yang-Mills magnetic monopole further supports the thesis that baryons are Yang-Mills magnetic monopoles, not only theoretically, *but based on experimentally-observed phenomenology. (5.6) says that Yang-Mills magnetic monopoles interact by emitting and absorbing mediating mesons!*

Importantly, however, the usual approaches to QCD do not provide a compelling deductive rationale for why mesons and not gluons are allowed to flow in and out of baryons, that is, they do not provide a natural deductive explanation for confinement and meson-based interaction. Often, confinement and meson flow are simply introduced through ad hoc mechanisms, again, see [7] section 18. Starting with Yang-Mills magnetic monopoles, this is fully explained on a deductive foundation, and so QCD is strengthened and supplemented, again, without contradiction.

Now, let's go a few steps step further: (5.6) tells us that mesons, with $\overline{R}R+\overline{G}G+\overline{B}B$ color structure, flow in and out of Yang-Mills magnetic monopoles. But what types of mesons? From (4.4) and (4.6) which expand the terms in (5.6), we see that the mesons which flow are: second rank (spin 2) antisymmetric tensor $\overline{\psi}\sigma^{\mu\nu}\psi$ mesons, which are designated phenomenologically as 2^+; first rank (spin 1) axial vector $\overline{\psi}\gamma^{\beta]}\gamma^5\psi$ mesons designated as 1^+; second rank (spin 2) axial tensor $\overline{\psi}i\sigma^{\beta]\delta}\gamma^5\psi$ mesons 2^-; and most importantly, zero-rank (spin 0) pseudoscalar $\overline{\psi}\gamma^5\psi$ mesons designated 0^-, which include the various π and K mesons and remaining generational mesons which dominate nuclear interactions and which Yukawa originally predicated in 1935 to be carrier particles of the strong nuclear force. This is

amply demonstrated to be experimentally true, see again, the extensive evidence at [8], [9]. In fact, the only mesons we have not yet come across when combining (4.4) and (4.6) with (5.6) are the spin 0 scalar $\overline{\psi}\gamma^5\psi$ mesons 0^+ and the spin 1 vector $\overline{\psi}\gamma^\nu\psi$ mesons 1^-. But these two will also make an appearance, as follows:

Designate axial wavefunctions via $\gamma^5 = i\gamma^0\gamma^1\gamma^2\gamma^3$ as $\psi_A = \gamma^5\psi_V$, where a "vector" (V) wavefunction ψ_V is defined as a wavefunction for which the related current density $J^\mu = \overline{\psi}_V\gamma^\mu\psi_V$ transforms as a Lorentz four-vector in spacetime. Based on combining the relationship $\gamma^5 = i\gamma^0\gamma^1\gamma^2\gamma^3$ with duality based on the work of Reinich [10] later elaborated by Wheeler [11] which uses the Levi-Civita formalism (see [12] at pages 87-89), it turns out that there is a whole system of "chiral duality" that is an integral, albeit (apparently) heretofore undeveloped feature of the Dirac algebra. For example, given a duality relationship $*A^{\mu\nu} \equiv \frac{1}{2!}\varepsilon^{\mu\nu\alpha\sigma}A_{\alpha\sigma}$, one may write $\gamma^5 = i\gamma^0\gamma^1\gamma^2\gamma^3$ in the alternative form $\sigma^{\mu\nu} = i*\sigma^{\mu\nu}\gamma^5$. Then, one may form $\overline{\psi}_V\sigma^{\mu\nu}\psi_V = i*\overline{\psi}_V\sigma^{\mu\nu}\psi_A$ by sandwiching between V wavefunctions.

Further, it is also well known because the second rank duality operator $**=-1$, that one can form continuous global rotations using $e^{*\theta} = \cos\theta + *\sin\theta$ (this is not to exclude local duality, which is also of interest). For example:

$$\begin{aligned}\overline{\psi}_V\sigma^{\mu\nu}\psi_V &\rightarrow \cos\theta\overline{\psi}_V\sigma^{\mu\nu}\psi_V + i\sin\theta\overline{\psi}_V\sigma^{\mu\nu}\psi_A \\ \overline{\psi}_V\sigma^{\mu\nu}\psi_A &\rightarrow i\sin\theta\overline{\psi}_V\sigma^{\mu\nu}\psi_V + \cos\theta\overline{\psi}_V\sigma^{\mu\nu}\psi_A\end{aligned} \quad (5.7)$$

Similar transformations may be developed for first / third and zeroth / fourth rank duality, with the result that tensors mix with axial tensors, vectors with axial vectors, and scalars with pseudoscalars. So in the end, we expect that the Yang-Mills magnetic monopoles will allow all of the spin $0^\pm$, $1^\pm$ and $2^\pm$ "vector" and "axial" mesons to pass through the closed surfaces (5.6). And $\gamma^5 = i\gamma^0\gamma^1\gamma^2\gamma^3$ can also be used to rewrite a spin *s* "vector" meson as a spin 4-*s* "axial" meson and a spin *s* "axial" meson as a spin 4-*s* "vector" meson. So $3^\pm$ and $4^\pm$ mesons will be permitted to flow as well. Further, there is nothing to prevent composite mesons such as $\overline{qqqq}$. And, when $\gamma^5 = i\gamma^0\gamma^1\gamma^2\gamma^3$ is applied to (3.10) as part of a Gordon decomposition (really, recomposition) of a vector current, it turns out that baryon and meson physics is endemically, organically *non-chiral*, which is consistent with what is experimentally observed, all with $\gamma^5 = i\gamma^0\gamma^1\gamma^2\gamma^3$ being the mainspring. Duality angle θ comes to be associated

with the strength of the running strong coupling α_S, and this in turn bears well-studied relationships, [13], [14] to experimental momentum transfer Q.

So, while we shall leave the development of this chiral duality to a separate paper, we simply note for now that fully developing the chiral duality of Dirac's equation and applying this to (4.6) may be one way to experimentally confirm the thesis that Baryons are Yang-Mills magnetic monopoles: simply probe nucleons at varying energies, study the chiral / spin $s^{\pm}$ characteristics of the meson debris that emerges from those probes, and correlate those chiral properties to the probe energies that were applied.

6. Yang-Mills Magnetic Monopoles Require the Topologically-Stable Gauge Group $SU(3)_C \times U(1)$

Now, let us examine the topological stability of the Yang Mills magnetic monopole baryons, by looking at several further aspects of (5.4) and (5.5). First, using the eight generators λ^i of $SU(3)_C$ let us write the left hand side of (5.5) as $P^{\sigma\mu\nu} = \lambda^i P_i^{\sigma\mu\nu}$. The off diagonal entries in (5.4) are manifestly zero, and as already discussed after (5.5), this leads to baryons and mesons respectively having $R[G,B]+G[B,R]+B[R,G]$ and $\overline{R}R+\overline{G}G+\overline{B}B$ color singlet wavefunctions, as required by QCD. This means that for the left and right hand sides of (5.4) to match up while having these required wavefunction color symmetries, all six of the $P_i^{\sigma\mu\nu}$ which sum with off-diagonal generators must be zero, i.e., $P_{1,2,4,5,6,7}{}^{\sigma\mu\nu} = 0$. Therefore:

$$P^{\sigma\mu\nu} = \lambda^i P_i^{\sigma\mu\nu} = \begin{pmatrix} \frac{1}{2\sqrt{3}} 2P_8^{\sigma\mu\nu} & 0 & 0 \\ 0 & -\frac{1}{2\sqrt{3}} P_8^{\sigma\mu\nu} + \frac{1}{2} P_3^{\sigma\mu\nu} & 0 \\ 0 & 0 & -\frac{1}{2\sqrt{3}} P_8^{\sigma\mu\nu} - \frac{1}{2} P_3^{\sigma\mu\nu} \end{pmatrix}. \qquad (6.1)$$

(Again, $tr(\lambda^i)^2 = \frac{1}{2}$.) However, because the assumed gauge group is the *simple* gauge group $SU(3)_C$ with all *traceless* generators, the trace of (6.1) is also zero, $\mathrm{Tr} P^{\sigma\mu\nu} = 0$. This contradicts (5.5), which has a non-zero trace, and leads us directly to an examination of topology.

In order for $P^{\sigma\mu\nu} = \lambda^i P_i^{\sigma\mu\nu}$ above to acquire a non-zero trace, we can no longer use $SU(3)_C$ alone, but *must* cross $SU(3)_C$ with a U(1) gauge group for which the generator has a non-zero trace. In particular, the U(1) generator will need to be a 3x3 unit matrix I_{3x3} times some constant number. We

designate this U(1) generator as λ^{15}, which we take for now to be a 3x3 remnant of the T^{15} generator of a simple gauge group $SU(N \geq 4)$. If we normalize this to $\mathrm{Tr}(\lambda^{15})^2 = \frac{1}{2}$, then $\lambda^{15} = \frac{1}{\sqrt{6}} I_{3x3}$. This should be reminiscent of electroweak theory in which a $U(1)_Y$ generator is crossed with the three $SU(2)_W$ isospin generators I^i to form $SU(2)_W \times U(1)_Y$ with the (left-chiral) quarks having the $U(1)_Y$ 2x2 hypercharge matrix generator $Y = \frac{1}{3} I_{2x2}$, the (left-chiral) leptons having the 2x2 hypercharge matrix generator $Y = -1 I_{2x2}$, and a *non-compact* embedding of the electromagnetic group with charge generator $Q = Y/2 + I^3$ across $SU(2)_W \times U(1)_Y$.

Once we employ $SU(3)_C \times U(1)$, rather than $SU(3)_C$ alone, we can now ensure that $\mathrm{Tr}P^{\sigma\mu\nu} = \frac{3}{\sqrt{6}} P_{15}{}^{\sigma\mu\nu}$ on the left hand side of (5.5) will be non-vanishing to match its non-vanishing right hand side, and that (5.6) will then describe a non-zero flow across the closed monopole surface of objects with the color symmetry $\overline{R}R + \overline{G}G + \overline{B}B$ of a meson. Specifically, with $SU(3)_C \times U(1)$ and $i = 1...8$ and 15, we write (5.4) as:

$$P^{\sigma\mu\nu} = \lambda^i P_i^{\sigma\mu\nu} = \begin{pmatrix} \frac{1}{\sqrt{6}} P_{15}{}^{\sigma\mu\nu} + \frac{1}{2\sqrt{3}} 2P_8^{\sigma\mu\nu} & 0 & 0 \\ 0 & \frac{1}{\sqrt{6}} P_{15}{}^{\sigma\mu\nu} - \frac{1}{2\sqrt{3}} P_8^{\sigma\mu\nu} + \frac{1}{2} P_3^{\sigma\mu\nu} & 0 \\ 0 & 0 & \frac{1}{\sqrt{6}} P_{15}{}^{\sigma\mu\nu} - \frac{1}{2\sqrt{3}} P_8^{\sigma\mu\nu} - \frac{1}{2} P_3^{\sigma\mu\nu} \end{pmatrix} \quad (6.2)$$

$$= -2 \begin{pmatrix} \partial^\sigma \frac{\overline{\psi}_R \sigma^{\mu,\nu} \psi_R}{" p_R - m_R "} & 0 & 0 \\ 0 & \partial^\mu \frac{\overline{\psi}_G \sigma^{\nu,\sigma} \psi_G}{" p_G - m_G "} & 0 \\ 0 & 0 & \partial^\nu \frac{\overline{\psi}_B \sigma^{\sigma,\mu} \psi_B}{" p_B - m_B "} \end{pmatrix}$$

The non-vanishing trace equation (5.5) then becomes:

$$\mathrm{Tr}P^{\sigma\mu\nu} = \frac{3}{\sqrt{6}} P_{15}{}^{\sigma\mu\nu} = -2 \left(\partial^\sigma \frac{\overline{\psi}_R \sigma^{\mu,\nu} \psi_R}{" p_R - m_R "} + \partial^\mu \frac{\overline{\psi}_G \sigma^{\nu,\sigma} \psi_G}{" p_G - m_G "} + \partial^\nu \frac{\overline{\psi}_B \sigma^{\sigma,\mu} \psi_B}{" p_B - m_B "} \right). \quad (6.3)$$

So the left and right hand sides are now both non-zero, but this is only achieved using $SU(3)_C \times U(1)$ rather than $SU(3)_C$ alone. We see that with (6.1) alone, i.e., with a simple gauge group $SU(3)_C$ alone, the right hand term would become zero. *This U(1) factor, which prevents the right hand sides of (6.2) and (6.3) from vanishing, is very important to providing topological stability.*

In section 7, we will examine the possible physical meaning of the quantum numbers associated with this new U(1) factor. But first, we point out the very vital benefit flowing from (6.3): *this U(1) factor, by making (6.3)*

non-zero, will allow us to ensure that these Yang-Mills magnetic monopole baryons are topologically stable. This is vital, because even though Yang-Mills magnetic monopoles with Fermi-Dirac exclusion lead us to all of the symmetries of QCD and baryons, to wit: gauge field confinement, three colored fermions, a $R[G,B]+G[B,R]+B[R,G]$ baryon wavefunction, mesons with $\overline{R}R+\overline{G}G+\overline{B}B$ wavefunctions, and spin 0, 1 and 2 "vector" and "axial" mesons but no gluons flowing across the baryon surface, we still cannot identify the Yang-Mills magnetic monopole with the physical, observed baryons, for example, proton and neutrons, until we have established that this magnetic monopole is a topologically stable with finite spatial expanse and finite total energy, and with the correct set of *flavor* quantum numbers (most importantly, electric charge and baryon number) which characterize the observed physical baryons. $SU(3)_C \times U(1)$ does just that!

Specifically, as is pointed out by Cheng and Li [15] at 472-473: "Topological considerations lead to the general result that stable monopole solutions occur for any gauge theories in which a *simple* gauge group G is broken down to a smaller group $H = h \times U(1)$ containing an explicit U(1) factor." Further, "the stable grand unified monopole . . . is expected to have both the 'ordinary' and the colour magnetic charges." So, while $SU(3)_C$ alone is incapable of supporting a topologically stable colored magnetic monopole, the group $SU(3)_C \times U(1)$ – when understood to be the residual group following symmetry breaking of a larger simple grand unified gauge group $G \supset SU(3)C \times U(1)$ – *will support topologically stable configurations.* Indeed, in this context, the thesis of this paper is that *the stable "colour magnetic charges" referred to by Cheng and Li are baryons.*

Weinberg makes a similar point in his definitive treatise [16] at 442:

> "The Georgi-Glashow model" [which was the basis for t'Hooft's monopole model in [1] discussed at length in section 9 below] "was ruled out as a theory of weak and electromagnetic interactions by the discovery of neutral currents, but magnetic monopoles are expected to occur in other theories, where a simply connected gauge group G is spontaneously broken not to U(1), but to some subgroup $H' \times U(1)$, where H' is simply connected. . . . There are no monopoles produced in the spontaneous breaking of the gauge group $SU(2) \times U(1)$ of the standard electroweak theory, which is not simply connected. . . . But we do find monopoles when the simply connected gauge group G of theories of unified strong

and electroweak interactions, such as $SU(4)\times SU(4)$ or $SU(5)$ or $Spin(10$, is spontaneously broken to the gauge group $SU(3)\times SU(2)\times U(1)$ of the standard model. . . ."

Consequently, the thesis that Yang-Mills magnetic monopoles are baryons, together with the exclusion principle as applied in (5.1), not only leads us to $SU(3)_C$ of QCD with no contradiction and delivers color confinement and the flow of mesons across monopole surface. Via the non-zero and non-trivial right hand side of (6.3), this thesis additionally forces us to employ the non-simple gauge group $SU(3)_C\times U(1)$ with a U(1) factor to ensure that the monopoles are non-vanishing. Not only does this, in turn, lay the foundation for a topologically stable monopole achieved by embedding this group in some (presently unspecified) simple group $G=SU(N\geq 4)\supset SU(3)_C\times U(1)$, but the right side of (6.3) will itself be the expression from which we may calculate a finite baryon rest mass, as we shall later see in section 11, based on a Gaussian *ansatz* borrowed from [3].

So, what we learn from (6.1) through (6.3) is the following: First, we must start from a simple GUT gauge group $SU(N\geq 4)$ because all the generators of this group are traceless and therefore the gauge theory based on these groups will be renormalizable, as will be in hidden form, any smaller group $H\subset SU(N\geq 4)$ theory which emerges from $SU(N\geq 4)$ following symmetry breaking. It is through the traceless $SU(N\geq 4)$ generators that we ensure renormalizability. But the traceless matrices of $SU(N\geq 4)$ will cause the monopole trace terms of such a theory to be zero, $\mathrm{Tr}P^{\sigma\mu\nu}=0$. Therefore, such a theory with a simple gauge group will itself will have no stable monopoles. The only way to *simultaneously* have renormalizability and have stable monopoles, as the above excerpts from [15], [16] illustrate, is to start with a simple G and break this down to a smaller group $H = h\times U(1)$. And, once we break symmetry and end up with $SU(N\geq 4)\rightarrow SU(3)_C\times U(1)$, we simultaneously have two benefits: First, the $SU(3)_C\times U(1)$ theory will inherit the renormalizability of $SU(N\geq 4)$ as a hidden symmetry. Second, the monopoles of $SU(3)_C\times U(1)$ will become non-zero as in (6.3), and the U(1) factor emerging from breaking symmetry will make the monopoles topologically stable. So the tracelessness of (6.1) based on $S(3)_C$, contrasted with the non-zero-non-trivial trace of (6.2) and (6.3) based on $SU(3)_C\times U(1)$, is a concrete illustration of the topological theorem that magnetic monopoles only exist in a theory with $H = h\times U(1)$ that is broken from a larger G.

This is what directly yields the monopole stability of the topological theorems as discussed above, and as we shall see, this is what will provide us with the ability to calculate finite monopole rest masses, for example, the proton and neutron "current" rest masses, and to obtain the electron rest mass from the up and down quark masses well within experimental errors and only about 3% from the experimental means for quark masses, and to obtain binding energies clearly in accord with measured nuclear phenomenology.

7. Protons and Neutrons Naturally Fit Fundamental $SU(3)_C \times U(1)_{B-L}$ Representations of Yang-Mills Magnetic Monopoles

Now let us take a closer look at the groups $G = SU(N \geq 4) \supset \mathrm{SU(3)_C} \times \mathrm{U(1)}$ which we came upon in section 6 and which will undergird the topological stability for the Yang-Mills magnetic monopole. Volovok, in [17] Section 12.2.2, employs an SU(4) group in which the normalized $\mathrm{diag}(\lambda^{15}) = \frac{1}{2\sqrt{6}}(3,-1,-1,-1)$ is associated with the difference between baryon number and lepton number, $B-L$. Specifically, $L-B = \frac{2\sqrt{2}}{\sqrt{3}}\mathrm{diag}(\lambda^{15}) = (1,-\frac{1}{3},-\frac{1}{3},-\frac{1}{3})$ provides a very natural fundamental representation for fermion eigenstates of one lepton and three (colored) quarks. The Volovok model then goes on to use preon eigenstates, but we shall not do so here. Instead, we shall show how this same approach, with the λ^{15} generator of SU(4) being proportional to $B-L$, may be used to directly represent protons and electrons on the one hand, and neutrons and neutrinos on the other, in relation to the Yang-Mills magnetic monopoles that we have developed this far.

Following [17], and using the simple gauge group SU(4), let us normalize via $Tr(\lambda^{i\,2}) = \frac{1}{2}$ the two λ^{15} and λ^{8} generators, and define a third embedded electric charge generator $Q \equiv B-L-\frac{2}{\sqrt{3}}\lambda^8 = -\frac{2}{\sqrt{3}}\left(\sqrt{2}\lambda^{15}+\lambda^8\right)$ sitting across these, as such:

$$B-L \equiv -\sqrt{\tfrac{8}{3}}\lambda^{15} = \begin{pmatrix} -1 & 0 & 0 & 0 \\ 0 & \frac{1}{3} & 0 & 0 \\ 0 & 0 & \frac{1}{3} & 0 \\ 0 & 0 & 0 & \frac{1}{3} \end{pmatrix}; \quad \tfrac{2}{\sqrt{3}}\lambda^8 = \begin{pmatrix} 0 & 0 & 0 & 0 \\ 0 & \frac{2}{3} & 0 & 0 \\ 0 & 0 & -\frac{1}{3} & 0 \\ 0 & 0 & 0 & -\frac{1}{3} \end{pmatrix}; \quad Q \equiv B-L-\tfrac{2}{\sqrt{3}}\lambda^8 = \begin{pmatrix} -1 & 0 & 0 & 0 \\ 0 & -\frac{1}{3} & 0 & 0 \\ 0 & 0 & \frac{2}{3} & 0 \\ 0 & 0 & 0 & \frac{2}{3} \end{pmatrix}. \quad (7.1)$$

In the fundamental representation we may then specify associated eigenvectors with the *flavor* quantum numbers:

$$\begin{pmatrix} e \\ 0 \\ 0 \\ 0 \end{pmatrix} \equiv \left|B=0;L=1;Q=-1\right\rangle \quad \begin{pmatrix} 0 \\ d_R \\ 0 \\ 0 \end{pmatrix} \equiv \left|B=\tfrac{1}{3};L=0;Q=-\tfrac{1}{3}\right\rangle \quad \begin{pmatrix} 0 \\ 0 \\ u_G \\ 0 \end{pmatrix} \equiv \left|B=\tfrac{1}{3};L=0;Q=\tfrac{2}{3}\right\rangle \quad \begin{pmatrix} 0 \\ 0 \\ 0 \\ u_B \end{pmatrix} \equiv \left|B=\tfrac{1}{3};L=0;Q=\tfrac{2}{3}\right\rangle \qquad .(7.2)$$

These quantum numbers are chiral symmetric, i.e., they are the same for both left and right handed states. Moreover, these exactly fit the expected baryon, lepton, and electric charge quantum numbers for the fermion quadruplet e,d_R,u_G,u_B. In contrast to many approaches which attempt to place all three colors of the same flavor of quark in the same multiplet, that is, u_R,u_G,u_B or d_R,d_G,d_B, the assignments (7.1) and (7.2) put one (red) down quark together with two (green and blue) up quarks in the fundamental representation. This flavor assemblage is exactly what we find in a proton! Moreover, because the election is the final member of this quadruplet, this representation yields a quadruplet for which all the generators remain traceless, which as discussed previously, yields a renormalizable gauge theory. Further, this renormalizability will be preserved during symmetry breaking to separate the electron from the three quarks comprising the proton. And the zero trace of the Q generator in (7.1) is what makes the combination of a proton plus and electron, which corresponds to a H^1 hydrogen atom, electrically neutral.

Because the color triplet in the SU(3) subgroup is a mix of flavor and color d_R,u_G,u_B and not a pure mono-flavored color triplet R,G,B, specifically because *u* and *d* also have a *weak isospin* relation between them, we shall refer to (7.2) as the "proton representation" of the "isospin-modified color group" *C'*, designated $SU(3)_{PC'}$. With (7.1) and (7.2), we now associate the $SU(3)_{PC'}$ subgroup which we have hitherto argued is a baryon, with perhaps the most important baryon of all, namely, the proton. The unbroken SU(4) group contains a proton and an electron. So we shall name this the $SU(4)_P$ "protium" group because it contains the precise same constituents as H^1 hydrogen, which is the most abundant chemical substance in the material universe. At the presumably very high GUT energies where this group is unbroken, the quarks may of course transform into electrons and vice versa. But because $SU(4)_P$ is a simple gauge group with all traceless matrices, the magnetic monopoles of this simple group itself will be topologically unstable, with $\mathrm{Tr}P^{\sigma\mu\nu}=0$, recall the discussion in section 6.

When symmetry breaking, we will wish to choose the Higgs sector such that this group breaks down via $SU(4)_P \to SU(3)_{PC'} \times U(1)_{B-L}$, where the $U(1)_{B-L}$ factor now represents the baryon minus lepton number generator

$\text{diag}(B-L)=\left(-1,\frac{1}{3},\frac{1}{3},\frac{1}{3}\right)$ of (7.1). Then, referring to (6.2) and (6.3), and using the $SU(3)_{PC'}$ subgroup for the three quarks, we see that $\text{Tr}P^{\sigma\mu\nu}=\left|B=1;Q=1\right\rangle$. Specifically: $\text{Tr}P^{\sigma\mu\nu}$ now represents a topologically stable magnetic monopole containing two up quarks and one down quark, with color symmetry $R[G,B]+G[B,R]+B[R,G]$, with its gauge fields confined, with mesons $\overline{R}R+\overline{G}G+\overline{B}B$ allowed to pass through the surface to mediate its interactions, with baryon number $B=+1$ and electric charge $Q=+1$, and it most naturally pairs with the electron with $L=1$ and $Q=-1$ from which it becomes broken at high energy when $SU(4)_P \rightarrow SU(3)_{PC'}\times U(1)_{B-L}$. *This is thus perfectly situated to represent an actual physical proton.* Because this group is $SU(3)_{PC'}\times U(1)_{B-L}$, the non-zero trace of the U(1) "remnant" generator $\text{diag}(B)=\left(\frac{1}{3},\frac{1}{3},\frac{1}{3}\right)$ is what prevents the term on the right hand side of (6.3) from being zeroed by the term on the left, and because of this U(1) factor, the topological theorems tell us that this Yang-Mills magnetic monopole proton is a stable field configuration, as it must be to represent the physical proton. Finally, as we shall soon see by borrowing a Gaussian *ansatz* from [3], $\text{Tr}P^{\sigma\mu\nu}=\left|B=1;Q=1\right\rangle$ is the term from which one can calculate explicitly that this magnetic monopole baryon proton has a finite, calculable energy!

Neutrons are developed in a somewhat similar manner to protons. Here, we note that $\frac{2}{\sqrt{3}}\lambda^8$ in (7.1) has the required eigenvalues to represent the electric charges of the three quarks in a neutron, plus a neutrino, and that the $B-L\equiv-\frac{2\sqrt{2}}{\sqrt{3}}\lambda^{15}$ of (7.1) will also properly characterize the baryon and lepton numbers of these fermions. So for neutrons and neutrinos, in contrast to (7.1), we use:

$$B-L\equiv-\sqrt{\tfrac{8}{3}}\lambda^{15}=\begin{pmatrix}-1&0&0&0\\0&\frac{1}{3}&0&0\\0&0&\frac{1}{3}&0\\0&0&0&\frac{1}{3}\end{pmatrix}\qquad Q\equiv\tfrac{2}{\sqrt{3}}\lambda^8=\begin{pmatrix}0&0&0&0\\0&\frac{2}{3}&0&0\\0&0&-\frac{1}{3}&0\\0&0&0&-\frac{1}{3}\end{pmatrix} \tag{7.3}$$

and then may specify the associated eigenvectors with the indicated quantum numbers:

$$\begin{pmatrix}\nu\\0\\0\\0\end{pmatrix}\equiv\left|B=0;L=1;Q=0\right\rangle\quad\begin{pmatrix}0\\u_R\\0\\0\end{pmatrix}\equiv\left|B=\tfrac{1}{3};L=0;Q=\tfrac{2}{3}\right\rangle\quad\begin{pmatrix}0\\0\\d_G\\0\end{pmatrix}\equiv\left|B=\tfrac{1}{3};L=0;Q=-\tfrac{1}{3}\right\rangle\quad\begin{pmatrix}0\\0\\0\\d_B\end{pmatrix}\equiv\left|B=\tfrac{1}{3};L=0;Q=-\tfrac{1}{3}\right\rangle \tag{7.4}$$

Here, the electric charge generators Q do *not* sit irregularly embedded across λ^{15} and λ^{8} as they do for the proton. Instead, the Q are directly, regularly embedded into λ^{8} alone. Here, the quadruplet ν, u_R, d_G, d_B contains a neutrino, together with one up quark and two down quarks. This specifies a neutron and a neutrino, and so we shall refer to this as the $SU(4)_N$ "neutrium" group. This too has a traceless (neutral sum) charge generator. Here, a "neutron representation" of the "isospin-modified color group" C' contains a neutron triplet of quarks u_R, d_G, d_B, and we shall designate this as $SU(3)_{NC'}$. When $SU(4)_N$ is broken down to $SU(3)_{NC'} \times U(1)_{B-L}$, the SU(3) magnetic monopole containing three quarks now has $\mathrm{Tr}P^{\sigma\mu\nu} = |B=1; Q=0\rangle$ with wavefunction type $R[G,B]+G[B,R]+B[R,G]$, and thus represents a neutron.

8. Protons and Neutrons and Electrons and Neutrinos Emerge from Spontaneous Symmetry Breaking of a Simple $SU(4)_{B-L}$ Group Down to $SU(3)_{C'} \times U(1)_{B-L}$

Exactly how do we break these SU(4) symmetries? The Georgi-Glashow SU(5) model [18] provides a good template, so let's briefly review that first. This model has 5x5-1=24 generators T^i. One specifies a set of 24 real Higgs scalars $\phi_i; i = 1 \ldots 24$ in the *adjoint* representation of SU(5), and from those, the 5x5 vacuum matrix $\Phi = T^i \phi_i$. Because the diagonal generators $\lambda^{24}, \lambda^{15}, \lambda^{8}, \lambda^{3}$ can be combined to form any 5x5 *traceless* matrix that one wishes, one uses these to form a hypercharge generator $\mathrm{diag}(Y/2) = \left(-\frac{1}{3}, -\frac{1}{3}, -\frac{1}{3}, \frac{1}{2}, \frac{1}{2}\right)$, which is $Y/2 = -\frac{\sqrt{10}}{6}T^{24} - \frac{5\sqrt{6}}{18}T^{15} - \frac{5\sqrt{3}}{9}T^{8}$ with the $\mathrm{Tr}(T^{i^2}) = \frac{1}{2}$ normalization. Then, using the regularly-embedded generator $\mathrm{diag}(I^3) = \left(0,0,0,\frac{1}{2},-\frac{1}{2}\right)$, one also irregularly embeds the electric charge $Q = Y/2 + I^3$, which leads to $\mathrm{diag}(Q) = Y/2 + I^3 = \left(-\frac{1}{3}, -\frac{1}{3}, -\frac{1}{3}, 1, 0\right)$. The right-chiral quintuplet $(d_R, d_G, d_B, e_C, -\nu_C)_R$ then matches up perfectly with these Q, Y, I^3 to form the fundamental SU(5) representation.

Symmetry breaking is specified using the Y generator *such that* $\mathrm{diag}(\Phi) = \mathrm{diag}(T^i \phi_i) = v_{GUT}\left(-\frac{1}{3}, -\frac{1}{3}, -\frac{1}{3}, \frac{1}{2}, \frac{1}{2}\right)$, that is, $\Phi = v_{GUT}\, Y/2$, where v_{GUT} is a vacuum expectation value at which the symmetry breaking takes place. The rest follows: Given the irregular embedding

$Y/2 = -\frac{\sqrt{10}}{6}T^{24} - \frac{5\sqrt{6}}{18}T^{15} - \frac{5\sqrt{3}}{9}T^{8}$, we must now set $\phi_{24} = -\frac{\sqrt{10}}{6}v_{GUT}$, $\phi_{15} = -\frac{5\sqrt{6}}{18}v_{GUT}$ and $\phi_{8} = -\frac{5\sqrt{3}}{9}v_{GUT}$ with the remaining $\phi_i = 0$, to obtain $\mathrm{diag}(\Phi) = v_{GUT}\left(-\frac{1}{3},-\frac{1}{3},-\frac{1}{3},\frac{1}{2},\frac{1}{2}\right)$. Thus, ${\phi_{24}}^2 + {\phi_{15}}^2 + {\phi_8}^2 = \frac{5}{3}v^2{}_{GUT} = C^2 v^2{}_{GUT}$, where $C^2 = \frac{5}{3}$ is the Clebsch-Gordon coefficient. If we then irregularly embed the usual $\lambda^i, i = 1\ldots8$ of $SU(3)_C$ into the 3x3 matrix in the upper left of SU(5) to form λ'^i, and assign the $I^i, i = 1,2,3$ of weak $SU(2)_W$ to the regularly embedded 2x2 matrix in the lower right, we find that the vacuum $\Phi = v_{GUT}\,Y/2$ commutes such that $\left[\Phi,\lambda'^i\right] = 0$, $i = 1\ldots8$, and $\left[\Phi,I^i\right] = 0$, $i = 1,2,3$, i.e., that the vacuum remains invariant under both $SU(3)_C$ and $SU(2)_W$ local gauge transformations $e^{i\lambda'^i\theta_i}$ and $e^{iI^i\theta_i}$. Additionally, the Y generator used to break the symmetry of course commutes with itself, $[\Phi,Y] = v_{GUT}[Y,Y]/2 = 0$, and so also leaves the vacuum invariant under $e^{iY\theta}$ $U(1)_Y$ transformations. This is how we arrive at $SU(3)_C \times SU(2)_W \times U(1)_Y$ following symmetry breaking, as it is these three subgroups which commute with the vacuum $\Phi = T^i\phi_i$. The further embedded $Q = Y/2 + I^3$ then leaves the ability to engage in a second stage of symmetry breaking, using an SU(2) Higgs doublet in the *fundamental* representation of SU(2) at another vev v~246 GeV which happens to be the Fermi vacuum. From this, one obtains the electromagnetic interaction.

An important feature of all of this, of course, is that by virtue of the topological theorems discussed earlier, the product group following SU(5) → $SU(3)_C \times SU(2)_W \times U(1)_Y$ symmetry breaking will contain stable magnetic monopoles, by virtue of SU(5) being a simple gauge group. And, of course, we are ensured that the broken theory will retain the renormalizability of the unbroken theory.

With Georgi-Glashow SU(5) [18] as a backdrop, we are now ready to break the symmetry of the protium and neutrium groups via $SU(4)_P \to SU(3)_{PC'} \times U(1)_{B-L}$ and $SU(4)_N \to SU(3)_{NC'} \times U(1)_{B-L}$. As reviewed above, in Georgi and Glashow, symmetry is broken using hypercharge generator $\mathrm{diag}(Y/2) = \left(-\frac{1}{3},-\frac{1}{3},-\frac{1}{3},\frac{1}{2},\frac{1}{2}\right)$. Here, we will instead use the generator $B-L$ of both (7.1) and (7.3), with $\mathrm{diag}(B-L) = \left(-1,\frac{1}{3},\frac{1}{3},\frac{1}{3}\right)$, to break the symmetry of both the protium and neutrium groups. In the former case, this will separate the electron from the proton, and in the latter, this will separate the neutrino from the neutron. In SU(5), we broke symmetry by

requiring (defining) that $\mathrm{diag}(\Phi)=\mathrm{diag}(T^i\phi_i)\equiv v_{GUT}\left(-\frac{1}{3},-\frac{1}{3},-\frac{1}{3},\frac{1}{2},\frac{1}{2}\right)$. Here, in contrast, we require that:

$$\mathrm{diag}(\Phi)=\mathrm{diag}(T^i\phi_i)\equiv v_{GUT}\left(-1,\tfrac{1}{3},\tfrac{1}{3},\tfrac{1}{3}\right)=v_{GUT}\mathrm{diag}(B-L),\text{i.e.,}\Phi=v_{GUT}(B-L),\quad(8.1)$$

Because $B-L\equiv-\sqrt{\frac{8}{3}}\lambda^{15}$ is regularly embedded in both $SU(4)_P$ and $SU(4)_N$, the symmetry breaking is somewhat easier than in SU(5). We merely set $\phi_{15}=-\sqrt{\frac{8}{3}}v_{GUT}$ and the remaining $\phi_i=0$ to obtain $\mathrm{diag}(\Phi)=v_{GUT}\left(-1,\frac{1}{3},\frac{1}{3},\frac{1}{3}\right)$. By inspection, ${\phi_{15}}^2=\frac{8}{3}{v^2}_{GUT}$, yielding a Clebsch Gordon coefficient $C^2=\frac{8}{3}$. Because $\left[\Phi,\lambda^i\right]=0,i=1\ldots8$, the vacuum is invariant under the $SU(3)_{C'}$ subgroup which for $SU(4)_P$ contains the proton triplet d_R,u_G,u_B, and which for $SU(4)_N$ contains the neutron triplet u_R,d_G,d_B. Additionally, of course, $[\Phi,B-L]=0$ is self-commuting, which yields the $U(1)_{B-L}$ subgroup for both the proton and neutron quark triplets.

For present purposes, where stable magnetic monopoles are of primary interest, the fact that we now have developed non-simple gauge groups $SU(3)_{C'}\times U(1)_{B-L}$ out of the simple gauge groups $SU(4)_P$ and $SU(4)_N$ for both protons and neutrons which we denote in consolidated form as $SU(4)_{P,N}$, tells us that these colored $SU(3)_{C'}$ magnetic monopoles will be topologically stable objects. Further, with L=0 for the fermions in the $SU(3)_{C'}$ representation, $U(1)_{B-L}\rightarrow U(1)_B$. Topologically speaking, referring again to Weinberg's [16] at 442, the homotopy groups associated with this symmetry breaking are:

$$\begin{aligned}\pi_2\left(SU(4)_{P,N}/SU(3)_{C'}\times U(1)_{B-L}\right)&=\pi_1\left(SU(3)_{C'}\times U(1)_B\right)\\&=\pi_1\left(SU(3)_{C'}\right)\times\pi_1\left(U(1)_B\right)=\pi_1\left(U(1)_B\right)=Z\end{aligned}\quad.(8.2)$$

The final terms, $\pi_1\left(SU(3)_{C'}\right)\times\pi_1\left(U(1)_B\right)=\pi_1\left(U(1)_B\right)=Z$, tell us that the topologically-stable magnetic monopoles are formed out of the $SU(3)_{C'}$ triplet of Fermions each with B=1/3 from $U(1)_B$, and so these stable $SU(3)_{C'}$ monopoles have B=1. *The baryons are now stable magnetic monopoles!*

Returning to (6.2) and (6.3) where this topological discussion began, following symmetry breaking the leptons separate from the quarks and $P^{\sigma\mu\nu}$ is formed only from the unbroken $SU(3)_{C'}$ subset of quarks, for which L=0. Thus, after symmetry breaking, $CP^{\sigma\mu\nu}=-BP_{15}{}^{\sigma\mu\nu}$ with $C=\sqrt{\frac{8}{3}}$. So the trace equation corresponding to (6.3) is then developed from the $SU(3)_{C'}$ subgroup, using the U(1) generator $\mathrm{diag}(B)=\left(\frac{1}{3},\frac{1}{3},\frac{1}{3}\right)$ for which $\mathrm{Tr}B=1$. Taking the trace

of each side of $CP^{\sigma\mu\nu} = -BP_{15}{}^{\sigma\mu\nu}$ thus yields $CTrP^{\sigma\mu\nu} = -P_{15}{}^{\sigma\mu\nu}$, which combined with (6.3) then yields:

$$C\mathrm{Tr}P^{\sigma\mu\nu} = -P_{15}{}^{\sigma\mu\nu} = -2C\left(\partial^{\sigma}\frac{\overline{\psi}_R\sigma^{\mu\vee\nu}\psi_R}{"p_R - m_R"} + \partial^{\mu}\frac{\overline{\psi}_G\sigma^{\nu\vee\sigma}\psi_G}{"p_G - m_G"} + \partial^{\nu}\frac{\overline{\psi}_B\sigma^{\sigma\vee\mu}\psi_B}{"p_B - m_B"}\right). \quad (8.3)$$

Contrasting (6.3) with (8.3), we see that $\mathrm{Tr}P^{\sigma\mu\nu} = \frac{3}{\sqrt{6}}P_{15}{}^{\sigma\mu\nu}$ in (6.3) is replaced above by $\mathrm{Tr}P^{\sigma\mu\nu} = -P_{15}{}^{\sigma\mu\nu}/C$ where the Clebsch-Gordon $C = \sqrt{\frac{8}{3}}$, that is, we see that the coefficient of $P_{15}{}^{\sigma\mu\nu}$ is different. In the (6.3) where the U(1) group was tacked on to SU(3), this coefficient emerged from establishing $\lambda^{15} = \frac{1}{\sqrt{6}}I_{3x3}$ normalized to $Tr\left(\lambda^{15^2}\right) = \frac{1}{2}$, hence $\mathrm{Tr}\lambda^{15} = \frac{3}{\sqrt{6}}$. In (8.3), this coefficient is now replaced simply by -1/C, which is a remnant from $SU(4)_{P,N}$ following symmetry breaking.

It is the presence of this Clebsch-Gordon coefficient in (8.3) which now incorporates the symmetry breaking which moved us from $SU(4)_P \to SU(3)_{PC'} \times U(1)_{B-L}$ and $SU(4)_N \to SU(3)_{NC'} \times U(1)_{B-L}$. Referring to (8.2), $P^{\sigma\mu\nu}$ in (8.3) is now the topologically-stable magnetic monopole $\pi_1\left(SU(3)_{C'}\right) \times \pi_1\left(U(1)_B\right) = \pi_1\left(U(1)_B\right) = Z$ that we obtain following symmetry breaking, and *the very presence of this coefficient C, rather than a normalization constant from the tacked-on U(1) of section 6, tells us that this is a stable monopole that emerged following symmetry breaking from a larger gauge group*. In other words, if a monopole has a Clebsch-Gordon C next to it as in (8.3), that signals that the monopole is topologically stable, because it emerged following symmetry breaking from a larger group.

For the stable proton monopole of $SU(3)_{PC'}$, the "red" quark will be associated with the down quark, see (7.2), and the "green" and "blue" quarks with the two up quarks, as a chosen convention. So we now write (8.3) as:

$$\mathrm{CTr}P^{\sigma\mu\nu}{}_{\mathrm{P}} = -P_{15}{}^{\sigma\mu\nu}{}_{\mathrm{P}} = -2C\left(\partial^{\sigma}\frac{\overline{\psi}_{dR}\sigma^{\mu\vee\nu}\psi_{dR}}{"p_{dR} - m_{dR}"} + \partial^{\mu}\frac{\overline{\psi}_{uG}\sigma^{\nu\vee\sigma}\psi_{uG}}{"p_{uG} - m_{uG}"} + \partial^{\nu}\frac{\overline{\psi}_{uB}\sigma^{\sigma\vee\mu}\psi_{uB}}{"p_{uB} - m_{uB}"}\right). \quad (8.4)$$

This expression, we associate directly with a physical proton and its duu constituents. For the stable neutron monopole of $SU(3)_{NC'}$, see (7.4), we similarly write:

$$\mathrm{CTr}P^{\sigma\mu\nu}{}_{\mathrm{N}} = -P_{15}{}^{\sigma\mu\nu}{}_{\mathrm{N}} = -2C\left(\partial^{\sigma}\frac{\overline{\psi}_{uR}\sigma^{\mu\vee\nu}\psi_{uR}}{"p_{uR} - m_{uR}"} + \partial^{\mu}\frac{\overline{\psi}_{dG}\sigma^{\nu\vee\sigma}\psi_{dG}}{"p_{dG} - m_{dG}"} + \partial^{\nu}\frac{\overline{\psi}_{dB}\sigma^{\sigma\vee\mu}\psi_{dB}}{"p_{dB} - m_{dB}"}\right). \quad (8.5)$$

This is now regarded as a physical neutron, with udd constituents.

9. Using a Gaussian *Ansatz* for Fermion Wavefunctions, the t'Hooft Monopole Model Fully Specifies the Dynamical Properties of Yang-Mills Magnetic Monopole Baryons

For the most part, the discussion thus far has attempted to show that Yang-Mills magnetic monopoles have all of the necessary symmetry characteristics to be regarded as baryons, and in sections 6 through 9, to show they have the topological stability based on symmetry breaking, and the correct baryon and electric charge quantum numbers, to further be regarded as protons and neutrons. Now, we will want to explore how these objects behave in spacetime, because to pass the test of being a proton or a neutron, these magnetic monopoles will have to be different from the magnetic monopoles with which we are familiar in two very important, and indeed, distinguishing features: First, they will have to interact only at short range, because that is what baryons do. They must *not* possess the inverse square field strength which characterizes other known monopoles. Second, they will have to possess masses on the order of 1 GeV. In contrast, the known magnetic monopoles are extremely massive. In GUT theories their mass is set by the scale of symmetry breaking, which can be 10^{16} GeV or more, and even in the t'Hooft model, they are on the order of the $137\times M_W$, which is over 10 TeV. So our monopoles here will have to obtain their masses in a very different way, with a much smaller mass scale.

In order to explore the radial behavior of the Yang-Mills magnetic monopole baryons, as well as their expected masses, it will now be helpful to carefully contrast the monopole developed here, with that laid out in t'Hooft's original paper [1]. It will be helpful in this section for the reader to have available the original t'Hooft paper, which can be found at www.phys.uu.nl/~thooft/gthpub/magnetic_monopoles.pdf. Where there are differences in notation, these will be noted in the discussion below.

For each of $SU(4)_P$ and $SU(4)_N$, we start with 15 Higgs scalar fields $\phi_i; i=1...15$. As in SU(5) reviewed above, we then form the 4x4 vacuum matrix in the *adjoint* SU(4) representation (t'Hooft uses Q_a):

$$\Phi = T^a\phi_a; a=1...15. \tag{9.1}$$

We have already used this expression in (8.1) to break symmetry via the $B-L$ generator of SU(4). We next specify a Lagrangian density in exactly the same way as in the t'Hooft model [1], namely (t'Hooft uses $G^a_{\mu\nu}$):

$$\mathcal{L} = -\tfrac{1}{4} F^a_{\mu\nu} F_a^{\mu\nu} - \tfrac{1}{2} D_\mu \phi_a D^\mu \phi^a - \tfrac{1}{2}\mu^2 \phi_a \phi^a - \tfrac{1}{8}\lambda\left(\phi_a \phi^a\right)^2 . \tag{9.2}$$

This specifies physical dynamics *identical* to t'Hooft's [2.1]. The gauge fields are related to the Yang-Mills field strength tensor according to (2.3), reproduced below with explicit internal symmetry indexes via $G^\mu \equiv T^i G_i^{\ \mu}$, $F^{\mu\nu} \equiv T^i F_i^{\mu\nu}$ and $f^{ijk} T_i = -i\left[T^j, T^k\right]$ (t'Hooft uses $W_a^{\ \nu}$):

$$F_a^{\ \mu\nu} = \partial^\mu G_a^{\ \nu} - \partial^\nu G_a^{\ \mu} + f_{abc} G^{b\mu} G^{c\nu} . \tag{9.3}$$

Finally, the gauge-covariant derivative of the Higgs vacuum field is:

$$D_\mu \phi_a = \partial_\mu \phi_a + f_{abc} G^b_\mu \phi^c . \tag{9.4}$$

The potential $V(\phi) = -\tfrac{1}{2}\mu^2 \phi_a^{\ 2} - \tfrac{1}{8}\lambda\left(\phi_a^{\ 2}\right)^2$ in (9.2) minimizes at:

$$\partial V(\phi_a)/\partial \phi_a = -\mu^2 \phi_a - \tfrac{1}{2}\lambda\left(\phi_a \phi^\alpha\right)\phi_a = 0 . \tag{9.5}$$

This allows us to define a symmetry-breaking vev energy v according to (t'Hooft uses $F^2 = \langle Q_a \rangle^2 = \tfrac{1}{4} v^2$):

$$-2\mu^2 / \lambda = \phi_a \phi^\alpha = 2\mathrm{Tr}\Phi^2 \equiv \tfrac{1}{4} v^2 . \tag{9.6}$$

So up to this juncture, we fully follow the t'Hooft model [1], aside from the fact that we employ the gauge groups $SU(4)_P$ and $SU(4)_N$ developed in section 7, while t'Hooft uses the SO(3) model of Georgi and Glashow [19]. But from here, we shall diverge onto a different path.

In the t'Hooft model, the next step – which we shall *not* employ here – is to hypothesize the form of an explicit radial solution to the foregoing, in which both fields G^a_μ and ϕ_a in (9.2) are written as functions of the space coordinates x_a and $r^2 = x_a x^a$, using the *ansatz* $G^a_\mu = \varepsilon_{\mu ab} x_b G(r)$ and $\phi_a = x_a \phi(r)$, see [2.8] in [1]. Boundary conditions are then imposed at $r \to \infty$, (9.2) is solved, and three main results are obtained: First, it is shown that there is a radial *magnetic* field strength that falls off via an inverse square relation $1/r^2$, [2.21] in [1]. This is clearly indicative of a magnetic monopole, but this would not be helpful for a baryon which interacts only at short range. Second, the total flux over a closed surface is shown to satisfy the Schwinger and in certain cases Dirac Quantization conditions $eg = 1$ and $eg = \tfrac{1}{2} n$, where e and g are the electric and magnetic charges respectively, with the strength of this inverse square law given by g/r^2. This is now not only a monopole, but a Schwinger / Dirac monopole.

Finally, keeping in mind that the canonical energy-momentum tensor for a given field φ is given by:

$$T^{\mu\nu} = \partial^{\mu}\varphi \frac{\partial \mathcal{L}}{\partial(\partial_{\nu}\varphi)} - g^{\mu\nu}\mathcal{L}, \tag{9.7}$$

and requiring L to be stationary under small variations in $\phi(r)$ and $G(r)$, so that $T^{\mu\nu} = -g^{\mu\nu}\mathcal{L}$, thus $T^{00} = -\mathcal{L}$ for $g^{00} = 1$, the total energy of the system (9.2) is $p^0 = E = \iiint T^{00} d^3x = -\iiint \mathcal{L} d^3x = -L$. This expression $E = -L$ ([2.10] in [1]) then gives the mass of the magnetic monopole, which is found to be on the order of the large vev v obtained in (9.6), which mass scale would not be suitable for a baryon.

Following t'Hooft, we shall also use the energy equation:

$$E = -L \tag{9.8}$$

to obtain the monopole mass, but as we shall see, by using a different *ansatz* for G^a_{μ}, *we will not only be able to uncover a short range interaction, but will also be able to obtain a much smaller mass*. For the moment, as regards the monopole mass, it is worth noting that the vev mass scale for the t'Hooft monopole enters through the parameterizations in [3.1] of [1]. Particularly, as regards the pure Yang-Mills gauge field sector of the Lagrangian density, $\mathcal{L}_{\text{gauge}} = -\frac{1}{4}F^a_{\mu\nu}F^{\mu\nu}_a$, given $F = \frac{1}{2}v$ as noted earlier, the mass scale appears through the parameterizations $w = W/F^2e$ and $x = eFr$. The remaining energy in the system based on $\mathcal{L}_V = -\frac{1}{2}D_{\mu}\phi_a D^{\mu}\phi^a - \frac{1}{2}\mu^2\phi_a\phi^a - \frac{1}{8}\lambda(\phi_a\phi^a)^2$, which involves the Higgs vacuum ϕ^a, appears through the additional parameterizations $q = Q/F^2e$ and $\beta = \lambda/e = M_H^2/M_W^2$. The term with $D_{\mu}\phi_a D^{\mu}\phi^a$ mixes both parameterizations, and as we shall discuss in section 11, also generates the vector boson masses.

While the energies based on vacuum terms with ϕ^a will be determined by the (very large) symmetry breaking vev, the monopole energies developed from the pure gauge field sector $\mathcal{L}_{\text{gauge}} = -\frac{1}{4}F^a_{\mu\nu}F^{\mu\nu}_a$ may in fact be decoupled from the vev, and shown by different means to be on an MeV to GeV order of magnitude. So, let us now examine what is different about the monopoles being developed here in relation to the t'Hooft monopoles, and lay the foundation for these monopoles to a) have short range and b) have MeV to GeV-order energies.

In the discussion to follow, we shall also introduce an *ansatz* about the behavior of the gauge fields $G^{\mu} \equiv T^{i} G_{i}^{\mu}$ as a function of radial distance, but shall do so in a different way. The first step of this *ansatz* is already to be found in (2.10), where as discussed following (2.5), rather than go straight to a condition such as t'Hooft's $G_{\mu}^{a} = \varepsilon_{\mu a b} x_{b} G(r)$, we instead employed (2.9) in (2.5), wherein (2.9) is the inverse $G_{\nu} \equiv I_{\sigma\nu} J^{\sigma}$ of the classical Maxwell's charge equation $J^{\nu} = \partial_{\mu} F^{\mu\nu} = \partial_{\mu} D^{[\mu} G^{\nu]}$ of (2.1) taken with zero perturbation $\partial_{\nu} G_{\sigma} \to 0$. That is, at the point in development where t'Hooft uses $G_{\mu}^{a} = \varepsilon_{\mu a b} x_{b} G(r)$, we instead use $G_{\mu}^{a} \equiv I_{\sigma\mu} J^{a\sigma}$ based on Maxwell's $J^{\nu} = \partial_{\mu} F^{\mu\nu}$, for zero perturbation, and then use $J_{i}^{\mu} = \overline{\psi} T_{i} \gamma^{\mu} \psi$ in (2.11) to introduce fermion wavefunctions. When we then follow this to the end of the trail in sections 2 through 5 including applying Fermi-Dirac exclusion at the start of section 5, we end up with a magnetic monopole (5.5) which contains three colored quark wavefunctions and has all of the color symmetries expected in QCD, plus confined gauge fields, plus mediation of interactions by mesons. *One may therefore think of (5.5) as being what emerges when one combines both of Maxwell's classical electric and magnetic charge equations (2.1), (2.2) in a non-commuting (Yang-Mills) gauge theory (2.3) and then applies Fermi-Dirac exclusion to Dirac wavefunctions that may be introduced via the currents* $J^{\nu} = \overline{\psi} \gamma^{\nu} \psi$.

Now, in place of the *ansatz* $G_{\mu}^{a} = \varepsilon_{\mu a b} x_{b} G(r)$ used by t'Hooft, and given that (5.5) which later became (8.3) contains terms of the form $\partial^{\sigma}\left(\overline{\psi}_{C} \sigma^{\mu,\nu} \psi_{C}\right)$ which contain Dirac wavefunctions ($C = R, G, B$ for shorthand), we shall instead borrow from equation [14] of Ohanian's [3], and will employ *Gaussian wavefunctions* with radial behavior specified by a Gaussian *ansatz*:

$$\psi(r) = u(p)\left(\pi \lambda\!\!\!^{-2}\right)^{-\frac{3}{4}} \exp\left(-\frac{1}{2}\frac{(r - r_{0})^{2}}{\lambda\!\!\!^{-2}}\right), \tag{9.9}$$

where $\lambda\!\!\!^{-}$ (presently unspecified) has dimensions of length, $r_{0} = (x_{0}, y_{0}, z_{0})$ designates the space coordinate of the center peak of the Gaussian, r is a radial coordinate distance from r_{0}, and $u(p)$ is a four-component Dirac spinor. (Because ψ represents a fermion, it makes sense to consider what occurs when $\lambda\!\!\!^{-} = \hbar / mc$ is the reduced Compton wavelength of the associated fermion, which will be further explored in section 11.) That is, t'Hooft's *ansatz* introduces radial behaviors through the spin 1 vector gauge fields via

$G^a_\mu(r)=\varepsilon_{\mu ab}x_b G(r)$. The *ansatz* (9.9), in contrast, introduces radial behaviors through the spin ½ fermion fields in (8.3) via (9.9), and in particular, hypothesizes that these fermion fields behave radially in spacetime as Gaussians. One may, if one wishes, employ some other *ansatz* than that of (9.9) if desired, but (9.9) seems to be a very natural course to explore, and provides a way to do definitive exploratory calculations of energies and interactions based on the monopole (8.3), particularly because of its easy integrability and other good behaviors discussed below.

The key distinguishing point of the present approach in relation to the t'Hooft monopole is this: *t'Hooft introduces radial behaviors at the gauge field level. Here, we introduce radial behaviors at the fermion field level.* Any sensible fermion field *ansatz* may be used with the present model, and indeed, it will be up to experimental observation to validate the correct *ansatz*. But, the *ansatz* in the present model must be introduced via the fermions, not via the gauge bosons. *This is the central difference between this approach and the t'Hooft model.*

Based on our *ansatz* choice (9.9), we easily show via $u^\dagger=\bar{u}\gamma^0$ and $\psi^\dagger=\bar{\psi}\gamma^0$ that:

$$\psi^\dagger\psi=\frac{1}{\pi^{\frac{3}{2}}\lambda^3}\exp\left(-\frac{(r-r_0)^2}{\lambda^2}\right)u^\dagger u=\frac{1}{\pi^{\frac{3}{2}}\lambda^3}\exp\left(-\frac{(r-r_0)^2}{\lambda^2}\right)\bar{u}\gamma^0 u=\bar{\psi}\gamma^0\psi=J^0 \qquad (9.10)$$

is a probability density which Lorentz transforms as the time component of a current four-vector. The Gaussian itself will thus experience Lorentz contractions $\propto 1/\sqrt{1-v^2/c^2}$ at relativistic energies. By inspection, at the boundary, $\psi(r\to\infty)=0$ and $\psi^\dagger\psi(r\to\infty)=0$. When integrated over the *entirety* of a three-dimensional space at a given time, from -∞ to +∞ over d^3x, this Gaussian of course integrates to unity:

$$\iiint\frac{1}{\pi^{\frac{3}{2}}\lambda^3}\exp\left(-\frac{(r-r_0)^2}{\lambda^2}\right)d^3x=1. \qquad (9.11)$$

Consequently, combining (9.10) and (9.11):

$$\iiint\psi^\dagger\psi d^3x=u^\dagger u\iiint\frac{1}{\pi^{\frac{3}{2}}\lambda^3}\exp\left(-\frac{(r-r_0)^2}{\lambda^2}\right)d^3x=u^\dagger u=\bar{u}\gamma^0 u. \qquad (9.12)$$

A primary reason to choose (9.9), is that this *ansatz* guarantees finite, well-behaved results both at $r\to\infty$, and when integrating out to infinity. That is, (9.9) *inherently* comes packaged with precisely the types of boundary conditions and finite integrability that will result in finite, stable, well-behaved

solutions. It should also be noted based on the mathematics of Gaussians that the variance (square standard deviation) $\sigma^2 = \frac{1}{2}\lambda\!\!\!^{-2}$. With the *ansatz* (9.9), we will need to re-normalize u so that it is dimensionless, because the +3 mass dimension of $\psi^\dagger\psi$ on the left hand side of (9.10) is balanced on the right-hand side by $1/\lambda\!\!\!^{-3}$, leaving $u^\dagger u$ dimensionless. Earlier, in (3.7), we normalized such that $u^\dagger u$ carried the +3 mass dimension, so we will soon need to change this. But the context for doing so will be our examination of the magnetic monopole baryon masses in Sections 11 and 12, and the normalization will be driven by empirical data.

10. Yang-Mills Magnetic Monopoles with a Gaussian *Ansatz* Interact only at Very Short Range as is Required for Nuclear Interactions

There are many beneficial consequences to using (9.9) in place of $G^a_\mu = \varepsilon_{\mu ab} x_b G(r)$ to specify how the monopoles behave as a function of radial distance. First, of course, Gaussians are well-behaved, finite, stable functions when integrated over an infinite spatial volume as in (9.12). Second, and related to this, the boundary conditions at $r \to \infty$ are implicitly imposed: because (9.9) is a Gaussian, we know that $\psi(r \to \infty) = 0$. This means that the field strength tensor $F^{\mu\nu}$ based on these Gaussian will also be well behaved. To see this explicitly, we first extract the integrand from (5.6) (ignoring for the moment the terms $\partial^\mu G^\nu - \partial^\nu G^\mu$ from (2.3) which can also be included when we extract the integrand because dd=0, but d≠0, see (11.1) infra where we shall include these terms):

$$\mathrm{Tr}F^{\mu\nu} = -2\left(\frac{\bar{\psi}_R \sigma^{\mu,\nu} \psi_R}{"\not{p}_R - m_R"} + \frac{\bar{\psi}_G \sigma^{\mu,\nu} \psi_G}{"\not{p}_G - m_G"} + \frac{\bar{\psi}_B \sigma^{\mu,\nu} \psi_B}{"\not{p}_B - m_B"}\right). \tag{10.1}$$

Then, we make use of (9.9) or (9.10) in (10.1) to write:

$$\mathrm{Tr}F^{\mu\nu}(r) = -2\begin{pmatrix} \exp\left(-\frac{(r-r_{0R})^2}{\lambda\!\!\!^{-2}_R}\right)\frac{1}{\pi^{\frac{3}{2}}\lambda\!\!\!^{-3}_R}\frac{\bar{u}_R \sigma^{\mu,\nu} u_R}{"\not{p}_R - m_R"} \\ +\exp\left(-\frac{(r-r_{0G})^2}{\lambda\!\!\!^{-2}_G}\right)\frac{1}{\pi^{\frac{3}{2}}\lambda\!\!\!^{-3}_G}\frac{\bar{u}_G \sigma^{\mu,\nu} u_G}{"\not{p}_G - m_G"} \\ +\exp\left(-\frac{(r-r_{0B})^2}{\lambda\!\!\!^{-2}_B}\right)\frac{1}{\pi^{\frac{3}{2}}\lambda\!\!\!^{-3}_B}\frac{\bar{u}_B \sigma^{\mu,\nu} u_B}{"\not{p}_B - m_B"} \end{pmatrix}, \tag{10.2}$$

where r_{0R}, r_{0G}, r_{0B} designate the space coordinates of the central Gaussian peaks for each of the R, G, B quarks. Clearly, at the boundary, $\mathrm{Tr}F^{\mu\nu}(r\to\infty)=0$. Similarly, using (9.10), the radial derivative of $\psi^{\dagger}\psi$ is:

$$\frac{\partial}{\partial r}\left(\psi^{\dagger}\psi\right)=-2\frac{r-r_0}{\pi^{\frac{3}{2}}\lambda^5}\exp\left(-\frac{(r-r_0)^2}{\lambda^2}\right)u^{\dagger}u\ , \tag{10.3}$$

and this also approaches zero at $r\to\infty$. Because a typical term in the magnetic monopole density (5.5) or (8.3) is of the form $\partial^{\sigma}\overline{\psi}_C\sigma^{\mu\nu}\psi_C$ with colors $C=R,G.B$, (10.3) implies that that in space coordinates $x^i=(r,\theta,\varphi)$, the radial component:

$$\partial^1\frac{\overline{\psi}_C\sigma^{\mu\nu}\psi_C}{"\not{p}_C-m_C"}=\frac{\partial}{\partial r}\frac{\overline{\psi}_C\sigma^{\mu\nu}\psi_C}{"\not{p}_C-m_C"}=-2\frac{r-r_0}{\pi^{\frac{3}{2}}\lambda^5}\exp\left(-\frac{(r-r_0)^2}{\lambda^2}\right)\frac{\overline{u}_C\sigma^{\mu\nu}u_C}{"\not{p}_C-m_C"}\ . \tag{10.4}$$

The underlying mathematical function $r\exp\left(-r^2/\lambda^2\right)$ becomes zero at $r\to\infty$, thus, via (5.5) or (8.3), so too will the monopole density $\mathrm{Tr}P^{\sigma\mu\nu}(r\to\infty)=0$.

This type of good boundary behavior and finite integrability are good characteristics to have for stability. But just as compelling is that the inherent concentration of the Gaussian wavefunctions about central peaks at $r_0=(x_0,y_0,z_0)$, together with a rapid decline in intensity just a few standard deviations way from the center, result in the type of short range – *not inverse square* – interaction that definitely needs to occur if we are going to be able to associate these Yang-Mills magnetic monopoles with physical baryons like the proton and the neutron. Indeed, even if one were to use a different *ansatz* than (9.9), so long as one selects well-behaved fermion wavefunctions which are concentrated near a central peak and taper to zero at infinity, one will also have well-behaved magnetic monopoles which interact only over short range and not via inverse square. Let us now examine this more closely.

First, we write the surface integral of (10.2) as in (5.6), over a given surface at $r=R$, as:

$$\oiint_{r=R}\mathrm{Tr}F=-2\oiint_{r=R}\left(\begin{array}{l}\exp\left(-\frac{(r-r_{0R})^2}{\lambda_R{}^2}\right)\frac{1}{\pi^{\frac{3}{2}}\lambda_R{}^3}\frac{\overline{u}_R\sigma^{\mu\nu}u_R}{"\not{p}_R-m_R"}\\ +\exp\left(-\frac{(r-r_{0G})^2}{\lambda_G{}^2}\right)\frac{1}{\pi^{\frac{3}{2}}\lambda_G{}^3}\frac{\overline{u}_G\sigma^{\mu\nu}u_G}{"\not{p}_G-m_G"}\\ +\exp\left(-\frac{(r-r_{0B})^2}{\lambda_B{}^2}\right)\frac{1}{\pi^{\frac{3}{2}}\lambda_B{}^3}\frac{\overline{u}_B\sigma^{\mu\nu}u_B}{"\not{p}_B-m_B"}\end{array}\right)dx_{\mu}dx_{\nu}\ . \tag{10.5}$$

Now, we need to be careful, because due to the Gaussian, this is *not* an inverse square field strength. For an inverse square field, it does not matter whether the charges are centered within the surface, situated near the edge of the surface, or arbitrarily distributed in between. Nor does the shape of the surface matter. The total flux across the surface will be the same no matter what, precisely because the surface area $A = 4\pi R^2$ runs reciprocally to the inverse square relationship g / R^2, so that the magnetic field flux $\oiint_{r=R} F = g$ is constant, *independent* of R no matter what the configuration or location of the surface about the charges. So, in evaluating (10.5), which does *not* use an inverse square relation, let us simplify calculation by stipulating that the surface is a *spherical* surface of radius R which is also situated such that the three r_0's are *at the center of the sphere*. Further, because (10.5) contains three quarks, each of which will have Gaussians centered at very close albeit different coordinates r_{0R}, r_{0G}, r_{0B}, we stipulate that R is sufficiently large so that any physical separation between respective quarks may be neglected and we may regard each of these quarks to be centered at the same central coordinate location r_0. Further, let us choose our coordinates such that $r_0 = 0$. All of these are simplifying stipulations, and if one wanted to do so, one could discard them and simply make careful use of unit vectors $\hat{r} = \vec{r} / r$ to further develop (10.5) as a three-body system, but that is not necessary for the preliminary calculations we shall do here.

With $r_0 = 0$, in polar coordinates $x^\mu = (t, r, \theta, \phi)$, and using the surface integral $4\pi R^2 = \oiint_{r=R} r^2 \sin^2\theta d\theta d\phi$, for each term from (10.5) we write:

$$-2\oiint_{r=R}\left(\exp\left(-\frac{r^2}{\lambda\!\!\!^{-}_C{}^2}\right)\frac{1}{\pi^{\frac{3}{2}}\lambda\!\!\!^{-}_C{}^3}\frac{\bar{u}_C\sigma^{2,3}u_C}{"\not{p}_C - m_C"}\right)\frac{1}{2!}dx_2\wedge dx_3 = -\frac{8R^2}{\sqrt{\pi}\lambda\!\!\!^{-}_C{}^3}\exp\left(-\frac{R^2}{\lambda\!\!\!^{-}_C{}^2}\right)\frac{\bar{u}_C\sigma^{2,3}u_C}{"\not{p}_C - m_C"}. \quad (10.6)$$

Based on these stipulations and (10.6), and adding the further simplifying stipulations that $\lambda\!\!\!^{-} \equiv \lambda\!\!\!^{-}_R = \lambda\!\!\!^{-}_G = \lambda\!\!\!^{-}_B$, $m \equiv m_R = m_G = m_B$ and $\not{p} \equiv \not{p}_R = \not{p}_G = \not{p}_B$ this means that (10.5), using (3.10) and $-2i\sigma^{\mu,\nu} = [\gamma^\mu{}_,\gamma^\nu]$, evaluates to:

$$g' \equiv \oiint_{r=R}\mathrm{Tr}F = -\frac{24R^2}{\sqrt{\pi}\lambda\!\!\!^{-3}}\exp\left(-\frac{R^2}{\lambda\!\!\!^{-2}}\right)\frac{\bar{u}\sigma^{2,3}u}{"\not{p}-m"} = -i\frac{12R^2}{\sqrt{\pi}\lambda\!\!\!^{-3}}\exp\left(-\frac{R^2}{\lambda\!\!\!^{-2}}\right)\frac{\bar{u}\gamma^{[2}(\not{p}+m)\gamma^{3]}u}{\rho^2 - m^2}. \quad (10.7)$$

That is, g' is the total flux of magnetic monopole charge that will be observed to flow across the closed surface at $r=R$, and it is indeed dependent on the radius R of the closed surface. Figure 2 below, illustrates this total flux in (10.7) for $\lambda\!\!\!^{-} = 1$, hence $\sigma^2 = \frac{1}{2}$, as a function of the spherical surface radius R.

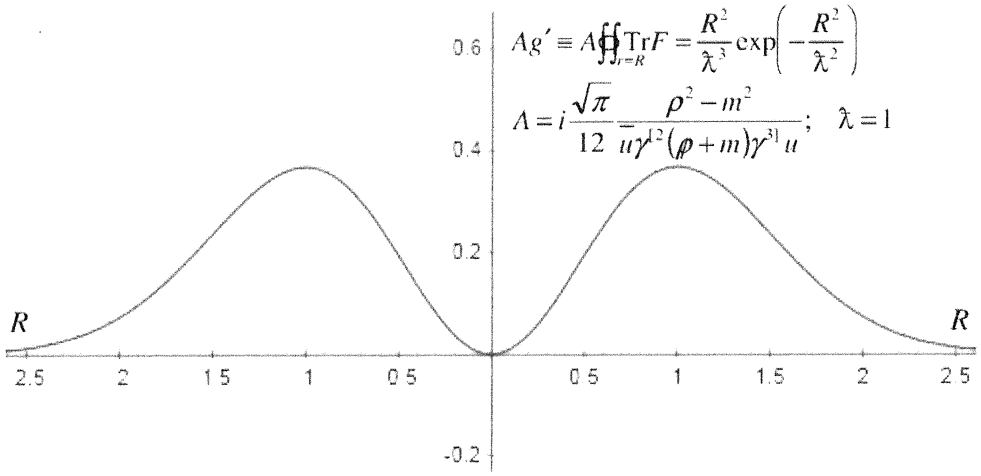

Figure 2

This is a magnetic-type flux because it is specified by $g'(R) = \oiint \mathrm{Tr}F$. But it obviously is of a very different character than the usual $g = \oiint F$ for a monopole with an inverse square law, such as the t'Hooft monopole. For this more familiar monopole, g is a *constant, independent of* R, and would be represented by a constant, horizontal line at the height g if drawn on Figure 2. But for the monopole of Figure 2, the total magnetic flux $g'(R) = \oiint \mathrm{Tr}F$ is clearly dependent on R, as it must be if this monopole is to represent a baryon, such as a proton or neutron, which interacts only at very short range.

In Figure 2, coefficient A merely determines the *amplitude* (height) of the curve (and note that γ^2 has imaginary elements to cancel the i in A). With a standard deviation $\sigma = \frac{1}{\sqrt{2}}$ the flux in Figure 2 peaks at $R = 1 = \sqrt{2}\sigma$ and falls off rapidly thereafter. In general, because $\sigma = \frac{1}{\sqrt{2}}\lambda\!\!\!^{-}$ (see after (9.12)), we see that by about $4\sigma \approx 3\lambda\!\!\!^{-}$ from the center, the total magnetic flux is virtually non-existent! So: (10.7), which is drawn in Figure 2, demonstrates clearly that while the magnetic monopole we have been developing here is indeed a magnetic monopole because its flux over closed surfaces is specified by $g'(R) = \oiint \mathrm{Tr}F$, this monopole does not produce an inverse-square field because the total flux depends upon R. Rather, it produces a field that falls off very sharply just a few standard deviations from its center. Such short range

fields are hallmarks of nuclear interactions, and further qualify Yang-Mills magnetic monopoles for serious consideration as baryons.

So, to summarize: we have applied an *ansatz* to the fermions rather than to the gauge bosons to specify the radial behavior of these Yang-Mills magnetic monopoles. Using a Gaussian for the *ansatz* (for which one may wish to substitute some other *ansatz* so long as it is applied to the fermions and not the gauge bosons), we have demonstrated (using some simplifying stipulations which can be lifted by more carefully using unit vectors $\hat{r} = \vec{r} / r$ to specify the fields of this three-body system) that these Yang-Mills magnetic monopoles do interact only at very short range, as do real, physical baryons such as protons and neutrons. In the next section, we shall show that this short range is on the order of 2 Fermi, as it is expected to be from empirical data.

But, as discussed at the start of Section 9, it is also necessary for the masses and energies associated with these monopoles to be in the MeV and GeV range, because that too is observed in the physical world. The energy physics of these monopoles will now be the focus of Sections 11 and 12, which will validate using well-established empirical data, that these Yang-Mills magnetic monopoles truly are baryons.

11. The Electron Mass is Predicted from Up and Down Quark Masses to about 3% from the Experimental Mean

We begin our examination of the energies associated with the magnetic monopoles with (8.3), which we rewrite using $\sigma^{\mu\vee\nu} = \frac{i}{2}\left[\gamma^{\mu}\vee\gamma^{\nu}\right]$. We then take the Gaussian surface integral $\oiint \mathrm{Tr}F = \iiint \mathrm{Tr}P$ as in (5.6) and extract the integrand. Finally, referring back to (2.3), we reintroduce the terms $\partial^{\mu}G^{\nu} - \partial^{\nu}G^{\mu}$ which are removed from the monopole via dd=0, but do <u>not</u> zero out for the field strength F=dA, and which we left out of (10.1). Thus:

$$\mathrm{Tr}F^{\mu\nu} = \partial^{\mu}G^{\nu} - \partial^{\nu}G^{\mu} - i\left(\frac{\overline{\psi}_R\left[\gamma^{\mu}\vee\gamma^{\nu}\right]\psi_R}{"p_R - m_R"} + \frac{\overline{\psi}_G\left[\gamma^{\mu}\vee\gamma^{\nu}\right]\psi_G}{"p_G - m_G"} + \frac{\overline{\psi}_B\left[\gamma^{\mu}\vee\gamma^{\nu}\right]\psi_B}{"p_B - m_B"}\right). \quad (11.1)$$

This is another way of expressing (10.1) in light of (2.3), and may be thought of as a way of rewriting the fundamental Yang-Mills field relation $F^{\mu\nu} = \partial^{\mu}G^{\nu} - \partial^{\nu}G^{\mu} - i\left[G^{\mu}, G^{\nu}\right]$ in (2.3) to capture much of our development so far. (Note: The above is quadratic in G^{μ} and so can be used to do *exact* calculations with the Gaussians employed in path integrals, see, e.g., Appendix A of [4].)

Now, back in (2.7), we derived the inverse for the classical Maxwell field equation $J^\nu = \partial_\mu F^{\mu\nu}$ of (2.1). But just prior to (2.9), we made the simplifying choice to develop the magnetic monopole *in the low-perturbation limit* by setting $\partial_\nu G_\sigma \to 0$, which we noted was more generally equivalent with setting a gauge invariant perturbation vector $-V^{\mu\nu} = \left(\partial^\mu G^\nu + G^\nu \partial^\mu\right) + G^\mu G^\nu \to 0$. Thus, all of our results thus far display the behavior of Yang-Mills magnetic monopoles for low, indeed, zero perturbation. We continue to examine *zero perturbation*, so consistently with the development thus far, we set $\partial_\nu G_\sigma \to 0$ in (11.1) as well. Thus, we now reduce (11.1) via $\partial_\nu G_\sigma \to 0$, back to:

$$\mathrm{Tr}F^{\mu\nu} = -i\left(\frac{\overline{\psi}_R\left[\gamma^\mu \vee \gamma^\nu\right]\psi_R}{"p_R - m_R"} + \frac{\overline{\psi}_G\left[\gamma^\mu \vee \gamma^\nu\right]\psi_G}{"p_G - m_G"} + \frac{\overline{\psi}_B\left[\gamma^\mu \vee \gamma^\nu\right]\psi_B}{"p_B - m_B"}\right). \tag{11.2}$$

This is (10.1) with $\sigma^{\mu\vee\nu} = \frac{i}{2}\left[\gamma^\mu \vee \gamma^\nu\right]$. Next, as in (8.4) and (8.5), we write this as two distinct expressions, one for the proton, and one for the neutron:

$$\begin{aligned}\mathrm{Tr}F^{\mu\nu}{}_{\mathrm{P}} &= -i\left(\frac{\overline{\psi}_d\left[\gamma^\mu \vee \gamma^\nu\right]\psi_d}{"p_d - m_d"} + \frac{\overline{\psi}_u\left[\gamma^\mu \vee \gamma^\nu\right]\psi_u}{"p_u - m_u"} + \frac{\overline{\psi}_u\left[\gamma^\mu \vee \gamma^\nu\right]\psi_u}{"p_u - m_u"}\right), \\ &= -i\left(\frac{\overline{\psi}_d\left[\gamma^\mu \vee \gamma^\nu\right]\psi_d}{"p_d - m_d"} + 2\frac{\overline{\psi}_u\left[\gamma^\mu \vee \gamma^\nu\right]\psi_u}{"p_u - m_u"}\right)\end{aligned} \tag{11.3}$$

$$\begin{aligned}\mathrm{Tr}F^{\mu\nu}{}_{\mathrm{N}} &= -i\left(\frac{\overline{\psi}_u\left[\gamma^\mu \vee \gamma^\nu\right]\psi_u}{"p_u - m_u"} + \frac{\overline{\psi}_d\left[\gamma^\mu \vee \gamma^\nu\right]\psi_d}{"p_d - m_d"} + \frac{\overline{\psi}_d\left[\gamma^\mu \vee \gamma^\nu\right]\psi_d}{"p_d - m_d"}\right). \\ &= -i\left(\frac{\overline{\psi}_u\left[\gamma^\mu \vee \gamma^\nu\right]\psi_u}{"p_u - m_u"} + 2\frac{\overline{\psi}_d\left[\gamma^\mu \vee \gamma^\nu\right]\psi_d}{"p_d - m_d"}\right)\end{aligned} \tag{11.4}$$

In the foregoing, we have suppressed the color designations as they will not be needed for the calculations following. In combining the two like terms for the up quark in (11.3) and the down quark in (11.4), and because we will shortly be integrating these over d^3x from -∞ to +∞ as part of the energy tensor, we make the simplifying stipulation that any physical separation between respective quarks may be neglected, as we did following (10.5).

Now, let us return to the t'Hooft monopole Lagrangian density (9.2). As noted following (9.8), the portion $\mathfrak{L}_V = -\frac{1}{2}D_\mu\phi_a D^\mu\phi^a - \frac{1}{2}\mu^2\phi_a\phi^a - \frac{1}{8}\lambda\left(\phi_a\phi^a\right)^2$ of this density which involves the Higgs vacuum ϕ^a will be determined by the GUT symmetry breaking scale at which the quarks are separated from the

leptons via the symmetry breaking of (8.1). For example, using (9.4) in the "kinetic energy" term $D_\mu\phi_a D^\mu\phi^a$ of (9.2) yields:

$$\mathcal{L}_{\text{kinetic}} = -\tfrac{1}{2} D_\mu\phi_a D^\mu\phi^a = -\tfrac{1}{2}\left(\partial_\mu\phi_a\partial^\mu\phi^a + 2f_{abc}\partial^\mu\phi^a G^b_\mu\phi^c + f_{abc}f^{ade}G^b_\mu G^\mu_d\phi^c\phi_e\right). \quad (11.5)$$

When we then apply $\phi_{15} = -\sqrt{\tfrac{8}{3}}v_{GUT}$ and the remaining $\phi_i = 0$ to break the symmetry as was done following (8.1), the final term becomes a sum of Lagrangian vector boson mass terms:

$$\mathcal{L}_{\text{boson mass}} = -\tfrac{1}{2}{v_{GUT}}^2 g^2\left(\tfrac{8}{3}f_{ab15}f^{ac15}G^b_\mu G^\mu_c\right) \rightarrow -\tfrac{1}{2}\Sigma M^2 G_\mu G^\mu, \quad (11.6)$$

where we have rescaled $G^b_\mu \rightarrow gG^b_\mu$ to restore the interaction charge strength heretofore absorbed into the bosons following (2.3). So the masses of the vector bosons clearly flow from this term, and the boson mass scale will be set by the extraordinarily high v_{GUT} energy at which quark and leptons decay into one another.

But as we shall now see, the pure gauge field sector $\mathcal{L}_{\text{gauge}} = -\tfrac{1}{4}F^a_{\mu\nu}F^{\mu\nu}_a$ of (9.2) *does not necessarily have to have its mass scale determined by* v_{GUT}. As pointed out following (9.8), t'Hooft uses the parameterizations $w = W / F^2 e$ and $x = eFr$ to set the scale for the magnetic monopole mass to be the same as the symmetry breaking energy scale v_{GUT}. But this is only because *the t'Hooft model does not introduce any other mass scale which would not be arbitrary*, and this in turn, is because the t'Hooft *ansatz* $G^a_\mu = \varepsilon_{\mu ab}x_b G(r)$ introduces radial behaviors into $F^{\mu\nu}_a$ *via the gauge fields* G^a_μ. Consequently, the masses of the monopoles become tied to the masses of the massive gauge bosons that emerge following symmetry breaking, and these are in turn tied to the GUT scale, as shown in (11.6) above.

Here, in important contrast, the Gaussian *ansatz* (9.9) introduces radial behaviors into $F^{\mu\nu}_a$ *via the fermion wavefunctions* ψ. Consequently, the monopole mass scales which emerge out of $\mathcal{L}_{\text{gauge}} = -\tfrac{1}{4}F^a_{\mu\nu}F^{\mu\nu}_a$ via (9.7) and (9.8) *will be tied to the masses of the fermions*, rather than to the gauge boson masses which in turn are tied to the GUT energy. Of course, the fermions have now been developed into up and down quarks, and the magnetic monopoles have been developed into protons and neutrons. So with this *ansatz* (9.9), the masses of the proton and neutron should be related in a precise way to the masses of the up and down quarks, and not to the GUT scale. We shall now show exactly how this is so.

We first return to (9.7), which specifies the canonical energy momentum tensor. The total energy of the dynamical system specified by $\mathfrak{L}$ is given by $E = p^0 = \iiint T^{00} d^3x$ as noted earlier. If Yang-Mills magnetic monopoles truly are baryons, then because we have turned off perturbations by setting $\partial_\nu G_\sigma \to 0$ throughout, E in this integral should give the "bare" proton and neutron masses absent perturbations. Following t'Hooft, we require $L = \iiint \mathfrak{L} d^3x$ to be stationary under small variations in the fields, which allows us to obtain the total energy from (9.8), namely, $E = -L$. Now the question becomes, which terms from L do we use?

The Lagrangian density (9.2), of course, contains multiple terms. We shall explore here, the energies specifically arising from the pure gauge field term $\mathfrak{L}_{\text{gauge}} = -\frac{1}{4} F^a_{\mu\nu} F_a^{\mu\nu}$, that is:

$$E = -L = -\iiint \mathfrak{L}_{\text{gauge}} d^3x = \tfrac{1}{4} \iiint F^a_{\mu\nu} F_a^{\mu\nu} d^3x = \tfrac{1}{2} \text{Tr} \iiint F_{\mu\nu} F^{\mu\nu} d^3x \,. \tag{11.7}$$

In exploring the pure gauge terms separately from those terms which contain the vacuum Φ, we are simultaneously doing two things: First, via $\partial_\nu G_\sigma \to 0$, we are turning off all perturbations. Second, by developing the energy only out of $\mathfrak{L}_{\text{gauge}} = -\frac{1}{4} F^a_{\mu\nu} F_a^{\mu\nu}$, we are turning off the vacuum. So the energies we obtain will be the barest energies resulting from the intrinsic structure of these monopoles with all perturbations and all vacuum effects turned off.

Next we substitute (11.3) and (11.4) into the above to write, for protons and neutrons respectively:

$$E_{\text{P}} = -\tfrac{1}{2} \iiint \left(\frac{\bar{\psi}_d [\gamma^\mu \vee \gamma^\nu] \psi_d}{\text{"}\rho_d - m_d\text{"}} + 2 \frac{\bar{\psi}_u [\gamma^\mu \vee \gamma^\nu] \psi_u}{\text{"}\rho_u - m_u\text{"}} \right) \times \left(\frac{\bar{\psi}_d [\gamma_\mu \vee \gamma_\nu] \psi_d}{\text{"}\rho_d - m_d\text{"}} + 2 \frac{\bar{\psi}_u [\gamma_\mu \vee \gamma_\nu] \psi_u}{\text{"}\rho_u - m_u\text{"}} \right) d^3x \tag{11.8}$$

$$= -\tfrac{1}{2} \iiint \left(\frac{\bar{\psi}_d [\gamma^\mu \vee \gamma^\nu] \psi_d}{\text{"}\rho_d - m_d\text{"}} \frac{\bar{\psi}_d [\gamma_\mu \vee \gamma_\nu] \psi_d}{\text{"}\rho_d - m_d\text{"}} + 4 \frac{\bar{\psi}_u [\gamma^\mu \vee \gamma^\nu] \psi_u}{\text{"}\rho_u - m_u\text{"}} \frac{\bar{\psi}_d [\gamma_\mu \vee \gamma_\nu] \psi_d}{\text{"}\rho_d - m_d\text{"}} + 4 \frac{\bar{\psi}_u [\gamma^\mu \vee \gamma^\nu] \psi_u}{\text{"}\rho_u - m_u\text{"}} \frac{\bar{\psi}_u [\gamma_\mu \vee \gamma_\nu] \psi_u}{\text{"}\rho_u - m_u\text{"}} \right) d^3x$$

$$E_{\text{N}} = -\tfrac{1}{2} \iiint \left(\frac{\bar{\psi}_u [\gamma^\mu \vee \gamma^\nu] \psi_u}{\text{"}\rho_u - m_u\text{"}} + 2 \frac{\bar{\psi}_d [\gamma^\mu \vee \gamma^\nu] \psi_d}{\text{"}\rho_d - m_d\text{"}} \right) \left(\frac{\bar{\psi}_u [\gamma_\mu \vee \gamma_\nu] \psi_u}{\text{"}\rho_u - m_u\text{"}} + 2 \frac{\bar{\psi}_d [\gamma_\mu \vee \gamma_\nu] \psi_d}{\text{"}\rho_d - m_d\text{"}} \right) d^3x \tag{11.9}$$

$$= -\tfrac{1}{2} \iiint \left(\frac{\bar{\psi}_u [\gamma^\mu \vee \gamma^\nu] \psi_u}{\text{"}\rho_u - m_u\text{"}} \frac{\bar{\psi}_u [\gamma_\mu \vee \gamma_\nu] \psi_u}{\text{"}\rho_u - m_u\text{"}} + 4 \frac{\bar{\psi}_d [\gamma^\mu \vee \gamma^\nu] \psi_d}{\text{"}\rho_d - m_d\text{"}} \frac{\bar{\psi}_u [\gamma_\mu \vee \gamma_\nu] \psi_u}{\text{"}\rho_u - m_u\text{"}} + 4 \frac{\bar{\psi}_d [\gamma^\mu \vee \gamma^\nu] \psi_d}{\text{"}\rho_d - m_d\text{"}} \frac{\bar{\psi}_d [\gamma_\mu \vee \gamma_\nu] \psi_d}{\text{"}\rho_d - m_d\text{"}} \right) d^3x$$

The above are a bit busy, but if we schematically refer to the terms with up quarks as "u terms" and the terms with down quarks as "d terms," the important pattern to glean from (11.8) and (11.9) is that:

$$E_{\text{P}}(duu) \propto (d + 2u)^2 = d^2 + 4ud + 4u^2 \,, \tag{11.10}$$

$$E_{\text{N}}(udd) \propto (u + 2d)^2 = u^2 + 4ud + 4d^2 \,. \tag{11.11}$$

This also means that the *difference* between the neutron and proton energies is schematically given by the relationship:

$$\Delta E \equiv E_{\mathrm{N}} - E_{\mathrm{P}} \propto 3\left(d^2 - u^2\right). \tag{11.12}$$

According to PDG's latest survey [20], the *unbound* neutron mass is 939.565379 MeV, the *unbound* proton mass is 938.272046 MeV, and so their difference ΔE is 1.293333 MeV. Meanwhile, the electron mass is known with great precision, and is listed in 2012 PDG data [21] as $m_e = 0.510998928$ MeV. This is all well known, and it is believed that the discrepancy between 1.293333 MeV and 0.510998928 MeV all arises due to the dynamical, non-linear interactions within the proton or neutron. If the "noise" of all this interaction was to be shut off, it is believed, then this discrepancy would vanish, and the electron mass m_e would be virtually identical to $\Delta E \equiv E_{\mathrm{Neutron}} - E_{\mathrm{Proton}}$. (Because neutrinos emitted during beta decay $n \to p + e^- + \bar{\nu}$ have such a small (<2 eV) mass, we neglect any such mass.)

But as just noted following (11.7), the proton and neutron expressions (11.8) and (11.9), or (11.3) and (11.4), were all developed for zero perturbation $V \to 0$, because we have zeroed out any perturbative terms throughout this development, and are further designed from the pure gauge fields only to filter out all vacuum effects. In common nomenclature, wherein the "current quark mass" is understood to represent the "constituent" or "effective quark mass," reduced by the mass of the respective "constituent quark coverings" arising from gluon fields and vacuum condensates surrounding the "current quarks," *we have in this development turned off all "coverings,"* of any origin. So, having stripped out the coverings, and solely looking at the "current quark masses," what (11.12) tells us is that the ΔE we will deduce from (11.8) and (11.9) is not from the difference between the *total, covered* masses of the proton and neutron, *but only from the difference between that portion of the total mass that is directly contributed by the current quark masses*. In other words, (11.12) as based on (11.8) and (11.9) is a difference between two bare, *uncovered* nucleon masses, which turns off the *noise*, and gets to the underlying undiluted "*signal*" arising from the current quarks only. As such, we should expect that $E_{\mathrm{Electron}} = \Delta E \equiv E_{\mathrm{Neutron}} - E_{\mathrm{Proton}}$ because our neglect of all perturbations and vacuum effects allows us to look at uncovered nucleon masses.

The "current" (uncovered) masses of the up and down quarks are $m_d = 4.8^{+.7}_{-.3}\,MeV$ and $m_u = 2.3^{+.7}_{-.5}\,MeV$ based on the most recent PDG data [22]. So based particularly on (11.12), we should see if the electron rest mass can in

fact be described in relation to these current quark masses, based on the relationships (11.8) and (11.9). Indeed, precisely because our development has turned off all perturbations and vacuum effects, we should not only expect this to work, but this must work in in order to validate the thesis we have presented. That is, we arrive at a point where our thesis and the development so far may be contradicted, if nature chooses to do so. So, let's do the calculations:

First, subtracting (11.8) from (11.9) to flesh out (11.12), we write:

$$\Delta E = -\tfrac{1}{2}\iiint 3\left(\frac{\overline{\psi}_d[\gamma^\mu \vee \gamma^\nu]\psi_d}{"\not{p}_d - m_d"} \frac{\overline{\psi}_d[\gamma_\mu \vee \gamma_\nu]\psi_d}{"\not{p}_d - m_d"} - \frac{\overline{\psi}_u[\gamma^\mu \vee \gamma^\nu]\psi_u}{"\not{p}_u - m_u"} \frac{\overline{\psi}_u[\gamma_\mu \vee \gamma_\nu]\psi_u}{"\not{p}_u - m_u"} \right) d^3x\,, \quad (11.13)$$

Then, we use the *ansatz* (9.9) in (11.13) to obtain:

$$\Delta E = -\tfrac{1}{2}\iiint 3\left(\begin{array}{l} \dfrac{1}{\pi^3 \lambda\!\!\!^{-}_d{}^6} \exp\left(-2\dfrac{(r-r_0)^2}{\lambda\!\!\!^{-}_d{}^2} \right) \dfrac{\overline{d}[\gamma^\mu \vee \gamma^\nu] d \overline{d}[\gamma_\mu \vee \gamma_\nu] d}{"\not{p}_d - m_d"^2} \\ - \dfrac{1}{\pi^3 \lambda\!\!\!^{-}_u{}^6} \exp\left(-2\dfrac{(r-r_0)^2}{\lambda\!\!\!^{-}_u{}^2} \right) \dfrac{\overline{u}[\gamma^\mu \vee \gamma^\nu] u \overline{u}[\gamma_\mu \vee \gamma_\nu] u}{"\not{p}_u - m_u"^2} \end{array} \right) d^3x\,. \quad (11.14)$$

Above, $d(p)$, $u(p)$ are Dirac spinors for the up and down quarks, respectively. Now, we may make use of (9.11) refashioned via scaling $\lambda\!\!\!^{-} \to \lambda\!\!\!^{-}/\sqrt{2}$, namely:

$$\iiint \frac{2^{\frac{3}{2}}}{\pi^{\frac{3}{2}} \lambda\!\!\!^{-}{}^3} \exp\left(-2\frac{(r-r_0)^2}{\lambda\!\!\!^{-}{}^2} \right) d^3x = 1 \quad (11.15)$$

to evaluate the Gaussian integral in (11.14). This means that:

$$\iiint \frac{1}{\pi^3 \lambda\!\!\!^{-}{}^6} \exp\left(-2\frac{(r-r_0)^2}{\lambda\!\!\!^{-}{}^2} \right) d^3x = \frac{1}{(2\pi)^{\frac{3}{2}} \lambda\!\!\!^{-}{}^3}\,. \quad (11.16)$$

Then, we use (11.16) in (11.14) to obtain:

$$\Delta E = -\tfrac{1}{2} \cdot 3\left(\frac{1}{(2\pi)^{\frac{3}{2}} \lambda\!\!\!^{-}_d{}^3} \frac{\overline{d}[\gamma^\mu \vee \gamma^\nu] d \overline{d}[\gamma_\mu \vee \gamma_\nu] d}{"\not{p}_d - m_d"^2} - \frac{1}{(2\pi)^{\frac{3}{2}} \lambda\!\!\!^{-}_u{}^3} \frac{\overline{u}[\gamma^\mu \vee \gamma^\nu] u \overline{u}[\gamma_\mu \vee \gamma_\nu] u}{"\not{p}_u - m_u"^2} \right), \quad (11.17)$$

Now, as a *test hypothesis*, let us see what occurs if we regard $\lambda\!\!\!^{-} = \hbar / mc$ as the reduced *bare* (uncovered, "current") Compton wavelength of the associated quarks. With $\hbar = c = 1$, this allows us via $m = 1/\lambda\!\!\!^{-}$ to directly employ quark masses in (11.17) instead of $\lambda\!\!\!^{-}$, thus:

$$\Delta E = -\tfrac{1}{2} \cdot 3\left(\frac{m_d{}^3}{(2\pi)^{\frac{3}{2}}} \frac{\overline{d}[\gamma^\mu \vee \gamma^\nu] d \overline{d}[\gamma_\mu \vee \gamma_\nu] d}{"\not{p}_d - m_d"^2} - \frac{m_u{}^3}{(2\pi)^{\frac{3}{2}}} \frac{\overline{u}[\gamma^\mu \vee \gamma^\nu] u \overline{u}[\gamma_\mu \vee \gamma_\nu] u}{"\not{p}_u - m_u"^2} \right), \quad (11.18)$$

By our test hypothesis $\lambda\!\!\!^{-} = \hbar / mc$, the mass scale for ΔE has now been established, *as has the mass scale for the proton and neutron masses*, and it is not the GUT scale. Importantly, and appropriately insofar as experimental observations are concerned, this mass scale is set by the masses of the up and down quark that comprise the neutron and the proton, rather than by the GUT energy of symmetry breaking. So the Gaussian *ansatz* (9.9), if we use $\lambda\!\!\!^{-} = \hbar / mc$, gets us into the right "ballpark" in orders of magnitude. And, it makes simple sense that the proton and neutron masses should be related in some fashion to the masses of the quarks of which they are comprised. We see that all the mass dimensions in (11.18) are correct, so long as we choose a normalization in which the Dirac spinors are dimensionless. We shall do so momentarily. But next, we come to the $"\not{p} - m"^2$ propagator denominators.

For this, we refer back to Figure 1 at the start of section 3, and also keep in mind section 12.2 of [5]. Specifically, we consider the circumstance in which the interactions shown in Figure 1 occur essentially at a point. In that situation, the propagator disappears, the *s* and *t* channels become indistinguishable, and we can set $"\not{p} - m"^2 \to m^2$ in (11.18) above. So, also applying (3.10) which defines $_{\nu} = 1$ and reverting from the quasi-commutator to the ordinary commutator, (11.18) becomes:

$$\Delta E = -\tfrac{1}{2} \cdot \frac{3}{(2\pi)^{\frac{3}{2}}} \left(m_d \cdot \bar{d}[\gamma^\mu, \gamma^\nu] d \bar{d}[\gamma_\mu, \gamma_\nu] d - m_u \cdot \bar{u}[\gamma^\mu, \gamma^\nu] u \bar{u}[\gamma_\mu, \gamma_\nu] u \right). \quad (11.19)$$

The remaining terms $\bar{d}[\gamma^\mu, \gamma^\nu] d \bar{d}[\gamma_\mu, \gamma_\nu] d$ and $\bar{u}[\gamma^\mu, \gamma^\nu] u \bar{u}[\gamma_\mu, \gamma_\nu] u$ are scalar numbers. They need to be normalized via the Dirac spinors into a dimensionless constant number *K*, so the only question now is to find the right normalization. For the moment, $K \equiv \bar{d}[\gamma^\mu, \gamma^\nu] d \bar{d}[\gamma_\mu, \gamma_\nu] d = \bar{u}[\gamma^\mu, \gamma^\nu] u \bar{u}[\gamma_\mu, \gamma_\nu] u$ is *defined* to be a dimensionless *experimental constant*, and we take this *K* to be an unknown. Now, (11.9) may be further reduced to:

$$\Delta E = -\tfrac{1}{2} K \cdot \frac{3}{(2\pi)^{\frac{3}{2}}} (m_d - m_u) \cdot \quad (11.20)$$

Now, we simply plug the experimental $m_d = 4.8^{+.7}_{-.3}\, MeV$ and $m_u = 2.3^{+.7}_{-.5}\, MeV$ from [22] into the above, to obtain:

$$\begin{aligned} \Delta E &= -\tfrac{1}{2} K \cdot 3(m_d - m_u)/(2\pi)^{\frac{3}{2}} = -\tfrac{1}{2} K \cdot 3\left(4.8^{+.7}_{-.3} - 2.3^{+.7}_{-.5}\right)/(2\pi)^{\frac{3}{2}} MeV \\ &= -\tfrac{1}{2} K \cdot \mathbf{.476^{+.228}_{-.190}\, MeV} = -\tfrac{1}{2} K \cdot \mathbf{(.286\ MeV\ to\ .704\ MeV)} \quad . \quad (11.21) \\ &= -\tfrac{1}{2} K \cdot \overline{\mathbf{.495 MeV}} \end{aligned}$$

This displays the *predicted* $\Delta E \equiv E_{\text{Neutron}} - E_{\text{Proton}}$ based on the up and down quark masses. Following (11.12) we suggested that this difference should turn out to be the electron rest mass, because we have turned off all the "noise" that distorts what is otherwise the electron mass into a ΔE of 1.293333 MeV between the observed, unbound, noisy, fully covered proton and neutron masses. The experimental electron mass, of course is m_e = 0.510998928 MeV. Using the high-side "down" and the low-side "up" masses, the high end of the term $3(m_d - m_u)/(2\pi)^{\frac{3}{2}} = .704 MeV$. Using the low-side "down" and high-side "up" masses, the low end of the term $3(m_d - m_u)/(2\pi)^{\frac{3}{2}} = .286 MeV$. Using the experimental mean for the up and down, however – and this is the striking result – this anticipated value of $3(m_d - m_u)/(2\pi)^{\frac{3}{2}} = .476 MeV$ And, the mean (denoted by the overbar) of the range between .286MeV and .704MeV is 0.495 MeV. The electron mass 0.510998928 MeV is perhaps one of the most tightly known natural constants, and so the 0.495 MeV electron mass *predicted* from the median of the experimental data differs only about 3% removed from the actual experimental mass! Not only is this prediction in the right ballpark, it is centered in the middle of a fairly wide experimental range, and so would appear to provide direct and compelling experimental confirmation that Yang-Mills magnetic monopoles as developed here, truly are baryons!

Given the closeness of the $3(m_d - m_u)/(2\pi)^{\frac{3}{2}}$ to the experimental electron mass based on the quark mass data, let us now regard the electron mass m_e to in fact be related to the quark *current* masses, *precisely*, by $E_{\text{Electron}} = m_e \equiv \Delta E$, and let us introduce this as a hypothesis supported by the experimental data. That is, we now hypothesize based on empirical data that:

$$m_e = 0.510998928\ MeV \equiv \Delta E = \frac{3}{(2\pi)^{\frac{3}{2}}}(m_d - m_u). \qquad (11.22)$$

This filters out the "noise" of the interactions within the proton and neutron, and shows the real "signal" behind the noise, which signal is the electron mass. It also makes general sense that the electron mass turns out to be a constant times the difference between the up and down quark masses, with the only real question being: what is the mathematical and physical basis for specifying that constant? As it turns out, the factor of 3 emerges from the $3(d^2 - u^2)$ schematic in (11.12) (and also happens to be the number of quarks in each nucleon) and the factor of $(2\pi)^{-\frac{3}{2}}$ comes straight from Gaussian integration over three dimensions. Given that the electron mass is known with

much more precision than the loosely-determined quark masses, we then use the electron mass to reverse the tables and predict *with precision*, the difference between these quark masses:

$$m_d - m_u = \frac{(2\pi)^{\frac{3}{2}}}{3} m_e = \mathbf{2.6826779329\ MeV} \tag{11.23}$$

This is a very precise number, and may be used to better constrain our the data for the current quark masses. Specifically, using $m_d = 4.8^{+.7}_{-.3}\ MeV$ and $m_u = 2.3^{+.7}_{-.5}\ MeV$, (11.23), in light of a $2.5^{+1.2}_{-1.0}\ MeV$ spread between the midpoint experimental data, tells us that the actual spread is slightly higher than the data indicates. Since there is more error on the high side of the down mass and less error on the low side of the up mass, the down mass is likely higher than 4.8 MeV, perhaps between 4.9 and 5.0 MeV and the up mass is likely a touch lower, perhaps 2.25 MeV. On average, the true masses should be about 3% higher based on (11.21). If we use (11.22) in an identity as:

$$m_d = \frac{m_d - m_u}{1 - m_u / m_d} = \frac{(2\pi)^{\frac{3}{2}}}{3} \frac{m_e}{1 - m_u / m_d}, \tag{11.24}$$

then because $m_d - m_u$ is now known with great precision from (11.23), the experimental determination of these quark masses can be made more precise to the degree that we can better tighten the *ratio* m_u / m_d.

Now, let's tie up the normalization, taking (11.22) as a given, empirical relationship. We combine (11.20) with (11.22) to find that:

$$-2 = K = \bar{d}[\gamma^\mu, \gamma^\nu] d \bar{d}[\gamma_\mu, \gamma_\nu] d = \bar{u}[\gamma^\mu, \gamma^\nu] u \bar{u}[\gamma_\mu, \gamma_\nu] u\,. \tag{11.25}$$

The *experimental constant* $K = -2$, now known, may now be discarded. What counts is that the spinors themselves now be normalized *such that* they accord with the *empirically-based* relation (11.25). We shall work with the "up" spinors, since the calculation is the same for either up or down. We first expand (11.25) using $g_{\mu\nu} = \eta_{\mu\nu}$:

$$-2 = \bar{u}[\gamma^\mu, \gamma^\nu] u \bar{u}[\gamma_\mu, \gamma_\nu] u = 8 \begin{pmatrix} -\bar{u}\gamma^0\gamma^1 u \bar{u}\gamma^0\gamma^1 u - \bar{u}\gamma^0\gamma^2 u \bar{u}\gamma^0\gamma^2 u - \bar{u}\gamma^0\gamma^3 u \bar{u}\gamma^0\gamma^3 u \\ + \bar{u}\gamma^1\gamma^2 u \bar{u}\gamma^1\gamma^2 u + \bar{u}\gamma^2\gamma^3 u \bar{u}\gamma^2\gamma^3 u + \bar{u}\gamma^3\gamma^1 u \bar{u}\gamma^3\gamma^1 u \end{pmatrix}. \tag{11.26}$$

We will want to calculate this with a sum over particle spin states for all the spinors. We first make use of $\Sigma u\bar{u} = N^2(\not{p} + m)/(\mathrm{E} + m)$ (see (3.1)) with an undetermined real normalization N. Via $\not{p} = p_\mu \gamma^\mu$, (11.26) becomes:

$$-2=8\frac{N^2}{\mathrm{E}+m}\begin{pmatrix}-\bar{u}\gamma^0\gamma^1(\boldsymbol{p}+m)\gamma^0\gamma^1 u-\bar{u}\gamma^0\gamma^2(\boldsymbol{p}+m)\gamma^0\gamma^2 u-\bar{u}\gamma^0\gamma^3(\boldsymbol{p}+m)\gamma^0\gamma^3 u\\+\bar{u}\gamma^1\gamma^2(\boldsymbol{p}+m)\gamma^1\gamma^2 u+\bar{u}\gamma^2\gamma^3(\boldsymbol{p}+m)\gamma^2\gamma^3 u+\bar{u}\gamma^3\gamma^1(\boldsymbol{p}+m)\gamma^3\gamma^1 u\end{pmatrix}. \quad (11.27)$$

$$=48\frac{N^2}{\mathrm{E}+m}\left(p_\mu\bar{u}\gamma^\mu u-m\bar{u}u\right)=48\frac{N^2}{\mathrm{E}+m}\bar{u}(\boldsymbol{p}-m)u$$

It is easy to show using Dirac spinors in the usual way, summing both particle spin states, that $m\bar{u}u=4N^2m^2/(E+m)$. On the other hand, we recognize that $p_\mu\bar{u}\gamma^\mu u$ is a variant of the conservation equation $\partial_\mu J^\mu=0$ written in momentum space. So we mandate $p_\mu\bar{u}\gamma^\mu u=0$ by continuity. Thus, we can use these two results in (11.27) to write:

$$-2=-192N^4\frac{m^2}{(E+m)^2}=\bar{d}[\gamma^\mu,\gamma^\nu]d\bar{d}[\gamma_\mu,\gamma_\nu]d=\bar{u}[\gamma^\mu,\gamma^\nu]u\bar{u}[\gamma_\mu,\gamma_\nu]u\,, \quad (11.28)$$

which means that:

$$N=\frac{1}{2\sqrt[4]{6}}\frac{\sqrt{E+m}}{\sqrt{m}};\quad N^2=\frac{1}{\sqrt{4!}}\frac{E+m}{2m}. \quad (11.29)$$

This is a *dimensionless covariant normalization* which keeps the Dirac spinors dimensionless, and which embeds into the Dirac algebra, the empirical relationships (11.22) and (11.23) between the quark and electron masses. In other words, the normalization (11.29) fully implements (hard-wires) the relationship (11.22), $m_e\equiv 3(m_d-m_u)/(2\pi)^{\frac{3}{2}}$ – which appears to yield the correct experimental relation between the electron mass and the up and down quark masses – into the Dirac algebra via the normalization of the Dirac spinors. To be clear: this is an *empirical normalization*, handed to us by nature, which reflects that $m_e\equiv 3(m_d-m_u)/(2\pi)^{\frac{3}{2}}$ appears to be an experimentally-correct mass relationship. We note, simply as an observation, via the Levi-Civita tensor in spacetime, that $4!=-\varepsilon_{\mu\nu\alpha\beta}\varepsilon^{\mu\nu\alpha\beta}$, and that $(E+m)/2m=1$ in the fermion rest frame $E=m$. Also, for any 4x4 matrix M in spacetime, the determinant $|M|=\varepsilon_{\alpha\beta\gamma\delta}M^{\alpha 0}M^{\beta 1}M^{\gamma 2}M^{\delta 3}$ has 24 additive terms. So the factor of 4!, while it emerges to implement an *experimental* mass observation, is a real integer number which does play a central role in field theory in four spacetime dimensions.

Moreover, we also observe that $4!=4\times3\times2$ is the number of known fermions of all flavors and colors and generations, and further describes the way in which these fermions are structured, as can be seen from Figure 3 below in which: *LRGB* represents leptons as a fourth color of quark at high

energies as discussed in section 7; e,μ,τ represents the three fermion *generations*; and $\Uparrow,\Downarrow$ represent isospin up and isospin down:

$$\begin{array}{ccccccc} & \leftarrow 3=e\mu\tau\rightarrow & & & \leftarrow 3=e\mu\tau\rightarrow & & \\ \uparrow & \nu_e & \nu_\mu & \nu_\tau & e & \mu & \tau \\ 4= & u_R & c_R & t_R & d_R & s_R & b_R \\ LRGB & u_G & c_G & t_G & d_G & s_G & b_G \\ \downarrow & u_B & c_B & t_B & d_B & s_B & b_B \\ & & \leftarrow 2=\Uparrow\Downarrow\rightarrow & & & & \end{array}$$

Figure 3

Therefore, if we let $n_f = 24 = 4!$ represent the number of fermions known in the natural world, the normalization (11.29), which applies to *each individual fermion* in this chart of 24, may be written on an entirely physical basis, without any "mysterious" numbers, as:

$$N^4 = \frac{1}{n_f}\frac{(E+m)^2}{(2m)^2} = \frac{1}{24}\frac{(E+m)^2}{(2m)^2}. \qquad (11.30)$$

While beyond the scope of this paper, this is suggestive of some sort of fermion "completeness relation" that entails accounting for all twenty-four of the fermion flavors shown in Figure 4 when normalizing individual Dirac spinors. We write (11.30) as N^4, because this is the power in which the normalization enters invariant amplitudes. So an amplitude which sums over all fermions will be summing a term with a 1/24 coefficient, over 24 distinct terms, one for each flavor of fermion in Figure 3.

Let us finally tie up one remaining aspect of section 10 and Figure 2, as to the short range of the nuclear interaction. In section 10, the reduced wavelength $\lambda\!\!\!^{-}$ was simply a parameter of the Gaussian *ansatz* (9.9). And we noted following (9.12) and again following Figure 2 that the Gaussian standard deviation $\sigma = \frac{1}{\sqrt{2}}\lambda\!\!\!^{-}$. But now, following (11.18), we set $\lambda\!\!\!^{-} = \hbar/mc$ to be the reduced Compton wavelength of the *current* quarks, and this led to the empirically-correct mass relationships (11.21)-(11.23). But given the current quark masses $m_d = 4.8^{+.7}_{-.3}\,MeV$ and $m_u = 2.3^{+.7}_{-.5}\,MeV$, and using the conversion scale $1F = 5.07GeV^{-1} = 1/(.197GeV)$, this means that $\lambda\!\!\!^{-}_u \sim 85.65F$ and $\lambda\!\!\!^{-}_d \sim 41.04F$, to which the standard deviation in Figure 2 is related by

$\sigma = \frac{1}{\sqrt{2}}\lambda\!\!\!^{-}$. This, of course, gives the nuclear interaction a short range, but not short enough, because the nuclear interaction is known to have a range on the order of 1 to 2 Fermi. So how do we explain this?

We now keep in mind that we have been using *current* quark masses which turn off any coverings due to perturbations of vacuum effects. But when we actually *observe* nuclear interactions, we are of course observing interactions based on the *effective, constituent* quark masses. If for very rough measure, we take these to be equal to 1/3 of the mass of the proton or neutron, say 939 MeV/3=313 MeV, then we have $\lambda\!\!\!^{-} \sim .63F$ and $\sigma = \frac{1}{\sqrt{2}}\lambda\!\!\!^{-} \sim .45F$. So now, the standard deviation for Figure 2 is slightly less than .5 F. Figure 2 and the discussion following then tells us that the nuclear interaction virtually ceases to be effective at about $4\sigma \approx 3\lambda\!\!\!^{-} \sim 2F$. So now, Figure 2, with $\lambda\!\!\!^{-}$ based on *constituent* quark masses, depicts just the right distance for the short range of nuclear interactions, which are now predicted to become insignificant at about 2 F.

12. Quark Confinement Results from Predicted Binding Energies which Coincide Extremely Closely with Nuclear Binding Energies

Finally, with the empirical fermion normalization (11.30) in place, we can directly derive the proton and neutron masses. However, because we have turned off all perturbation and turned off the vacuum, the masses in (11.8) and (11.9) are not expected to be the *observed* masses. Rather, these will the *structural* proton and neutron masses based only on the current quark masses, with no perturbations and no accounting for vacuum condensates. These, once again, are "signal" relationships with "noise" stripped out. While these masses are given formally in (11.8) and (11.9), the schematic relationships (11.10) through (11.12) provide a shortcut to calculate these masses. If we compare (11.12) to our eventual result (11.22) for the electron mass, we may schematically express this as:

$$E_{\text{Electron}} \propto 3\left(d^2 - u^2\right) \Rightarrow E_{\text{Electron}} = 3(m_d - m_u)/(2\pi)^{\frac{3}{2}}. \tag{12.1}$$

The key thing that we learn via the Gaussian integration, is to use the three-dimensional Gaussian integration number $(2\pi)^{\frac{3}{2}}$ as a divisor to find the correct mass relationships. Careful consideration of (11.8) through (11.11) and the Gaussian *ansatz* should make clear that the proton and neutron structural (noise-free signal) masses follow an identical pattern, i.e.:

$$E_{\text{P}} \propto d^2 + 4ud + 4u^2 \Rightarrow E_{\text{P}} = \left(m_d + 4\sqrt{m_u m_d} + 4m_u\right)/(2\pi)^{\frac{3}{2}}, \tag{12.2}$$

$$E_N \propto u^2 + 4ud + 4d^2 \Rightarrow E_N = \left(m_u + 4\sqrt{m_u m_d} + 4m_d\right)/(2\pi)^{\frac{3}{2}}. \quad (12.3)$$

Then, making use of the mid-valued experimental quark masses from [22] (which we know from (11.21) are low by about 3%), we obtain:

$$E_P = \left(m_d + 4\sqrt{m_u m_d} + 4m_u\right)/(2\pi)^{\frac{3}{2}} = 1.733\,MeV\ , \quad (12.4)$$

$$E_N = \left(m_u + 4\sqrt{m_u m_d} + 4m_d\right)/(2\pi)^{\frac{3}{2}} = 2.209\,MeV\ . \quad (12.5)$$

This proves in energy terms, that these magnetic monopoles are topologically stable with definite, finite energies.

Now, while (12.4) and (12.5) seem odd at first blush in light of E_N = 939.565379 MeV and E_P = 938.272046 MeV, this is actually a fascinating and very revealing result: We have turned off all perturbative terms, which means that "interaction" energy and other "noise" accounts for about 99.8% of the observed mass of the proton and neutron, according to the above. The underlying quarks, absent interactions and absent vacuum effects, appear to contribute only about 0.2% of the total. But of even more interest, is this: If the "naked" proton and neutron masses were simply a linear sum of their component quark masses which are $m_d = 4.8^{+.7}_{-.3}\,MeV$ and $m_u = 2.3^{+.7}_{-.5}\,MeV$ based on the best PDG data, we would expect to have about $E_{\text{Proton}} = 9.4MeV$ and $E_{\text{Neutron}} = 11.9MeV$ based on the PDG experimental means. So here, "the whole is *a lot less* than the sum of the parts," and there is a stunning energy diminution. What does this mean that we can put three quarks together and have a system where the total mass is less than 20% of the mass of the component quarks, before we turn on the perturbative interactions? Imagine putting ten pounds of anything into a black box, and then finding that the black box weighs less than two pounds. *It means that there is a fantastically-large, intrinsic, negative binding energy holding these quarks together in a confined system!*

We can calculate this inherent binding energy B directly: Using the additive relationships $E_{\text{Proton}} = 9.4MeV = m_d + 2m_u$, $E_{\text{Neutron}} = 11.9MeV = m_\mu + 2m_d$ for mean data per above, and (12.4) and (12.5), the inherent proton and neutron binding energies, respectively, are simply:

$$B_P = 2m_u + m_d - \left(m_d + 4\sqrt{m_u m_d} + 4m_u\right)/(2\pi)^{\frac{3}{2}} = 9.4MeV - 1.733MeV = 7.667MeV \quad (12.6)$$

$$B_N = 2m_d + m_u - \left(m_u + 4\sqrt{m_u m_d} + 4m_d\right)/(2\pi)^{\frac{3}{2}} = 11.9MeV - 2.209MeV = 9.691MeV\ . \quad (12.7)$$

For a system with an equal number of protons and neutrons, the *average* binding energy *per nucleon* will then be:

$$\overline{B} = (7.667\,MeV + 9.691MeV)/2 = 8.679\,MeV \quad (12.8)$$

This is a fascinating result, because these are exactly the magnitudes of per-nucleon binding energies that are observed throughout nuclear physics for all elements from He^4 and C^{12} through the balance of the periodic table, as shown in Figure 4 below which can be obtained in like-form from virtually any hardcopy or online reference on nuclear physics. Is (12.8) a prediction that the per-nucleon binding energy is between 8 and 9 MeV, which is *exactly what is observed throughout Figure 4?* If so, then the validation of the thesis that baryons are Yang-Mills magnetic monopoles advances well beyond predicting the electron rest mass from the quark masses in (11.21)-(11.23), to perhaps predicting the precisely-known binding energies that permeate nuclear physics. How might this work?

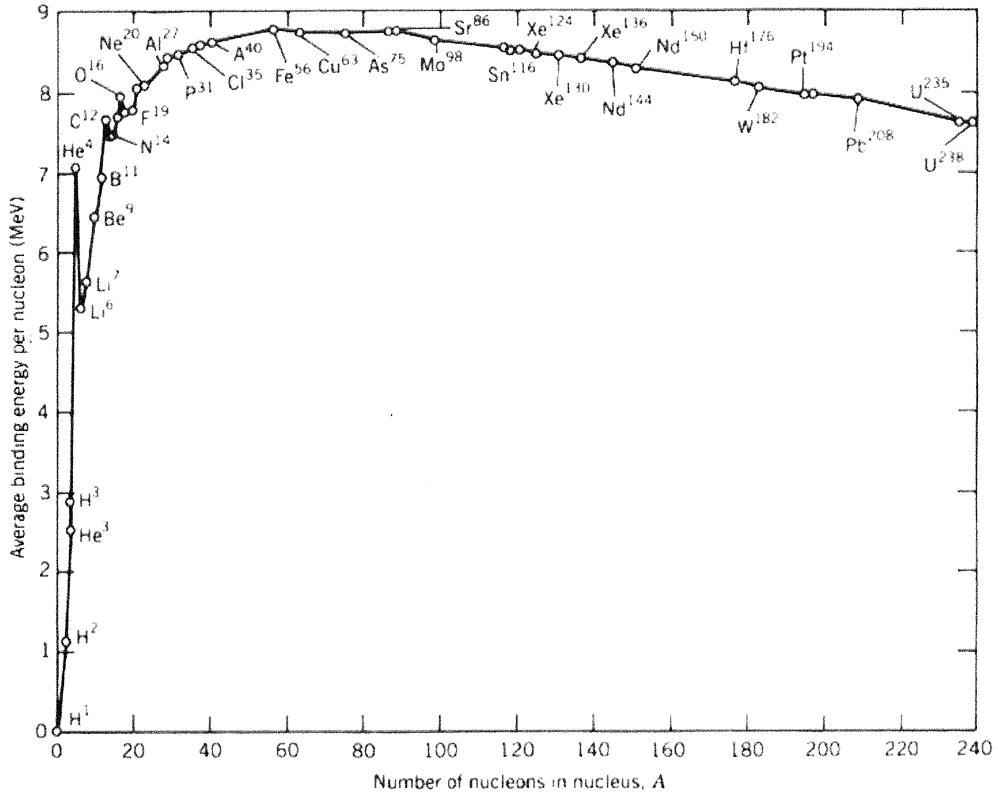

Figure 4

Based on the data in Figure 4 and (12.6)-(12.8), what one might observe as a preliminary matter is the following: First, when we state that the neutron and proton masses are E_N = 939.565379 MeV and E_P = 938.272046 MeV, we have to be careful to be clear that these are *unbound* masses for *free* nucleons, as we were with emphasis following (11.12). Fuse a proton and a

neutron into a deuteron (H^2 nucleus), however, and the mass of each is reduced by a well-established binding energy *per nucleon* of $B_{H^2}/2 = 1.112283 MeV$, the first non-zero data point in Figure 4. (In general, for the discussion to follow, we shall use binding energies calculated from nuclei masses in [23].) Fuse two of these into a four-nucleon alpha particle (He^4 nucleus) and the binding energy per nucleon spikes rapidly to just over 7 MeV per nucleon, entering the range predicted in (12.8). Why is He^4 understood to spike so quickly, whereby the Li and Be nuclei drop back down to under 6 MeV per nucleon before C and N rise back to about 7.5 MeV per nucleon before the heavier elements move smack into the middle of what is predicted by (12.8)? Because for the He^4 nucleus, all of the nuclei (two protons and two neutrons, one each with spin up, one each with spin down) can remain in a ground state, but for any element that has more than 4 nuclei, the remainder of the nuclei *must* go into higher energy states because of the fermion Exclusion Principle. This means that some of the nuclei in Li and Be must "steal" some of the energy that is otherwise available for binding, and instead use this energy to excite to a higher energy state to be able to coexist in the same nucleus with the first four nucleons of the alpha particle. All of these observations are part of the known understanding of Figure 4.

So based on these observations, one might fashion the following *preliminary* explanation of what (12.6) – (12.8) are saying: Each nucleon apparently has what we shall refer to as a "latent binding energy," or "energy *available* for binding." When a nucleon is free, *all* of that binding energy is contained within the nucleon, and serves to *confine* the quarks within the nucleon through *intra-nucleon* binding. This confinement is structural based on differential spacetime geometry, as established in section 1. But to fuse one nucleon with another nucleon, some of that internal "latent" binding energy must become devoted to binding together the two nucleons. So in the deuteron, $B_{H^2}/2 = 1.112283 MeV$ per nucleon is channeled into the fusion of the two nucleons (and thus is released as fusion energy) and the total masses (including the *observed* masses) of the proton and neutron drop slightly by an equivalent amount. Some, but not all, of the latent binding energy has now gone into *inter-nucleon* binding, rather than *intra-nucleon* binding. As one goes up the nuclear mass scale, more and more of the latent binding energy is apparently channeled into inter-nucleon binding, and less into intra-nucleon binding. And some of that energy – for which Li and Be are good examples – can be channeled into providing the energy needed for the "fifth" and additional nucleons to excite into a higher energy state so that they can fuse to

the rest of the nucleus. So what (12.6)-(12.8) appear to be saying, in this context, is that each nucleon has available for binding, a maximum latent binding energy of about 7.7 MeV per proton and 9.7 MeV per neutron. How much of that is used, and what it is used for, depends on the particular nucleus that one seeks to fuse together.

Let's go a step further and look at Fe^{56} and Ni^{62}, which have the highest binding energy per nucleon of any nuclei, and are highly illustrative. Fe^{56} contains 30 neutrons and 26 protons. Based on (12.6) and (12.7) (which again, are based on quark masses that appear to be about 3% off on the low side), one would expect a total binding energy of 490.072 MeV. The observed experimental biding energy is a remarkably-close, slightly *higher* 492.253892 MeV. Ni^{62} contains 34 neutrons and 28 protons. Based on (12.6) and (12.7), (again, about 3% low) one would expect a total binding energy of 544.17 MeV. The empirical binding energy is the slightly higher 545.259 MeV. What does this mean?

First, the closeness of these numbers is further validation of the thesis of this paper that baryons are indeed Yang-Mills magnetic monopoles. Second, however, the empirical binding energies should in principle be *slightly lower rather than slightly higher* than the theoretical maximum available for binding via (12.6) and (12.7), otherwise it would become possible to de-confine quarks which must in principle be impossible based on section 1 as well as a general understanding of confinement principles. As we shall momentarily show, the 3% correction noted in earlier in (11.21) will fix this, so that *no nucleus* will *exceed* the maximum available latent binding energy. Rather, these "lightest per nucleon" nuclei Fe^{56} and Ni^{62} will use up just a tad less than the total available binding energy, with (12.6) and (12.7) (with energy numbers we will shortly update) establishing *in principle energy limits*.

As to the lighter elements, the amount of latent binding energy used for actual binding is lower, but let's look at the very lightest nuclei containing more than one nucleon. First, the H^2 deuteron which consists of one proton and one neutron, as a "two body" system, is the very simplest composite nucleus, and is known to have a binding energy $B_{H^2} = 2.224566 MeV$. This is intriguingly close to the mass of the up quark $m_u = 2.3^{+.7}_{-.5}\, MeV$, especially since there is a good likelihood that the up mass is just slightly smaller, as suggested following (11.23). Might it be that $m_u = 2.3^{+.7}_{-.5}\, MeV \overset{??}{=} B_{H^2} = 2.224566\ MeV$ are *one and the same*, i.e., that the deuteron binding energy is another "signal,"

like the electron mass, which cuts through the "noise" of the nucleons to tell us what is really going in inside? Specifically, might it be that the deuteron binding energy is a signal that tells us the *exact* current mass of the up quark? If this is so, then the up and down quark masses can be calculated to six-decimal precision in MeV using B_{H^2} and (11.23).

Based on the tantalizing closeness of these energies, let us introduce the *hypothesis* that this is so, i.e., that:

$$m_u \equiv B_{H^2} = \mathbf{2.224566\ \ MeV}\ , \tag{12.9}$$

in which case, via (11.23), we may obtain with similar precision:

$$m_d = \frac{(2\pi)^{\frac{3}{2}}}{3} m_e + m_u = 2.6826779329\ \ MeV + 2.224566\ \ MeV\ , \tag{12.10}$$

$$= \mathbf{4.907244\ \ MeV}$$

and the ratio:

$$m_u / m_d = \mathbf{.4533229}\ . \tag{12.11}$$

Both of these masses fit well within the current quark masses $m_u = 2.3^{+.7}_{-.5}\, MeV$ and $m_d = 4.8^{+.7}_{-.3}\, MeV$ given in [22] and the ratio $m_u / m_d = .46(5)$ in equation [5] of [24]. We shall momentarily discuss the *theoretical* basis upon which this hypothesis might be justified, but first, let's do some calculations.

If hypothesis (12.9) is true, then via (12.6) and (12.7) we may do a more precise calculation:

$$B_{\mathrm{P}} = 2m_u + m_d - \left(m_d + 4\sqrt{m_u m_d} + 4m_u\right)/(2\pi)^{\frac{3}{2}} = 9.356376\ \text{MeV} - 1.715697\, MeV \tag{12.12}$$

$$= \mathbf{7.640679MeV}$$

$$B_{\mathrm{N}} = 2m_d + m_u - \left(m_u + 4\sqrt{m_u m_d} + 4m_d\right)/(2\pi)^{\frac{3}{2}} = 12.039054\ \text{MeV} - 2.226696\, MeV\ . \tag{12.13}$$

$$= \mathbf{9.812358MeV}$$

Based on the discussion preceding (12.9), this says that every proton in a nucleus has a latent (maximum available) binding energy of 7.640679 MeV, and every neutron has available 9.812358 MeV. For a *free, unbound* nucleon, *all* of this energy is used to confine the quarks within the nucleon. But when one nucleon binds to another, some of this energy is released as fusion energy, and an equivalent deficit of energy goes into binding the nucleons. For Fe^{56}, with 26 protons and 30 neutrons, we may calculate that this *maximum available* binding energy is:

$$B_{\max}(\mathrm{Fe}^{56}) = 26 \times 7.640679 MeV + 30 \times 9.812358 MeV = \mathbf{493.028394MeV} \tag{12.14}$$

What does the empirical data show to be the *actual* binding energy? **492.253892 MeV!** So precisely 99.8429093% of the *available* binding energy

predicted by this model of nucleons as Yang-Mills magnetic monopoles goes into binding together the Fe^{56} nucleus. The remaining 0.1570907%, which is equal to .774502 MeV total, or a relatively scant 13.83040 KeV *per nucleon*, goes into confining the quarks within the nucleons. A calculation similar to (12.14) based on (12.12) and (12.13) for Ni^{62} reveals a predicted *available* binding energy of 547.559184 MeV compared to an empirical binding energy of 545.2590 MeV. So Ni^{62} uses 99.57992% of the *available* binding energy, with the balance continuing to confine the quarks. Calculations for other nuclei and isotopes and isobars reveal that *no known nucleus ever gets up to using 100% of the available binding energy*, and that Fe^{56} achieves the maximum utilization at 99.8429093%. This appears to provide compelling experimental validation that baryons, including protons and neutrons, are indeed Yang-Mills magnetic monopoles.

What would it mean to get over 100%? It would mean that the balance has been tipped, so that the energies within individual nucleons would no longer confine the quarks, but would free them. The peak in Figure 4 at Fe^{56}, is nature saying that she will *never* allow quarks to be de-confined from a nucleon, any more than she will allow material signals to reach the speed of light! Fe^{56} is the closest that one can come to taking all the energy that is used to confine the quarks inside a nucleon, and using it to instead bind nuclei together. But even here, we never get to the point where we can remove the quark from a nucleus; we only approach a natural limit. There is always *at least* 13.83040 KeV per nucleon continuing to confine the quarks, even for Fe^{56}. After reaching these peaks at Fe^{56} and Ni^{62}, the Figure 4 curve heads back down into the fission zone, and the quarks again become more tightly confined inside the nucleon. While quarks always stay confined, however, this does suggest that Fe^{56} and Ni^{62} and other nuclei which commit a very high percentage of available binding energy to inter-nucleon binding are the best nuclei to use, experimentally, in order to observe the behaviors of quarks inside the nucleons. This is because for these nuclei, the *intra-nucleon* energies confining the quarks inside the nuclei are at their lowest strength, having all been channeled into *inter-nucleon* binding. In these nuclei, quarks have more freedom, asymptotic and otherwise, than in any other nuclei.

While the hypothesis (12.9) that $m_u \equiv B_{H^2}$ appears to be confirmed based on the empirical data, both directly and via (12.12) to (12.14) deduced therefrom, it is important to try to understand the *theoretical* reasons why (12.9) would make sense. Figure 4, which is entirely empirical, makes clear that to fuse a nucleon to any given nucleus, the amount of energy which is

either liberated (fusion) or needs to be supplied (fission) is a *discreet* amount of energy. For example, in fusing a proton and a neutron into a deuteron, one will liberate exactly 2.224566 MeV (equation (12.9)) of energy, each and every time, *as opposed to some continuous spread of energy*. To add another neutron to a deuteron to form the tritium H^3 isotope with a total 8.481799 MeV binding energy, one will liberate exactly another 6.257233 MeV, which is the difference between the H^2 and H^3 binding energies. Not a continuous spread. The same, discrete amount of energy, each and every time. What determines that precise energy values like these, and no others, will be released (or must be supplied)? Hypothesis (12.9), which leads to predictions such as (12.14) which are borne out by empirical data binding, adds new information to the semi-empirical Bethe-Weizsäcker mass formula which accounts for binding energies in general terms based on nucleus volume in light of limited nuclear range, surface versus central position of particular nuclei, Coulomb repulsion between protons, and exclusion based on both spin and internal symmetry quantum numbers. What (12.9) adds to all of these considerations, is this:

Take a proton and a neutron. Think of each as a *resonant cavity*. Try to fuse them into a deuteron. Experiments tell us that the same amount of energy – 2.224566 MeV – will be released each and every time following a successful fusion. Some attribute of these two nucleons must determine that this amount of energy is 2.224566 MeV, and not some other energy. So what is that attribute? Each of these nucleons contains up quarks and down quarks. These have associated Compton wavelengths. Not unlike in the early Bohr / deBroglie models used to explain atomic spectra, those wavelengths will establish preferred, discreet resonant energy levels which can be detected, to the exclusion of all other energies which cannot be detected. And nature will follow least action principles and so choose a lower energy level (such as that set by the up quark) over a higher energy level (such as that set by the down quark) whenever it can. So to create a two body system – a deuteron – from a proton and a neutron, the energy released resonates *precisely* with the mass of the down quark, which is why 2.224566 MeV is <u>both</u> the mass of the up quark <u>and</u> the energy released in this simplest, most elemental fusion of a proton and a neutron into a deuteron. The energy released from this fusion (and presumably other fusions) appears to depend on what wavelengths "fit" with respect to the components being fused. And at least for fusing a deuteron, the wavelength / mass that "fits" is established directly, equivalently by the mass of the up quark which is contained twice in a proton and once in a neutron.

To start with a deuteron H^2 and add another neutron to form an H^3 tritium nucleus (which does not add the complication of a p—p repulsion that occurs for He^3) then also becomes a problem of asking: what resonates? But now, the problem is a three body problem. One of the "cavities" is now a deuteron. So while the empirical answer is 6.257233 MeV, there is no simple apparent way to get this number, at least linearly, from (12.9) and (12.10). But, to find the basis for this 6.257233 MeV energy needed to go from H^2 to H^3 adds another consideration to the semi-empirical mass formula: what is the lowest energy, most natural resonance of the two systems that one is trying to fuse, namely, an H^2 and a neutron? That resonance is 6.257233 MeV, and some careful analysis of the resonance between a two body system and a one-body system, together with some employment of the quark masses (12.9), (12.10), should yield that number.

So, in sum, (12.9) becomes justified for a deuteron on the basis of the proposition that the fusion resonance for a cavity (proton) that already contains a quark with a mass of 2.224566 MeV with a second cavity (neutron) that also contains a quark with a mass of 2.224566 MeV, is just that mass: 2.224566 MeV. For other nuclei, this introduces a resonant cavity analysis to supplement the other considerations in the semi-empirical mass formula.

This also leads one to consider the technological possibility that a new type of "resonant fusion" in which nuclei are bathed in oscillations at their known binding energies, might serve to catalyze fusion and extract energy without the need to supply excessive heat or large particle accelerations.

And, (12.12) and (12.13) modify our thinking about Bethe-Weizsäcker in one other very important way: the first two terms of this formula, $a_V A + a_s A^{2/3}$, where A is the number of nucleons, are designed to account for the volume and surface geometry of a larger nucleon based upon the fact that because of the short range of the nuclear force (see Figure 2 in section 10 and the discussion at the end of section 11 suggesting a standard deviation of $\sigma = \frac{1}{\sqrt{2}}\lambda\!\!\!^{-} \sim .45F$ for nuclear interactions and a virtual cessation of interaction at around $4\sigma \approx 3\lambda\!\!\!^{-} \sim 2F$), each nucleon will only interact with its immediately-adjacent neighbors, and nucleons on the surface will have less neighbors with which to interact. But (12.12) and (12.13) introduce the same considerations from a different standpoint: it sets in very precise terms, a maximum available binding energy, and that energy limit flows from the Gaussian distribution of Figure 2 for the field flux across any closed surface. That is why the first two terms of Bethe-Weizsäcker are $a_V A + a_s A^{2/3}$, rather than $a_V A^2 + a_s A^{4/3}$.

To further develop this *preliminary* understanding of nuclear binding, it will be very useful to carefully scour the wealth of data for various nuclear isotopes and isobars to see exactly how much binding energy is added or subtracted each time a proton or neutron is added to or removed from a nucleus, and compare those with the predicted binding energies in (12.12) and (12.13), as this may provide a more "granular" insight into the specific data points on nuclear binding charts such as Figure 4. For example, start with Fe^{56}. Add a single neutron to turn it into the Fe^{57} isotope. The empirical data shows that this adds 931.919288 MeV (with no new electron) to the atomic weight of Fe^{56} while adding one more neutron with an *unbound* mass of 939.565379 MeV. So, the additional binding energy introduced (and the fusion energy released) by adding this one neutron is:

$$B(Fe^{57}) - B(Fe^{56}) = \mathbf{7.646090\ MeV} \qquad (12.15)$$

This *empirical* binding energy differs from the *theoretical prediction* of **7.640679MeV** in (12.12) for the intrinsic binding energy of a proton, by a paltry 5.412 KeV, or 0.0708%. Apparently, adding one *neutron* to Fe^{56}, within a small fraction of one percent, liberates an intrinsic binding energy virtually equal to that of a single *proton*. Similar exercises for other isotopes and isobars of all nuclei should be quite instructive, and with (12.12) and (12.13) available for guidance, can help us better understand what happens each time one adds or subtracts a proton or a neutron to or from a nucleus, and how the biding energies are allocated.

But the *seven parts in ten thousand* closeness of the *empirical* energy (12.15) to a *predicted* energy in (12.12), taken together with all of the other predictions in Sections 11 and 12 which appear to be experimentally supported, cannot be dismissed as coincidence. There are too many such predictions, they are all intertwined, and they all come too close to observational data to be merely coincidental.

All of this, and especially the 99.8429093% of the available binding energy which goes into binding together the Fe^{56} nucleus, and the fact that *nothing goes over100%*, brings us full circle back to where we started in section 1, when we showed how Yang-Mills magnetic monopoles naturally confine their gauge fields, and how this was due to the very structure of spacetime via Gauss' / Stokes' integration and the geometric relationship $dd=0$. Now, in (12.12) and (12.13), when we are finally looking at energies, we see that once three quarks are put into a baryon, the very structure of the baryon creates an intrinsic latent binding energy that is equal to more than 80% of the component quark masses. This latent binding energy is

fundamental to the structure of baryons. As we showed in section 1, confinement flows from the very structure of spacetime, and as we showed here, it explains with precision the experimental data for nucleon binding of the heaviest elements and especially explains why Figure 4 has a maximum binding energy per nucleon which is never exceeded and grows smaller as one moves away from the fusion / fission boundary.

So, expressed in terms of proton and neutron energies, quark confinement is signaled by the fact that for three quarks in a baryon, there is an inherent negative latent binding energy that is equal to more than 80% of the quark masses themselves, and that even for the most tightly bound nuclei, some small amount of energy from this binding energy reservoir is always retained to keep the quarks confined. This is how the energy physics of a baryon conspires to keep the quarks confined. When nucleons are fused, some of that binding energy migrates into a negative binding energy holding the nucleons together to form nuclei and a positive equivalent is released as fusion energy. If one can maximize the latent binding energy that goes into inter-nucleon binding, the confinement of the quarks within any given nucleon does loosen up, because the latent binding energy is used less for confinement and more for actual inter-nucleon binding. In an iron nucleus, for example, quarks will come close (within 0.16% per nucleon) of being able to deconfine from the nucleus. But one never quite goes beyond that, because precisely at the point where the quarks comes closest to deconfinement, one starts onto the downward fission slope where *more, not less*, of the latent binding energy starts to go back into keeping quarks confined. *So, the well-known empirical peak in Figure 4 is fundamentally a confinement phenomenon* whereby quarks step back from the brink of becoming de-confined in Fe^{56}, and remain confined *in principle* no matter what the element. Iron-56 thus is seen to sit at the theoretical crossroads of fission, fusion, and quark confinement.

Knowing now that nucleons very likely are Yang-Mills magnetic monopoles, and given the stark binding energy "tea leaves" just noted, it may become possible to develop a more coherent and detailed granular understanding of nuclear structure. Such an understanding, in light of what has been developed here, now boils down to understanding in detail, how *collections* of such magnetic monopoles – which monopole collections we now understand to be nuclei when the monopoles are protons and neutrons – organize and structure themselves.

Conclusion

The very vast preponderance of the material universe consists of baryons, and particularly, protons and neutrons. The results developed here, especially the empirical concurrences developed in sections 11 and 12, firmly validate that for non-commuting Yang-Mills gauge fields, the long-sought and ever-elusive magnetic monopoles of Maxwell do exist in the physical world, everywhere and anywhere that there is matter in the universe, hiding in plain sight, in the form of protons and neutrons!

These Yang-Mills Magnetic Monopoles naturally confine their gauge fields, naturally contain three colored fermions in a color singlet, and mesons also in color singlets are the only particles they are allowed to emit or absorb. $SU(3)_C$ QCD as it has been extensively studied and confirmed is understood in broader context, with no contradiction, to be a consequence of baryons being Yang-Mills magnetic monopoles. Protons and neutrons are naturally represented in the fundamental representation of this group. The t'Hooft monopole Lagrangian with a Gaussian *ansatz* for fermion wavefunctions demonstrates that these monopoles can be made to interact only at very short range as is required for nuclear interactions. These monopoles are topologically stable following symmetry breaking from an SU(4) group using the B-L (baryon minus lepton number) generator. The mass of the electron is accurately predicted based on the masses of the up and down quarks to about 3% from the experimental mean for the quark masses, and confinement of quarks occurs energetically via fantastically strong negative binding energies. And, the predicted binding energies per nucleon are completely consistent with experimental data. All of this compels serious consideration and further development of baryons as Yang-Mills magnetic monopoles.

Acknowledgement

The author wishes to express grateful thanks and appreciation to Dr. Andrej (Andy) Inopin of Kharkov, Ukraine for all of his feedback in helping the author develop and review this manuscript, and in working with me on various occasions since 2005 when he first got me interested in quark and color confinement which forms a central part of this paper.

References

[1] t'Hooft, G., *Magnetic Monopoles in Unified Gauge Theories*, Nuclear Physics B79, 276-284, (1974)
[2] A.M. Polyakov, *Particle Spectrum in the Quantum Field Theory*, JETP Lett. 20, 194-195 (1974)
[3] Ohanian, H. C., *What is spin?*, Am. J. Phys. 54 (6), 500-505 (June 1986)
[4] Zee, A., *Quantum Field Theory in a Nutshell*, Princeton (2003)
[5] Halzen, F., and Martin A. D., *Quarks and Leptons: An Introductory Course in Modern Particle Physics*, J. Wiley & Sons (1984)
[6] Ryder, L., *Quantum Field Theory*, Cambridge (1996)
[7] Close, F. E., *An Introduction to Quarks and Partons*, Academic Press (1979)
[8] J. Beringer et al.(PDG), PR D86, 010001 (2012), see specifically, *Chapter 14. Quark Model,* http://pdg.lbl.gov/2012/reviews/rpp2012-rev-quark-model.pdf.
[9] J. Beringer et al. (Particle Data Group), PR D86, 010001 (2012) http://pdg.lbl.gov/2012/tables/rpp2012-sum-mesons.pdf
[10] Reinich, G.Y., *Electrodynamics in the General Relativity Theory*, Trans. Am. Math. Soc., Vol. 27, pp. 106-136 (1925)
[11] Wheeler, J. A., *Geometrodynamics*, Academic Press, pp. 225-253 (1962)
[12] Misner, C. W., Thorne, K. S., and Wheeler, J. A., *Gravitation*, W. H. Freeman & Co. (1973)
[13] K. Hagiwara *et al.*, Quantum, Chromodynamics , Physical Review D66, 010001-1 (2002), http://pdg.lbl.gov/2002/qcdrpp.pdf
[14] S. Bethke, The 2009 World Average of αS, Eur. Phys. J. C64, 689 (2009) http://arxiv.org/abs/0908.1135
[15] Cheng, T-P and Li, L-F, *Gauge theory of elementary particle physics*, Oxford (1984) (2011 reprint)
[16] Weinberg, S., *The Quantum Theory of Fields, Volume II, Modern Applications*, Cambridge (1996)
[17] Volovok, G. E., *The Universe in a Helium Droplet*, Clarendon Press – Oxford (2003)
[18] Howard Georgi and Sheldon Glashow, *Unity of All Elementary-Particle Forces*, Physical Review Letters, 32 at 438 (1974)
[19] Georgi, H. and Glashow, S. L., *Unified Weak and Electromagnetic Interactions without Neutral Currents*, Phys. Rev. Lett. 28, 1494–1497 (1972)

[20] J. Beringer et al. (Particle Data Group), PR D86, 010001 (2012)
http://pdg.lbl.gov/2012/tables/rpp2012-sum-baryons.pdf
[21] J. Beringer et al. (Particle Data Group), PR D86, 010001 (2012)
http://pdg.lbl.gov/2012/tables/rpp2012-sum-leptons.pdf
[22] J. Beringer et al. (Particle Data Group), PR D86, 010001 (2012)
http://pdg.lbl.gov/2012/tables/rpp2012-sum-quarks.pdf
[23] http://physics.nist.gov/cuu/Constants/index.html
[24] J. Beringer et al. (Particle Data Group), PR D86, 010001 (2012)
http://pdg.lbl.gov/2012/reviews/rpp2012-rev-quark-masses.pdf